July 2009
Research Report: UCPRC-RR-2009-02

Warm-Mix Asphalt Study: First-Level Analysis of Phase 2 HVS and Laboratory Testing and Phase 1 and Phase 2 Forensic Assessments

Authors:
D. Jones, R. Wu, B. Tsai, and J.T. Harvey

Partnered Pavement Research Program (PPRC) Contract Strategic Plan Element 4.18:
Warm-Mix Asphalt

PREPARED FOR:

California Department of Transportation
Division of Research and Innovation
Office of Roadway Research

PREPARED BY:

University of California
Pavement Research Center
UC Davis, UC Berkeley

DOCUMENT RETRIEVAL PAGE			**Research Report: UCPRC-RR-2009-02**
Title: Warm-Mix Asphalt Study: First-Level Analysis of Phase 2 HVS and Laboratory Testing, and Phase 1 and Phase 2 Forensic Assessments			
Authors: David Jones, Rongzong Wu, Bor-Wen Tsai, and John T. Harvey			
Prepared for: Caltrans	**FHWA No:** CA112221A	**Work submitted:** 05-24-2011	**Date:** July 2009
Strategic Plan Element No: 4.18	**Status:** Final		**Version No.:** 1

Abstract:

This first-level report describes the second phase of a warm-mix asphalt study, which compares the performance of a control mix, produced and constructed at conventional hot-mix asphalt temperatures, with three mixes produced with warm-mix additives, produced and compacted at approximately 35°C (60°F) lower than the control. The additives tested included *Advera WMA*®, *Evotherm*™, and *Sasobit*®. The results of the second phase of Heavy Vehicle Simulator (HVS) and laboratory testing are discussed. The study includes these key findings:

- Based on the results of HVS testing and a forensic investigation of the test track, it is concluded that the use of any of the three warm-mix asphalt technologies included in this experiment will not significantly influence the rutting performance or moisture sensitivity of the mix.
- The duration and rut depths of the embedment phase of the warm-mix sections were approximately half that of the control, an opposite trend to that observed in Phase 1, indicating that the effects of oxidation of the binder at lower temperatures may only influence rutting performance in the first few months after construction.
- No difficulty was experienced in the preparation of field-mixed, laboratory-compacted specimens at actual construction temperatures. Lower air-void contents were achieved in the laboratory-prepared specimens compared to specimens sampled from the HVS test track.
- Limited laboratory moisture sensitivity testing confirmed that all the mixes tested were potentially susceptible to moisture damage. There was, however, no difference in the level of moisture sensitivity between the control mix and mixes with the additives assessed in this study.

The HVS and laboratory testing completed in this phase of the study support the findings of the first phase of testing in that no results were obtained to suggest that the warm-mix technologies assessed in this study should not be used in new construction, rehabilitation, or pavement preservation applications in California. Final recommendations on the use of warm-mix asphalt will only be made after further research and monitoring of full-scale pilot studies on in-service pavements is completed. It is recommended that use of warm-mix technologies continue in full-scale pilot studies on in-service pavements until a decision is made on statewide use.

Keywords:
Warm-mix asphalt, WMA, accelerated pavement testing, Heavy Vehicle Simulator

Proposals for implementation:
Continue with Phase 3 (warm mix in rubber hot-mix asphalt). Continue with implementation.

Related documents:
Work plan (UCPRC-WP-2007-01) and Phase 1 report (UCPRC-RR-2008-11).

Signatures:

D. Jones **1st Author**	J. Harvey **Technical Review**	D. Spinner **Editor**	J. Harvey **Principal Investigator**	T.J. Holland **Caltrans Contract Manager**

DISCLAIMER

The contents of this report reflect the views of the authors who are responsible for the facts and accuracy of the data presented herein. The contents do not necessarily reflect the official views or policies of the State of California or the Federal Highway Administration. This report does not constitute a standard, specification, or regulation.

PROJECT OBJECTIVES

The objective of this project is to determine whether the use of additives that reduce the production and construction temperatures of hot-mix asphalt influences the performance of the mix. This will be achieved through the following tasks:

1. Preparation of a work plan to guide the research;
2. Monitoring the construction of Heavy Vehicle Simulator (HVS) and in-service test sections;
3. Sampling of mix and mix components during asphalt concrete production and construction;
4. Trafficking of demarcated sections with the HVS in a series of tests to assess performance;
5. Conducting laboratory tests to identify comparable laboratory performance measures;
6. Monitoring the performance of in-service pilot sections; and
7. Preparation of first- and second-level analysis reports and a summary report detailing the experiment and the findings.

This report describes work undertaken to satisfy Tasks 4, 5, and 7.

ACKNOWLEDGEMENTS

The University of California Pavement Research Center acknowledges the following individuals and organizations who contributed to the project:

- Ms. Terrie Bressette, Ms. Cathrina Barros, Mr. Glenn Johnson, and Dr. Joe Holland, Caltrans
- Mr. Mike Cook and Dr. Hongbin Xie, Graniterock Company
- The management and staff, Graniterock Company and Pavex Construction
- Ms. Annette Smith, PQ Corporation
- Dr. Everett Crews, Meadwestvaco
- Mr. John Shaw and Mr. Larry Michael, Sasol Wax Americas
- Mr. Matthew Corrigan and Mr. Satish Bellaguti, Federal Highway Administration Turner Fairbanks Highway Research Center
- The Heavy Vehicle Simulator testing crew
- The UCPRC Richmond Field Station laboratory staff

EXECUTIVE SUMMARY

The objective of the comprehensive, phased California Department of Transportation (Caltrans) warm-mix asphalt study being undertaken by the University of California Pavement Research Center (UCPRC) is to determine whether the use of additives that reduce the production and construction temperatures of asphalt concrete will influence performance of the mix. The first two phases of the study compared the performance of a control mix, produced and constructed at conventional hot-mix asphalt temperatures, with three warm-mixes, produced and compacted at temperatures approximately 35°C (60°F) lower than the control. The additives tested in these phases included *Advera WMA®*, *Evotherm DAT™*, and *Sasobit®*.

The first phase of the study, based on a work plan approved by Caltrans, included the identification of an appropriate site for the experiment, the design and monitoring of construction of a test track, accelerated loading tests using the Heavy Vehicle Simulator (HVS) to assess rutting behavior, and a series of laboratory tests on specimens sampled from the test track. The second phase of the study, which is the focus of this report, included accelerated loading tests to assess the moisture sensitivity of the mixes and a series of laboratory rutting and fatigue tests on specimens prepared at the test track on the day of construction using laboratory (rolling wheel) compaction. The test track, constructed in September 2007, is located at the Graniterock Company's A.R. Wilson Quarry and Asphalt Plant near Aromas, California.

The second phase of Heavy Vehicle Simulator (HVS) testing commenced in August 2008 and was completed in June 2009. This testing compared rutting performance under wet conditions at elevated temperatures (pavement temperature of 50°C at 50 mm [122°F at 2.0 in.] pavement depth), using 40 kN, 60 kN, and 90 kN (9,000 lb, 13,500 lb, and 18,000 lb) loads on a standard dual-wheel configuration and a unidirectional trafficking mode. Laboratory testing to compare results from a limited number of field-mixed, laboratory-compacted specimens with results from the first phase field-mixed, field-compacted specimens commenced in October 2008 and was completed in January 2009. Due to the limited number of specimens produced, this phase of laboratory testing only included rutting and fatigue testing. Moisture sensitivity testing was limited to fatigue testing on unsoaked and soaked specimens.

Key findings from this phase of the study include:

- HVS trafficking on each of the four sections revealed that the duration and rut depths of the embedment phases (high early-rutting phase of typical two-phase rutting processes) on the warm-mix sections were approximately half that of the Control, a trend opposite to that observed in Phase 1. This indicates that the effects of oxidation of the binder at lower production temperatures may only influence performance in the first few months after construction.

- Rutting behavior of the Control and Evotherm sections after the embedment phase was distinctly different than that of the Sasobit and Advera sections. This was attributed to the Control and Evotherm sections being predominantly in the shade of an adjacent shed for most of the day, while the Advera and Sasobit sections were predominantly in the sun for most of the day. It is believed that the rate of aging of the two shaded sections was consequently slower than the other two sections, leading to the difference in performance. This is being investigated in a separate study and the results will be presented with the Phase 3 laboratory and HVS test results (on rubberized asphalt) when that testing is complete.
- The Control and Evotherm tests followed similar trends to each other after the first 80,000 HVS load repetitions and reached the 12.5 mm (0.5 in.) failure point at about 300,000 load repetitions. The Advera and Sasobit tests followed similar trends to the Control after the embedment phase, but with a much slower increase in rut depth. In the interests of completing this phase of the study, the Advera test was terminated after 625,000 when the rut depth was 11.5 mm (0.45 in.) repetitions (i.e., before reaching the failure point of 12.5 mm), while the Sasobit test was terminated after 420,000 repetitions when the rut depth was 9.9 mm (0.39 in.).
- A forensic investigation of all test sections indicated that the rutting was confined to the upper lift of the asphalt concrete. No evidence of moisture damage was noted on any of the sections, although some evidence of debonding between the two lifts of asphalt was noted on the Control section. All sections had some top-down cracking.
- Laboratory test results indicate that use of the warm-mix technologies assessed in this study does not significantly influence the performance of the asphalt concrete when compared to control specimens produced and compacted at conventional hot-mix asphalt temperatures. However, moisture sensitivity testing indicated that all the mixes tested were potentially susceptible to moisture damage. There was, however, no difference in the level of moisture sensitivity between the Control mix and mixes with warm-mix additives.

The HVS and laboratory testing completed in this phase have provided no new results to suggest that warm-mix technologies should not be used in California. The use of warm-mix technologies should therefore continue in full-scale pilot studies on in-service pavements until a decision is made on statewide implementation.

TABLE OF CONTENTS

EXECUTIVE SUMMARY ..... **v**
LIST OF TABLES ..... **xi**
LIST OF FIGURES ..... **xiii**
LIST OF ABBREVIATIONS ..... **xvi**
LIST OF TEST METHODS AND SPECIFICATIONS ..... **xvii**
CONVERSION FACTORS ..... **xviii**
1 INTRODUCTION **1**
1.1 Background 1
1.2 Project Objectives 1
1.3 Overall Project Organization 2
1.3.1 Deliverables 3
1.4 Structure and Content of this Report 3
1.5 Measurement Units 4
1.6 Terminology 4
2 SUMMARY OF FINDINGS FROM PHASE 1 TESTING **5**
3 TEST TRACK LAYOUT AND HVS TEST CRITERIA **9**
3.1 Protocols 9
3.2 Test Track Layout 9
3.3 HVS Test Section Layout 9
3.4 Pavement Instrumentation and Monitoring Methods 9
3.5 HVS Test Criteria 12
3.5.1 Test Section Failure Criteria 12
3.5.2 Environmental Conditions 12
3.5.3 Test Duration 15
3.5.4 Loading Program 15
4 PHASE 2 HVS TEST DATA SUMMARY **17**
4.1 Introduction 17
4.2 Rainfall 18
4.3 Section 604FD: Control 19
4.3.1 Test Summary 19
4.3.2 Outside Air Temperatures 20
4.3.3 Air and Water Temperatures in the Temperature Control Unit 20
4.3.4 Temperatures in the Asphalt Concrete Layers 22
4.3.5 Permanent Surface Deformation (Rutting) 22
4.3.6 Asphalt Concrete Moisture Content 25
4.3.7 Visual Inspection 26
4.4 Section 605FD: Advera 28
4.4.1 Test Summary 28
4.4.2 Outside Air Temperatures 29
4.4.3 Air and Water Temperatures in the Temperature Control Unit 29
4.4.4 Temperatures in the Asphalt Concrete Layers 30
4.4.5 Permanent Surface Deformation (Rutting) 31
4.4.6 Asphalt Concrete Moisture Content 34
4.4.7 Visual Inspection 35
4.5 Section 606FD: Evotherm 37
4.5.1 Test Summary 37
4.5.2 Outside Air Temperatures 37
4.5.3 Air and Water Temperatures in the Temperature Control Unit 38
4.5.4 Temperatures in the Asphalt Concrete Layers 38

4.5.5 Permanent Surface Deformation (Rutting) ... 40
4.5.6 Asphalt Concrete Moisture Content ... 42
4.5.7 Visual Inspection ... 43
4.6 Section 607FD: Sasobit ... 44
4.6.1 Test Summary ... 44
4.6.2 Outside Air Temperatures ... 45
4.6.3 Air and Water Temperatures in the Temperature Control Unit ... 45
4.6.4 Temperatures in the Asphalt Concrete Layers ... 47
4.6.5 Permanent Surface Deformation (Rutting) ... 47
4.6.6 Asphalt Concrete Moisture Content ... 50
4.6.7 Visual Inspection ... 51
4.7 Test Summary and Discussion ... 52
4.8 Comparison of Phase 1 and Phase 2 HVS Test Results ... 55
4.9 Fatigue Performance Testing ... 56
5 FORENSIC INVESTIGATION ... 57
5.1 Introduction ... 57
5.2 Forensic Investigation Procedure ... 57
5.3 Coring and Test Pit Excavation ... 58
5.4 Core Evaluation ... 58
5.5 Test Pit Profiles and Observations ... 62
5.5.1 Section 600FD: Phase 1 Control ... 63
5.5.2 Section 601FD: Phase 1 Advera ... 63
5.5.3 Section 602FD: Phase 1 Evotherm ... 63
5.5.4 Section 603FD: Phase 1 Sasobit ... 64
5.5.5 Section 604FD: Phase 2 Control ... 64
5.5.6 Section 605FD: Phase 2 Advera ... 64
5.5.7 Section 606FD: Phase 2 Evotherm ... 65
5.5.8 Section 607FD: Phase 2 Sasobit ... 65
5.6 Base-Course Density and Moisture Content ... 73
5.7 Dynamic Cone Penetrometer ... 75
5.8 Forensic Investigation Summary ... 76
6 PHASE 2a LABORATORY TEST DATA SUMMARY ... 77
6.1 Introduction ... 77
6.1.1 Specimen Preparation ... 77
6.2 Experiment Design ... 77
6.2.1 Shear Testing ... 77
6.2.2 Fatigue Testing ... 78
6.3 Test Results ... 79
6.3.1 Shear Tests ... 79
6.3.2 Resilient Shear Modulus (G) ... 81
6.3.3 Fatigue Beam Tests ... 84
6.4 Summary of Laboratory Testing Results ... 95
6.5 Comparison of Phase 1 and Phase 2 Laboratory Test Results ... 95
7 CONCLUSIONS ... 99
7.1.1 Comparative Energy Usage ... 100
7.1.2 Achieving Compaction Density at Lower Temperatures ... 100
7.1.3 Optimal Temperature Ranges for Warm-Mixes ... 100
7.1.4 Cost Implications ... 100
7.1.5 Rutting Performance ... 101
7.1.6 Moisture Sensitivity ... 101
7.1.7 Fatigue Performance ... 101
7.1.8 Rubberized and Open-Graded Mixes ... 101

8 REFERENCES 103
APPENDIX A: TEST PIT PROFILES 105
APPENDIX B: FATIGUE BEAM SOAKING PROCEDURE 111

LIST OF TABLES

Table 3.1: Test Duration for Phase 2 HVS Moisture Sensitivity Tests 15
Table 3.2: Summary of Phase 2 HVS Loading Program 15
Table 4.1: Rainfall Summary for Phase 2 HVS Testing 18
Table 4.2: 604FD: Temperature Summary for Air and Pavement 22
Table 4.3: 604FD: Moisture Content after Testing 25
Table 4.4: 605FD: Temperature Summary for Air and Pavement 31
Table 4.5: 605FD: Moisture Content after Testing 34
Table 4.6: 606FD: Temperature Summary for Air and Pavement 39
Table 4.7: 606FD: Moisture Content after Testing 43
Table 4.8: 607FD: Temperature Summary for Air and Pavement 47
Table 4.9: 607FD: Moisture Content after Testing 51
Table 5.1: Average Asphalt Concrete Thicknesses from Cores 58
Table 5.2: Average Asphalt Concrete Thicknesses from Test Pit Profiles (Station 9) 62
Table 5.3: Summary of Base Course Density and Moisture Content Measurements 74
Table 5.4: Summary of Dynamic Cone Penetrometer Measurements 76
Table 6.1: Theoretical Maximum Specific Gravity (RICE) Values 77
Table 6.2: Summary of Shear Test Results on FMLC Specimens 80
Table 6.3: Summary of Air-Void Contents of FMLC Shear Test Specimens 81
Table 6.4: Summary of Fatigue Beam Test Results on FMLC Specimens 85
Table 6.5: Summary of Air-Void Contents of Fatigue Beam Specimens 86
Table 6.6: Summary of Air-Void Contents of Flexural Frequency Sweep Specimens 86
Table 6.7: Summary of Master Curves and Time-Temperature Relationships 92

LIST OF FIGURES

Figure 3.1: Layout of test track and HVS test sections. 10
Figure 3.2: Phase 2 test section layout and thermocouple locations. 11
Figure 3.3: Location of presoaking dam and soak holes. 13
Figure 3.4: Soaking dam and presoaking holes. 13
Figure 3.5: Soaking dam with water. 14
Figure 3.6: Water flow across test section during trafficking. 14
Figure 4.1: Illustration of maximum rut depth and average deformation of a leveled profile. 17
Figure 4.2: Measured rainfall during Phase 2 HVS testing. 19
Figure 4.3: Seepage during presoaking. 19
Figure 4.4: 604FD: Load history. 20
Figure 4.5: 604FD: Daily average outside air temperatures. 21
Figure 4.6: 604FD: Daily average inside air temperatures. 21
Figure 4.7: 604FD: Daily average temperatures at pavement surface and various depths. 22
Figure 4.8: 604FD: Profilometer cross section at various load repetitions. 23
Figure 4.9: 604FD: Average maximum rut. 24
Figure 4.10: 604FD: Average deformation. 24
Figure 4.11: 604FD: Contour plot of permanent surface deformation at start and end of test. 25
Figure 4.12: Location of cores for moisture content determination. 25
Figure 4.13: 604FD: Cores for moisture content determination. 26
Figure 4.14: 604FD: Crystallized salt on edges of wheelpaths during testing. 27
Figure 4.15: 604FD: Cracks in wheelpaths during testing. 27
Figure 4.16: 604FD: Final crack pattern. 27
Figure 4.17: 604FD: Fines pumped from holes drilled for presoaking. 27
Figure 4.18: 604FD: Section photographs at test completion. 28
Figure 4.19: 605FD: Load history. 29
Figure 4.20: 605FD: Daily average outside air temperatures. 30
Figure 4.21: 605FD: Daily average inside air temperatures. 30
Figure 4.22: 605FD: Daily average temperatures at pavement surface and various depths 31
Figure 4.23: 605FD: Profilometer cross section at various load repetitions. 32
Figure 4.24: 605FD: Average maximum rut. 33
Figure 4.25: 605FD: Average deformation. 33
Figure 4.26: 605FD: Contour plot of permanent surface deformation at start and end of test. 34
Figure 4.27: 605FD: Cores for moisture content determination. 34
Figure 4.28: 605FD: Crystallized salt on edges of wheelpaths during early testing. 35
Figure 4.29: 605FD: Cracks in wheelpaths during testing. 35
Figure 4.30: 605FD: Final crack pattern. 35
Figure 4.31: 605FD: Fines pumped from holes drilled for presoaking. 36
Figure 4.32: 605FD: Section photographs at test completion. 36
Figure 4.33: 606FD: Load history. 37
Figure 4.34: 606FD: Daily average outside air temperatures. 38
Figure 4.35: 606FD: Daily average inside air temperatures. 39
Figure 4.36: 606FD: Daily average temperatures at pavement surface and various depths 40
Figure 4.37: 606FD: Profilometer cross section at various load repetitions. 40
Figure 4.38: 606FD: Average maximum rut. 41
Figure 4.39: 606FD: Average deformation. 41
Figure 4.40: 606FD: Contour plot of permanent surface deformation at start and end of test. 42
Figure 4.41: 606FD: Cores for moisture content determination. 43

Figure 4.42: 606FD: Final crack pattern. 44
Figure 4.43: 606FD: Section photographs at test completion. 44
Figure 4.44: 607FD: Load history. 45
Figure 4.45: 607FD: Daily average outside air temperatures. 46
Figure 4.46: 607FD: Daily average inside air temperatures. 46
Figure 4.47: 607FD: Daily average temperatures at pavement surface and various depths. 47
Figure 4.48: 607FD: Profilometer cross section at various load repetitions. 48
Figure 4.49: 607FD: Average maximum rut. 49
Figure 4.50: 607FD: Average deformation. 49
Figure 4.51: 607FD: Contour plot of permanent surface deformation at start and end of test. 50
Figure 4.52: 607FD: Cores for moisture content determination. 50
Figure 4.53: 607FD: Final crack pattern. 51
Figure 4.54: 607FD: Section photographs at test completion. 52
Figure 4.55: Comparison of average maximum rut. 53
Figure 4.56: Comparison of average deformation. 53
Figure 4.57: Afternoon shade from the shed on Sections 604FD and 606FD. 54
Figure 4.58: Comparison of Phase 1 and Phase 2 rutting performance. 55
Figure 5.1: Test pit layout. 59
Figure 5.2: 600FD: Core from Trafficked Area. 60
Figure 5.3: 601FD: Core from Trafficked Area. 60
Figure 5.4: 602FD: Core from Trafficked Area. 60
Figure 5.5: 603FD: Core from Trafficked Area. 60
Figure 5.6: 604FD: Core from Trafficked Area. 61
Figure 5.7: 605FD: Core from Trafficked Area. 61
Figure 5.8: 606FD: Core from Trafficked Area. 61
Figure 5.9: 607FD: Core from Trafficked Area. 61
Figure 5.10: 600FD: Test pit photographs. 66
Figure 5.11: 601FD: Test pit photographs. 67
Figure 5.12: 602FD: Test pit photographs. 68
Figure 5.13: 603FD: Test pit photographs. 69
Figure 5.14: 604FD: Test pit photographs. 70
Figure 5.15: 605FD: Test pit photographs. 71
Figure 5.16: 606FD: Test pit photographs. 72
Figure 5.17: 607FD: Test pit photographs. 73
Figure 6.1: Air-void contents of FMLC shear specimens. 81
Figure 6.2: Summary boxplots of resilient shear modulus. 82
Figure 6.3: Summary boxplots of cycles to 5% permanent shear strain. 83
Figure 6.4: Summary boxplots of cumulative permanent shear strain at 5,000 cycles. 83
Figure 6.5: Cycles to 5% permanent shear strain versus permanent shear strain after 5,000 cycles. 84
Figure 6.6: Air-void contents of fatigue beam specimens (dry and wet). 86
Figure 6.7: Air-void contents of flexural frequency sweep specimens (dry and wet). 87
Figure 6.8: Summary boxplots of initial stiffness. 88
Figure 6.9: Summary boxplots of initial phase angle. 88
Figure 6.10: Initial stiffness versus phase angle for fatigue beam specimens. 89
Figure 6.11: Summary boxplots of fatigue life. 90
Figure 6.12: Flexural complex modulus (E^*) master curves (dry) 93
Figure 6.13: Temperature-shifting relationship (dry) 93
Figure 6.14: Complex modulus (E^*) master curves (wet) 93
Figure 6.15: Temperature-shifting relationship (wet). 93
Figure 6.16: Comparison of dry and wet complex modulus master curves. 94
Figure 6.17: Air-void content comparison between FMFC and FMLC shear specimens. 96

Figure 6.18: Air-void content comparison between FMFC and FMLC fatigue specimens. 96
Figure 6.19: Resilient shear modulus comparison between FMFC and FMLC shear tests. 96
Figure 6.20: Permanent shear strain comparison between FMFC and FMLC shear tests. 96
Figure 6.21: Cycles to 5% permanent shear strain comparison between FMFC and FMLC shear tests. .. 97
Figure 6.22: Initial stiffness comparison between FMFC and FMLC fatigue tests. 97
Figure 6.23: Phase angle comparison between FMFC and FMLC fatigue tests. 97
Figure 6.24: Fatigue life comparison between FMFC and FMLC fatigue tests. 97
Figure 6.25: Comparison of cycles to 5% permanent shear strain after air-void content correction. 98
Figure 6.26: Comparison of fatigue life after air-void content correction. 98
Figure 6.27: Comparison of predicted cycles to 5% permanent shear strain at same air-void content. 98
Figure 6.28: Comparison of predicted fatigue life at same air-void content. 98

LIST OF ABBREVIATIONS

AASHTO	American Association of State Highway and Transport Officials
ASTM	American Society for Testing and Materials
Caltrans	California Department of Transportation
DCP	Dynamic Cone Penetrometer
DGAC	Dense-graded asphalt concrete
ESAL	Equivalent standard axle load
FHWA	Federal Highway Administration
FMFC	Field-mixed, field-compacted
FMLC	Field-mixed, laboratory-compacted
FWD	Falling Weight Deflectometer
HMA	Hot-mix asphalt
HVS	Heavy Vehicle Simulator
LMLC	Laboratory-mixed, laboratory-compacted
MDD	Multi-Depth Deflectometer
MPD	Mean profile depth
PPRC	Partnered Pavement Research Center
RHMA-G	Gap-graded rubberized hot-mix asphalt
RSD	Road Surface Deflectometer
SPE	Strategic Plan Element
TSR	Tensile strength retained
UCPRC	University of California Pavement Research Center
WMA	Warm-mix asphalt

LIST OF TEST METHODS AND SPECIFICATIONS

AASHTO T-275	Standard Method of Test for Bulk Specific Gravity of Compacted Bituminous Mixtures Using Paraffin-Coated Specimens
AASHTO T-320	Standard Method of Test for Determining the Permanent Shear Strain and Stiffness of Asphalt Mixtures using the Superpave Shear Tester
AASHTO T-321	Flexural Controlled-Deformation Fatigue Test
AASHTO T-324	Standard Method of Test for Hamburg Wheel-Track Testing of Compacted Hot-Mix Asphalt (HMA)
CT 371	Method of Test for Resistance of Compacted Bituminous Mixture to Moisture Induced Damage

CONVERSION FACTORS

SI* (MODERN METRIC) CONVERSION FACTORS				
Symbol	**Convert From**	**Convert To**	**Symbol**	**Conversion**
LENGTH				
mm	millimeters	inches	in	mm x 0.039
m	meters	feet	ft	m x 3.28
km	kilometers	mile	mile	km x 1.609
AREA				
mm^2	square millimeters	square inches	in^2	mm^2 x 0.0016
m^2	square meters	square feet	ft^2	m^2 x 10.764
VOLUME				
m^3	cubic meters	cubic feet	ft^3	m^3 x 35.314
kg/m^3	kilograms/cubic meter	pounds/cubic feet	lb/ft^3	kg/m^3 x 0.062
L	liters	gallons	gal	L x 0.264
L/m^2	liters/square meter	gallons/square yard	gal/yd^2	L/m^2 x 0.221
MASS				
kg	kilograms	pounds	lb	kg x 2.202
TEMPERATURE (exact degrees)				
C	Celsius	Fahrenheit	F	°C x 1.8 + 32
FORCE and PRESSURE or STRESS				
N	newtons	poundforce	lbf	N x 0.225
kPa	kilopascals	poundforce/square inch	lbf/in^2	kPa x 0.145

*SI is the symbol for the International System of Units. Appropriate rounding should be made to comply with Section 4 of ASTM E380. (Revised March 2003)

1 INTRODUCTION

1.1 Background

The California Department of Transportation (Caltrans) has expressed interest in warm-mix asphalt with a view to reducing stack emissions at plants, to allow longer haul distances between asphalt plants and construction projects, to improve construction quality (especially during nighttime closures), and to extend the annual period for paving. However, use of warm-mix asphalt technologies require the addition of an additive into the mix, and/or changes in production and construction procedures, specifically related to temperature, which could influence the short- and long-term performance of the pavement. Therefore, research is required to address a range of concerns related to these changes before statewide implementation of the technology is approved.

1.2 Project Objectives

The research presented in this report is part of Partnered Pavement Research Center Strategic Plan Element 4.18 (PPRC SPE 4.18), titled "Warm-Mix Asphalt Study," undertaken for Caltrans by the University of California Pavement Research Center (UCPRC). The objective of this project is to determine whether the use of additives intended to reduce the production and construction temperatures of asphalt concrete influence mix production processes, construction procedures, and the short-, medium-, and/or long-term performance of hot-mix asphalt. The potential benefits of using the additives will also be quantified. This is to be achieved through the following tasks:

1. Develop a detailed work plan *(1)* for Heavy Vehicle Simulator (HVS) and laboratory testing *(Completed in September 2007).*
2. Construct a test track (subgrade preparation, aggregate base-course, tack coat, and asphalt wearing course) at the Graniterock A.R. Wilson quarry near Aromas, California, with four sections as follows *(Completed in September 2007 [2])*:
   i. Conventional dense-graded asphalt concrete (DGAC) mix. This will serve as the control section.
   ii. DGAC warm-mix asphalt with *Advera WMA*® additive (referred to as Advera in this report).
   iii. DGAC warm-mix asphalt with *Evotherm DAT*™ additive (referred to as Evotherm in this report).
   iv. DGAC warm-mix asphalt with *Sasobit*® additive (referred to as Sasobit in this report).
3. Identify and demarcate three HVS test sections on each section *(Completed in September 2007 [2]).*
4. Test each section with the HVS in separate phases (rutting performance, moisture sensitivity performance, fatigue performance), with later phases dependent on the outcome of earlier phases and laboratory tests *(Phase 1 [rutting performance] completed in April 2008 [2] and Phase 2 [moisture sensitivity performance] completed in June 2009 and the subject of this report).*

5. Carry out a series of laboratory tests to assess rutting and fatigue behavior *(Phase 1 [field-mixed, laboratory-compacted specimens] completed in August 2008 [2], Phase 2a [field-mixed, laboratory-compacted specimens] completed in January 2009, and Phase 2b [laboratory-mixed, laboratory-compacted specimens], testing in progress as of this writing).*
6. Prepare a series of reports describing the research *(Phase 1 report submitted in December 2008 [2])*.
7. Prepare recommendations for implementation.

If agreed upon by the stakeholders (Caltrans and warm-mix technology suppliers), the sequence listed above or a subset of the sequence will be repeated for gap-graded rubberized asphalt concrete (RHMA-G), and again for open-graded mixes.

Pilot studies with the technology on in-service pavements will also be supported as part of the study.

1.3 Overall Project Organization

This UCPRC project has been planned as a comprehensive study to be carried out in a series of phases, with later ones dependent on the results of the initial phase. The revised planned testing phases include *(1)*:

- Phase 1 compared early rutting potential at elevated temperatures (pavement temperature of 50°C at 50 mm [122°F at 2.0 in.] pavement depth). HVS trafficking started approximately 30 days after construction. Cores and beams sawn from the sections immediately after construction were subjected to rutting, fatigue, and moisture sensitivity testing in the laboratory. The results from this phase are discussed in a report entitled *Warm-Mix Asphalt Study: Test Track Construction and First-Level Analysis of Phase 1 HVS and Laboratory Testing (2).*
- Phase 2 compared rutting potential at elevated temperatures (pavement temperature of 50°C at 50 mm [122°F at 2.0 in.] pavement depth) and under wet conditions. HVS trafficking started approximately 90 days after completion of the Phase 1 HVS testing was completed. The decision to undertake this phase was based on Phase 1 laboratory test results. Phase 1 laboratory testing did not indicate that the warm-mix asphalt technologies tested would influence fatigue performance and although fatigue testing with the HVS was allowed for in the work plan, it was not carried out.
- Depending on the outcome of the above testing phases and if agreed upon by the stakeholders (Caltrans and warm-mix technology suppliers), the sequence listed above or a subset of the sequence will be repeated for gap-graded rubberized asphalt concrete (RHMA-G) and for open-graded mixes.

This test plan is designed to evaluate short-, medium-, and long-term performance of the mixes.

- Short-term performance is defined as failure by rutting of the asphalt-bound materials.
- Medium-term performance is defined as failure caused by moisture and/or construction-related issues.
- Long-term performance is defined as failure from fatigue cracking, reflective cracking, or rutting of the asphalt-bound and/or unbound pavement layers.

These are some of the questions that will be answered during the various phases of the study *(1)*:

- What is the approximate comparative energy usage between HMA and WMA during mix preparation? This will be determined from asphalt plant records/observations in pilot studies where sufficient tonnages of HMA and WMA are produced to undertake an assessment.
- Can satisfactory compaction be achieved at lower temperatures? This will be established from construction monitoring and subsequent laboratory tests.
- What is the optimal temperature range for achieving compaction requirements? This will be established from construction monitoring and subsequent laboratory tests.
- What are the cost implications? These will be determined with basic cost analyses from pilot studies where sufficient tonnages of HMA and WMA are produced to undertake an assessment.
- Does the use of warm-mix asphalt technologies influence the rutting performance of the mix? This will be determined from Phase 1 HVS and laboratory tests.
- Is the treated mix more susceptible to moisture sensitivity given that the aggregate is heated to lower temperatures? This will be determined from Phase 1 laboratory tests and Phase 2 HVS testing.
- Does the use of warm-mix asphalt technologies influence fatigue performance? This will be determined from Phase 1 and Phase 2 laboratory tests and potential additional laboratory and HVS testing.
- Does the use of warm-mix asphalt technologies influence the performance of the mix in any other way? This will be determined from HVS and laboratory tests (all phases).
- If the experiment is extended to rubberized and open-graded mixes, are the impacts of using the additives in these mixes the same as for conventional mixes?

1.3.1 Deliverables

Deliverables from the study will include:

- A detailed work plan for the entire study *(1)*;
- A report detailing construction, first-level data analysis of the Phase 1 HVS testing, first-level data analysis of the Phase 1 laboratory testing, and preliminary recommendations *(2)*;
- A report detailing first-level data analysis of the Phase 2 HVS testing, first-level data analysis of the Phase 2a laboratory testing, and preliminary recommendations (this report);
- Reports detailing the first-level data analyses of subsequent HVS and laboratory testing phases;
- A detailed second-level analysis report for the entire study if appropriate; and
- A summary report for the entire study.

A series of conference and journal papers documenting various components of the study will also be prepared.

1.4 Structure and Content of this Report

This report presents an overview of the work carried out in Phase 2 to continue meeting the objectives of the study, and is organized as follows:

- Chapter 2 summarizes the findings of the Phase 1 study to provide context to this report.
- Chapter 3 details the HVS test section layout and HVS test criteria.
- Chapter 4 provides a summary of the Phase 2 HVS test data collected from each test.
- Chapter 5 summarizes the observation from a forensic investigation after HVS testing.

- Chapter 6 discusses the Phase 2a laboratory testing on field-mixed, laboratory-compacted (FMLC) specimens compacted at the same time as construction of the HVS test track and compares the results to the Phase 1 field-mixed, field-compacted (FMFC) specimen results.
- Chapter 7 provides conclusions and preliminary recommendations.

1.5 Measurement Units

Although Caltrans has recently returned to the use of U.S. standard measurement units, metric units have always been used by the UCPRC in the design and layout of HVS test tracks, and for laboratory and field measurements and data storage. In this report, metric and English units (provided in parentheses after the metric units) are provided in general discussion. In keeping with convention, only metric units are used in HVS and laboratory data analyses and reporting. A conversion table is provided on Page xviii at the beginning of this report.

1.6 Terminology

The term “asphalt concrete” is used in this report as a general descriptor for the surfacing on the test track. The terms “hot-mix asphalt (HMA)” and “warm-mix asphalt (WMA)” are used as descriptors to differentiate between the two technologies discussed in this study.

2 SUMMARY OF FINDINGS FROM PHASE 1 TESTING

The first phase of a comprehensive study into the use of warm-mix asphalt was completed in 2008 for the California Department of Transportation (Caltrans) by the University of California Pavement Research Center (UCPRC). This phase, based on a work plan *(1)* approved by Caltrans, included the identification of an appropriate site for the experiment, the design and construction of a test track, an accelerated loading test using the Heavy Vehicle Simulator (HVS) to assess rutting behavior, and a series of laboratory tests on specimens sampled from the test track *(2)*. The study compared the performance of a control mix, produced and constructed at conventional hot-mix asphalt temperatures, with three warm-mixes, produced and compacted at approximately 35°C (60°F) lower than the control. The additives tested were *Advera WMA*®, *Evotherm DAT*™, and *Sasobit*®.

The test track is located at the Graniterock Company's A.R. Wilson Quarry and Asphalt Plant near Aromas, California. The design and construction of the test track was a cooperative effort between Caltrans, the UCPRC, Graniterock, and the three warm-mix technology suppliers. The test track was constructed in September 2007, using asphalt from the commercial asphalt mix plant at the quarry. The track is 80 m by 8.0 m (262 ft by 26 ft) divided into four test sections (Control, Advera, Evotherm, and Sasobit). The pavement structure consists of the existing subgrade/subbase material overlying bedrock, with 300 mm (12 in.) of imported aggregate base, and two 60 mm (2.4 in.) lifts of asphalt concrete. A standard mix design was used and no adjustments were made to accommodate the additives. Target production temperatures were set at 155°C (310°F) for the Control mix and 120°C (250°F) for the warm-mixes. Specimens were removed from the test track for laboratory testing.

The first phase of Heavy Vehicle Simulator (HVS) testing commenced in October 2007 after a six-week curing period and was completed in April 2008. This testing compared early rutting performance at elevated temperatures (pavement temperature of 50°C at 50 mm [122°F at 2.0 in.]), using a 40 kN (9,000 lb) load on a standard dual-wheel configuration and a unidirectional trafficking mode. Laboratory testing commenced in December 2007 and was completed in July 2008. The test program included shear testing, wet and dry fatigue testing, Hamburg Wheel-Track testing, and determination of the wet-to-dry tensile strength ratio.

Key findings from the Phase 1 study include:

- A Hveem mix design that met Caltrans requirements for Type A 19 mm maximum dense-graded asphalt concrete was used in the study. The target gradation met Caltrans requirements for both the

Coarse and Medium gradations. The recommended bitumen content was 5.1 to 5.4 percent by mass of aggregate, which was based on the minimum air-void content under standard kneading compaction. The mix design had very high Hveem stabilities.

- A consistent base-course was constructed on the test track using material produced at the nearby quarry. Some overwatering occurred in the early stages of construction resulting in some moist areas in the pavement, which influenced measured densities and deflections. These areas are unlikely to effect later performance of the test track. The very stiff base is likely to complicate any planned fatigue cracking experiments in that a very high number of HVS repetitions will likely be required before any distress occurs.
- Minimal asphalt plant modifications were required to accommodate the warm-mix additives.
- No problems were noted with producing the asphalt mixes at the lower temperatures. The target mix production temperatures (i.e., 155°C and 120°C [310°F and 250°F]) were achieved.
- Although a PG 64-16 asphalt binder was specified in the work plan, subsequent tests by the Federal Highway Administration indicated that the binder was rated as PG 64-22. This should not have affected the outcome of the experiment.
- The Control, Advera, and Evotherm mixes met the project mix design requirements. The binder content of the Sasobit was 0.72 percent below the target binder content and 0.62 percent below the lowest permissible binder content. This probably influenced performance and was taken into consideration when interpreting the HVS and laboratory test results presented in this report.
- Graniterock Company did not perform Hveem compaction or stability tests for quality control purposes as there is no protocol for adjusting the standard kneading compaction temperature for mixes with warm-mix additives. Instead, Marshall and Superpave Gyratory compaction were performed in the Graniterock laboratory next to the asphalt plant on mix taken from the silo.
- Laboratory quality control tests on the Control mix (specimens compacted with Marshall and Superpave Gyratory compaction) showed it to have a higher specific gravity and lower air-void content, compared to the mixes with additives. It is not clear whether this was a testing inconsistency or was linked to the lower production and specimen preparation temperatures. This will need to be investigated during Phase 2b laboratory investigations.
- Moisture contents of the mixes with additives were notably higher than in the Control mix, indicating that potentially less moisture will evaporate from the aggregate at lower production temperatures. All mixes were, however, well within the minimum Caltrans-specified moisture content level. Aggregate moisture contents will need to be monitored in the stockpiles and production times adjusted accordingly to ensure that specified end-of-production moisture contents are met when using warm-mix technologies.
- Construction procedures and final pavement quality did not appear to be influenced by the lower construction temperatures. The Advera mix showed no evidence of tenderness, and acceptable compaction was achieved. Some tenderness was noted on the Evotherm and Sasobit sections resulting in shearing under the rollers at various stages of breakdown and/or rubber-tired rolling, indicating that the compaction temperatures were still higher than optimal. No problems were observed after final rolling at lower temperatures.
- Interviews with the paving crew after construction revealed that no problems were experienced with construction at the lower temperatures. Improved working conditions were identified as an advantage. Tenderness on the Evotherm and Sasobit sections was not considered to be significantly different from that experienced with conventional mixes during normal construction activities.
- Although temperatures at the beginning of compaction on the warm-mix sections were considerably lower than the Caltrans-specified limits, the temperatures recorded on completion of compaction were within limits, indicating that the rate of temperature loss in the mixes with additives was lower than that on the Control mix, as expected.
- Some haze/smoke was evident on the Control mix during transfer of the mix from the truck to the paver. No haze or smoke was observed on the mixes with additives.

- Average air-void contents of the Control and Advera sections were 5.6 percent and 5.4 percent respectively. Those on the Evotherm and Sasobit sections, which showed signs of tenderness during rolling, were approximately 7.0 percent, with the caveat that the Sasobit mix binder content was lower than the target while that for the Evotherm sections was not. Based on these observations, it was concluded that adequate compaction can be achieved on warm-mixes at the lower temperatures. Optimal compaction temperatures are likely to differ between the different warm-mix technologies.
- Skid resistance measurements indicated that the warm-mix additives tested do not influence the skid resistance of an asphalt mix.
- HVS trafficking on each of the four sections revealed that the duration of the embedment phases (high early-rutting phase of typical two-phase rutting processes) on the Advera and Evotherm sections were similar to the Control. However, the rut depths at the end of the embedment phases on these two sections was slightly higher than the Control, which was attributed to less oxidation of the binder during mix production at lower temperatures. Rutting behavior on the warm-mix sections followed similar trends to the Control after the embedment phase. The performance of the Sasobit section could not be directly compared with the other three sections given that the binder content of the mix was significantly lower.
- Laboratory test results indicate that use of the warm-mix technologies assessed in this study does not significantly influence the performance of the asphalt concrete when compared to control specimens produced and compacted at conventional hot-mix asphalt temperatures. However, moisture sensitivity testing indicated that all the mixes tested were potentially susceptible to moisture damage. There was, however, no difference in the level of moisture sensitivity between the Control mix and mixes with warm-mix additives.

The Phase 1 HVS and laboratory testing provided no results to suggest that the warm-mix technologies assessed in this study should not be used in California. Final recommendations on the use of these and other warm-mix technologies will only be made after further research and monitoring of full-scale pilot studies on in-service pavements is completed. Interim recommendations from the Phase 1 study include the following:

- The use of warm-mix technologies should continue in full-scale pilot studies on in-service pavements.
- Although laboratory testing indicated that the warm-mix technologies assessed in this study did not increase the moisture sensitivity of the mix, HVS testing to assess moisture sensitivity should continue as recommended in the work plan to confirm these findings. Subsequent laboratory testing of moisture sensitivity should assess a range of different aggregates given that all of the mixes tested in this study where considered to be moisture sensitive.
- Phase 2 laboratory testing on field-mixed, laboratory-compacted specimens should proceed to determine whether representative mixes can be produced in the laboratory and to determine how and whether laboratory test results on these specimens differ from those on field-mixed, field-compacted specimens.
- As part of the Phase 2 laboratory study, protocols need to be developed for adjusting laboratory specimen-preparation compaction temperatures for mixes with warm-mix additives. It is unlikely that any national studies will develop these protocols for Hveem mix designs, which are still used in California.

3 TEST TRACK LAYOUT AND HVS TEST CRITERIA

3.1 Protocols

Heavy Vehicle Simulator (HVS) test section layout, test setup, trafficking, and measurements followed standard University of California Pavement Research Center (UCPRC) protocols *(3)*.

3.2 Test Track Layout

The Warm-Mix Asphalt Study test track layout is shown in Figure 3.1. Four HVS Test Sections were demarcated for the second phase of HVS testing for moisture sensitivity performance assessment. The section numbers allocated were as follows:

- Section 604FD: Control
- Section 605FD: Advera
- Section 606FD: Evotherm
- Section 607FD: Sasobit

3.3 HVS Test Section Layout

The general test section layout for each of the rutting sections is shown in Figure 3.2. Station numbers (0 to 16) refer to fixed points on the test section and are used for measurements and as a reference for discussing performance.

3.4 Pavement Instrumentation and Monitoring Methods

Measurements were taken with the instruments listed below. Instrument positions are shown in Figure 3.2. Detailed descriptions of the instrumentation and measuring equipment are included in Reference 3. Intervals between measurements, in terms of load repetitions, were selected to enable adequate characterization of the pavement as damage developed.

- Laser profilometer, measuring surface profile. Measurements are taken at each station.
- Thermocouples, measuring pavement temperature (at Stations 4 and 12) and ambient temperature at one-hour intervals during HVS operation.

Air temperatures were measured at a weather station approximately 150 m (500 ft) from the test section and recorded at the same intervals as the thermocouples.

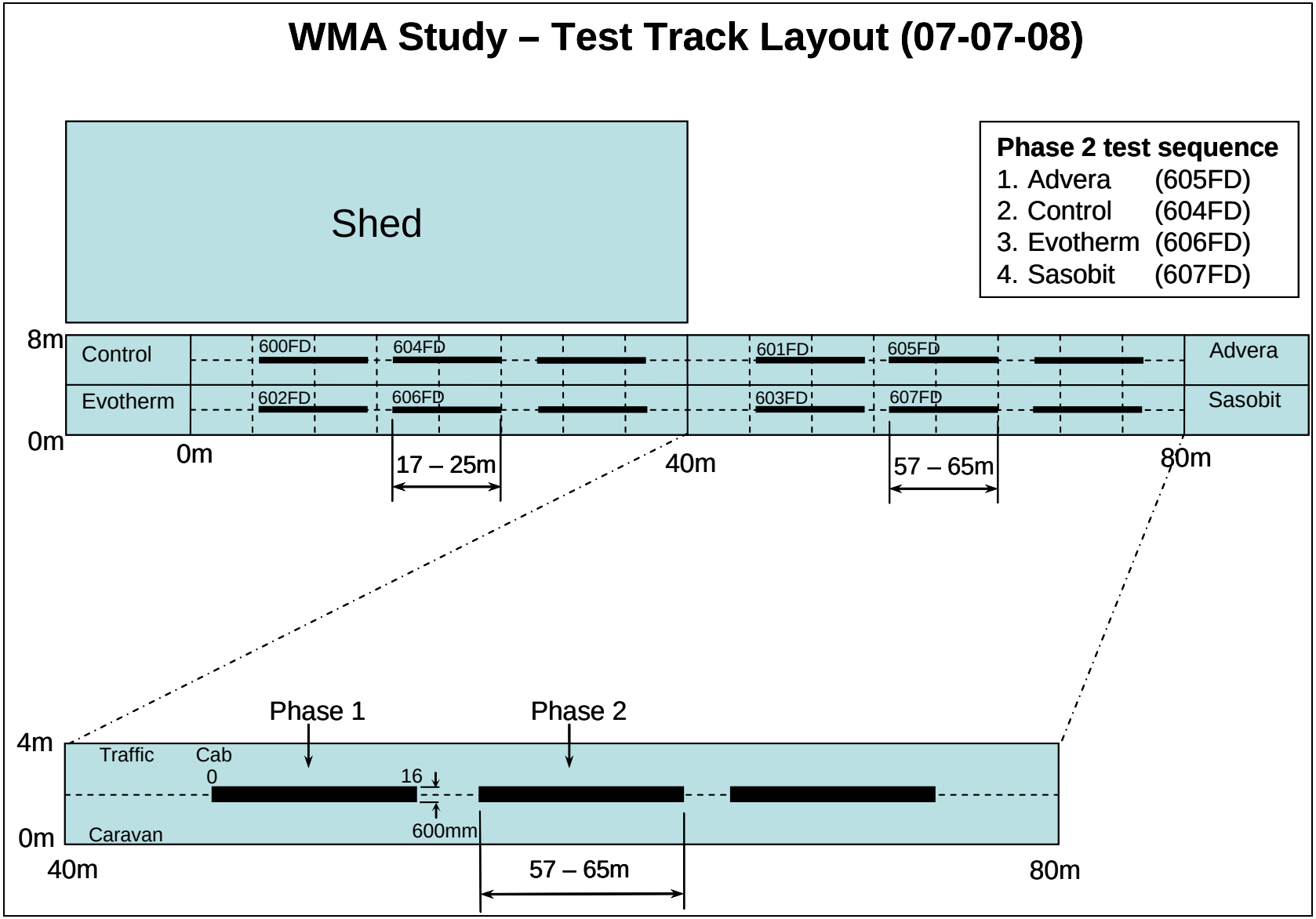

Figure 3.1: Layout of test track and HVS test sections.

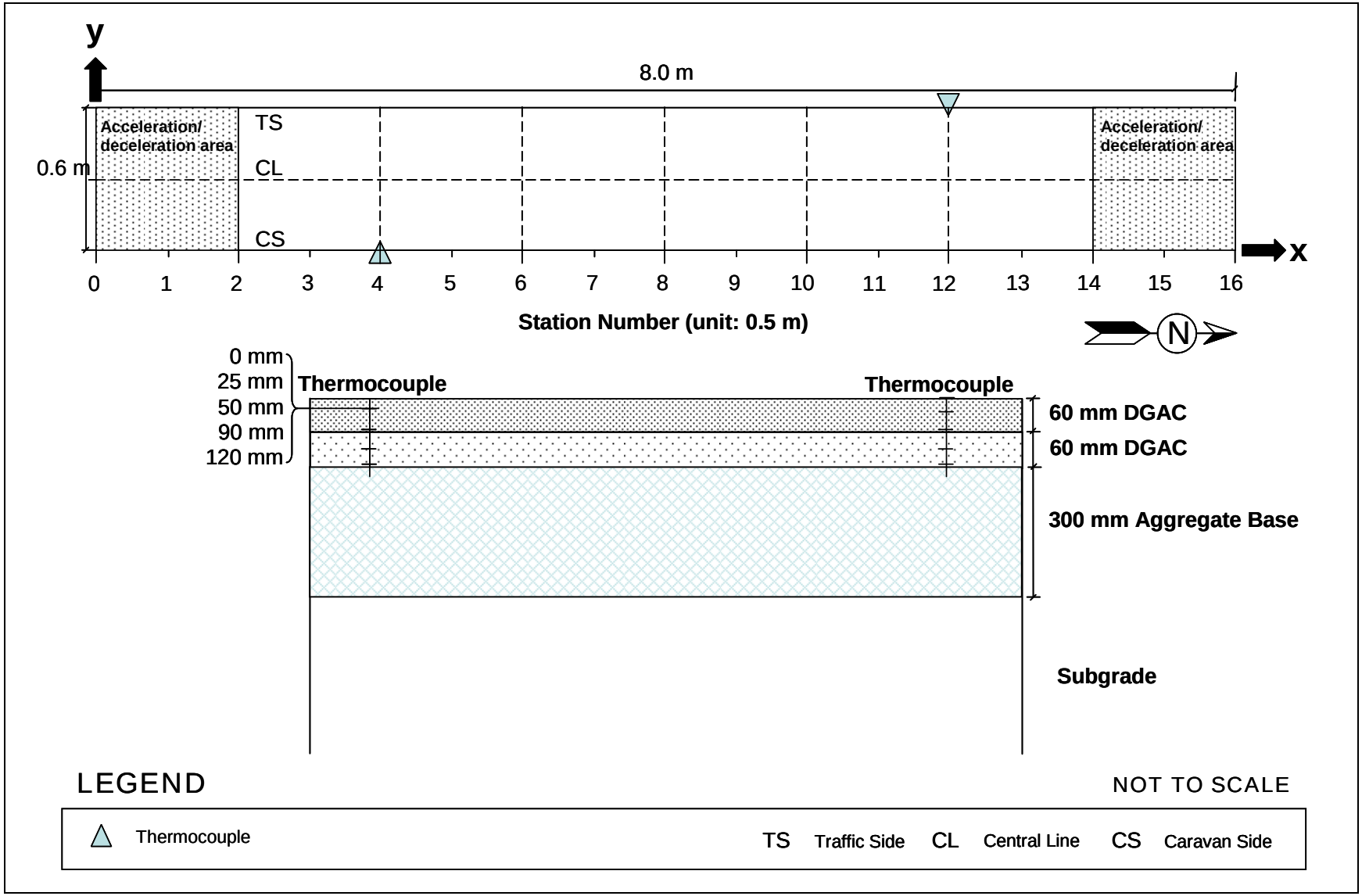

Figure 3.2: Phase 2 test section layout and thermocouple locations.

Surface and in-depth deflections were not measured. Surface deflection cannot be measured with the Road Surface Deflectometer (RSD) on rutted pavements. In-depth deflection measured with Multi-Depth Deflectometers (MDD) was not possible due to difficulties with installing and anchoring the instruments in the bedrock.

3.5 HVS Test Criteria

The HVS test criteria for Phase 2 were essentially the same as those for Phase 1 *(2)*, except that each section was subjected to a 14-day presoaking with water prior to HVS trafficking, and a constant flow of water across each section was maintained throughout HVS trafficking (see Section 3.5.2).

3.5.1 Test Section Failure Criteria

An average maximum rut of 12.5 mm (0.5 in.) over the full monitored section (Station 3 to Station 13) and/or severe stripping of the surface aggregate were set as the failure criteria for the experiment.

3.5.2 Environmental Conditions

Presoaking with Water

Given that the demarcated test sections had not been subjected to any traffic and that the asphalt concrete was relatively new, each section was soaked with water for a period of 14 days prior to HVS testing, thereby accelerating the onset of any potential moisture damage. A row of holes was drilled to the bottom of the top lift of asphalt concrete on one side of each test section to facilitate water ingress. The holes were 25 mm (1.0 in.) in diameter, 250 mm (10 in.) from the edge of the HVS test section, and 250 mm (10 in.) apart. A wooden dam, 150 mm (6.0 in.) high and 300 mm (12 in.) from the edge of the test section, was then glued to the pavement with silicone to provide a head of water. The dam was kept full of water for the duration of the soaking period.

The presoaking dam and location of the soak holes are illustrated in Figure 3.3 through Figure 3.5.

Pavement Temperature

The pavement temperature at 50 mm (2.0 in.) was maintained at 50°C±4°C (122°F±7°F) to assess rutting potential under typical pavement conditions in a similar manner to the Phase 1 testing. Infrared heaters inside a temperature control chamber were used to maintain the pavement temperature.

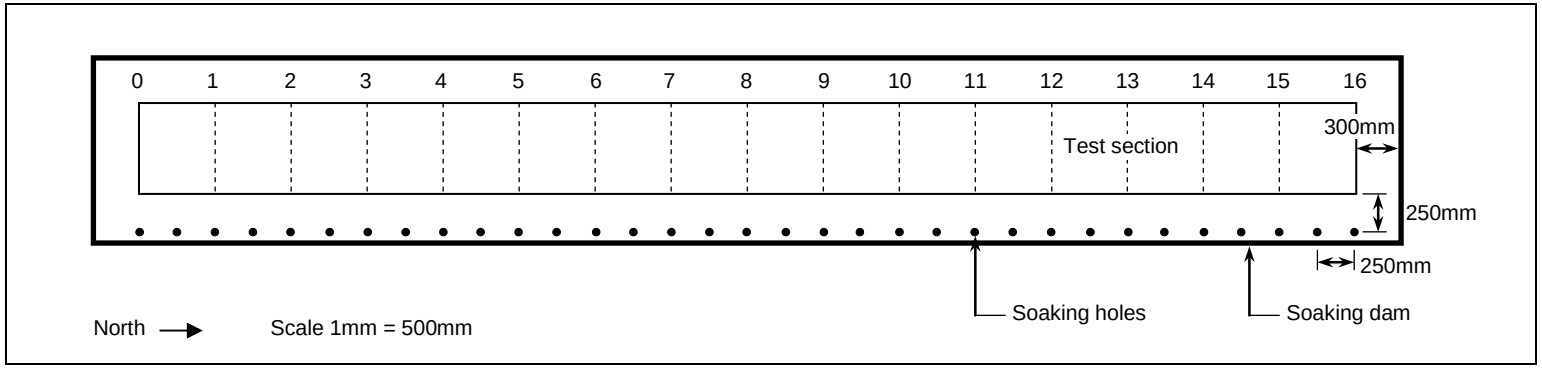

Figure 3.3: Location of presoaking dam and soak holes.

Figure 3.4: Soaking dam and presoaking holes.

Figure 3.5: Soaking dam with water.

Surface Water

A flow of surface water across the test sections during HVS trafficking was necessary to identify whether the warm-mix asphalt sections were more sensitive to moisture-related damage (stripping, raveling, and/or rutting) than the Control section. The study focused on rut damage related to moisture retained in the aggregate as a result of lower production temperatures, which would typically materialize as load-related stripping throughout the layer, as opposed to stripping and raveling of the surface aggregate caused by scour from tires on the wet surface. Soaking regimes and surface water flows for this study were determined from a short HVS experiment on a section demarcated between Section 600FD and Section 602FD from the Phase 1 study. Based on observations from this experiment, all Phase 2 HVS testing was carried out with a constant flow of approximately 1.5 liters (0.4 gallons) of water per hour across the section. The water was preheated to 50°C±4°C (122°F±7°F) to prevent cooling of the pavement surface. The test conditions are shown in Figure 3.6.

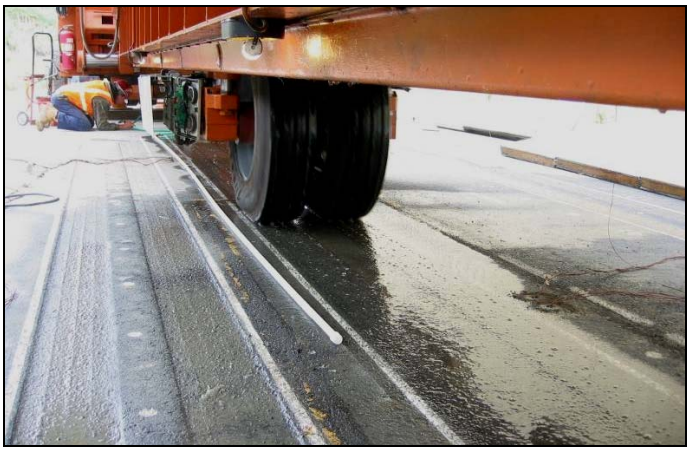

Figure 3.6: Water flow across test section during trafficking.

3.5.3 Test Duration

HVS trafficking on each section was initiated and completed as shown in Table 3.1.

Table 3.1: Test Duration for Phase 2 HVS Moisture Sensitivity Tests

Section	Overlay	Start Date	Finish Date	Repetitions
604FD	Control	12/11/2008	02/19/2009	371,000
605FD	Advera	08/14/2008	11/24/2008	620,500
606FD	Evotherm	03/07/2009	04/24/2009	352,000
607FD	Sasobit	04/05/2009	06/18/2009	464,500

3.5.4 Loading Program

The HVS loading program for each section is summarized in Table 3.2. The point at which load changes were made depended on HVS operation schedules and differed slightly among the test sections. Equivalent Standard Axle Loads (ESALs) were determined using the following Caltrans conversion (Equation 3.1):

$$ESALS = (\text{axle load}/18000)^{4.2} \quad \textbf{(3.1)}$$

Table 3.2: Summary of Phase 2 HVS Loading Program

Section	Overlay	Wheel Load[1] (kN)	Repetitions	ESALs[2]
604FD	Control	40	185,000	185,000
		60	80,000	439,200
		90	106,000	3,195,000
		Total	371,000	3,819,200
605FD	Advera[3]	40	157,000	157,000
		60	32,000	175,700
		90	431,500	13,006,100
		Total	620,500	13,338,800
606FD	Evotherm	40	166,000	166,000
		60	118,000	647,800
		90	68,000	2,049,600
		Total	352,000	2,863,400
607FD	Sasobit[3]	40	152,000	152,000
		60	137,000	752,000
		90	175,500	5,289,900
		Total	464,500	6,194,000
		Total	**1,807,500**	**26,200,400**

[1] 40 kN = 9,000 lb. 60 kN = 13,500 lb. 90 kN = 20,250 lb.
[2] ESAL: Equivalent Standard Axle Load
[3] Testing terminated before rut depth of 12.5 mm was reached.

All trafficking was carried out with a dual-wheel configuration, using radial truck tires (Goodyear G159 - 11R22.5- steel-belted radial) inflated to a pressure of 720 kPa (104 psi), in a channelized, unidirectional loading mode.

Wheel loads were checked with a portable weigh-in-motion pad at the beginning of each test and after each load change.

4 PHASE 2 HVS TEST DATA SUMMARY

4.1 Introduction

This chapter provides a summary of the data collected from the four HVS tests (Sections 604FD through 607FD) and a brief discussion of the first-level analysis. Data collected includes rainfall, air temperatures inside and outside the temperature control chamber, pavement temperatures, and surface permanent deformation. Each section was visually assessed every day for any indication of moisture-related damage.

Pavement temperatures were controlled using the temperature control chamber. Both air (inside and outside the temperature box) and pavement temperatures were monitored and recorded hourly during the entire loading period. Permanent deformation at the pavement surface (rutting) was monitored with the Laser Profilometer. In-depth permanent deformation at various depths within the pavement was not monitored due to the presence of bedrock and associated difficulties with the installation of Multi-Depth Deflectometers (MDDs). The following rut parameters were determined from these measurements:

- Average maximum rut depth (Figure 4.1),
- Average deformation (Figure 4.1),
- Location and magnitude of the maximum rut depth, and
- Rate of rut development.

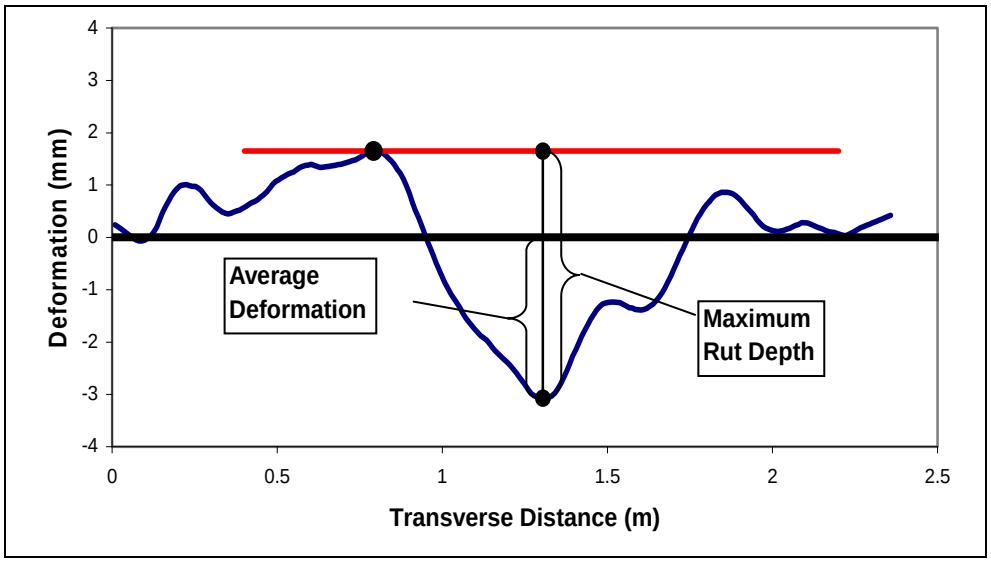

Figure 4.1: Illustration of maximum rut depth and average deformation of a leveled profile.

The Laser Profilometer provides sufficient information to evaluate the evolution of permanent surface deformation of the entire test section at various loading stages. The rut depth figures in this report show

the average values over the entire section (Stations 3 through 13) as well as values for half sections between Stations 3 and 8 and Stations 9 and 13. These two additional data series were plotted to identify any differences along the length of the section. The precise nature of the permanent deformation was identified during a forensic investigation (cores and test pits) undertaken after completion of all HVS testing and is discussed in Chapter 5.

The data from each HVS test is presented separately in Sections 4.3 through 4.6, with the presentation of each test following the same format. Data plots are presented on the same scale to facilitate comparisons of performance. Interpretation of the data in terms of pavement performance will be discussed in a separate second-level analysis report once all HVS and laboratory testing has been completed.

4.2 Rainfall

Figure 4.2 shows the monthly rainfall data from July 2008 through July 2009 as measured at the weather station close to the test track. Rainfall was measured during all four Phase 2 HVS tests (Table 4.1), although considerably more rainfall was recorded during testing on the Control section compared to the other three sections. It is unlikely that the rainfall events that occurred during Phase 2 HVS testing had any influence on the performance of the test sections.

Table 4.1: Rainfall Summary for Phase 2 HVS Testing

Section	Overlay	Rain days	Total (mm [in.])	Highest 24 Hour (mm [in.])
604FD	Control	32	212.4 (8.36)	24.9 (0.98)
605FD	Advera	9	25.9 (1.02)	10.7 (0.42)
606FD	Evotherm	6	22.9 (0.90)	11.5 (0.45)
607FD	Sasobit	9	12.4 (0.49)	7.6 (0.30)

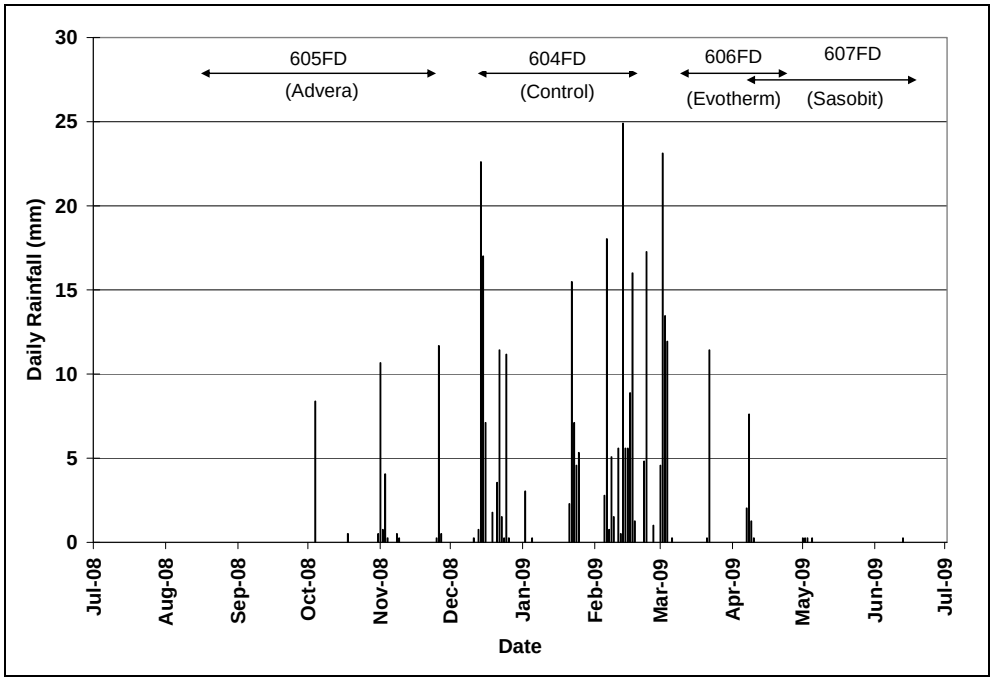

Figure 4.2: Measured rainfall during Phase 2 HVS testing.

4.3 Section 604FD: Control

4.3.1 Test Summary

During presoaking of the section some seepage through the pavement (patched area from earlier sampling after construction of the test track) was observed adjacent to the test section (Figure 4.3) implying that water was possibly seeping between the top and bottom lifts of asphalt.

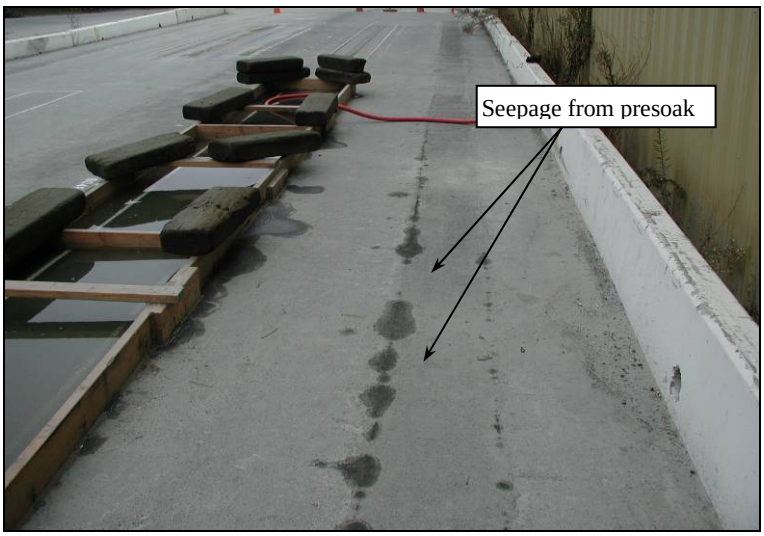

Figure 4.3: Seepage during presoaking.

Loading commenced on December 11, 2008, and ended on February 19, 2009. A total of 371,000 load repetitions were applied and 64 datasets were collected. Testing was interrupted on three occasions during equipment breakdowns. The HVS loading history for Section 604FD is shown in Figure 4.4.

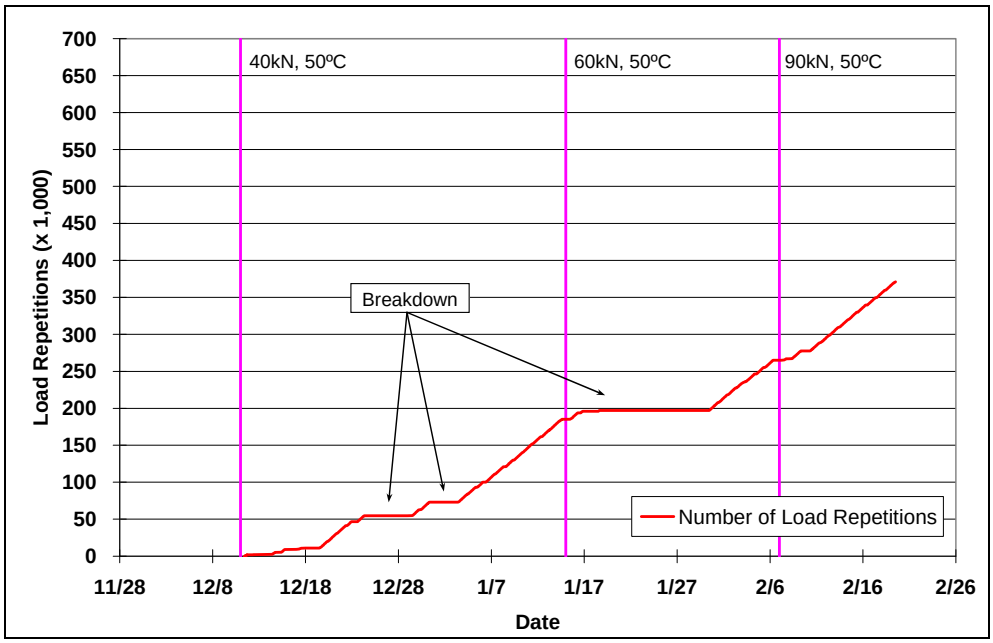

Figure 4.4: 604FD: Load history.

4.3.2 Outside Air Temperatures

Outside air temperatures while the HVS was running are summarized in Figure 4.5. Vertical error bars on each point on the graph show the daily temperature range. Temperatures ranged from -0.4°C to 24.8°C (31°F to 77°F) during the course of HVS testing, with a daily average of 9.4°C (49°F), an average minimum of 5.0°C (41°F), and an average maximum of 15.6°C (60°F). Maximum temperatures varied considerably during the test (between 6.8°C and 24°C [44°F and 77°F]).

4.3.3 Air and Water Temperatures in the Temperature Control Unit

During the test, air temperatures inside the temperature control chamber ranged from 21°C to 49°C (70°F to 120°F) with an average of 37°C (99°F) and standard deviation of 2.7°C (5°F). Air temperature was adjusted as required throughout the test to maintain a pavement temperature as close as possible to 50°C±4°C (122°F±7°F), which is expected to promote rutting damage. Air temperatures were not maintained during breakdowns. The daily average air temperatures recorded in the temperature control unit, calculated from the hourly temperatures recorded during HVS operation, are shown in Figure 4.6. Vertical errors bars on each point on the graph show daily temperature range.

The surface water temperature was maintained at 50°C±4°C (122°F±7°F) to prevent cooling of the pavement.

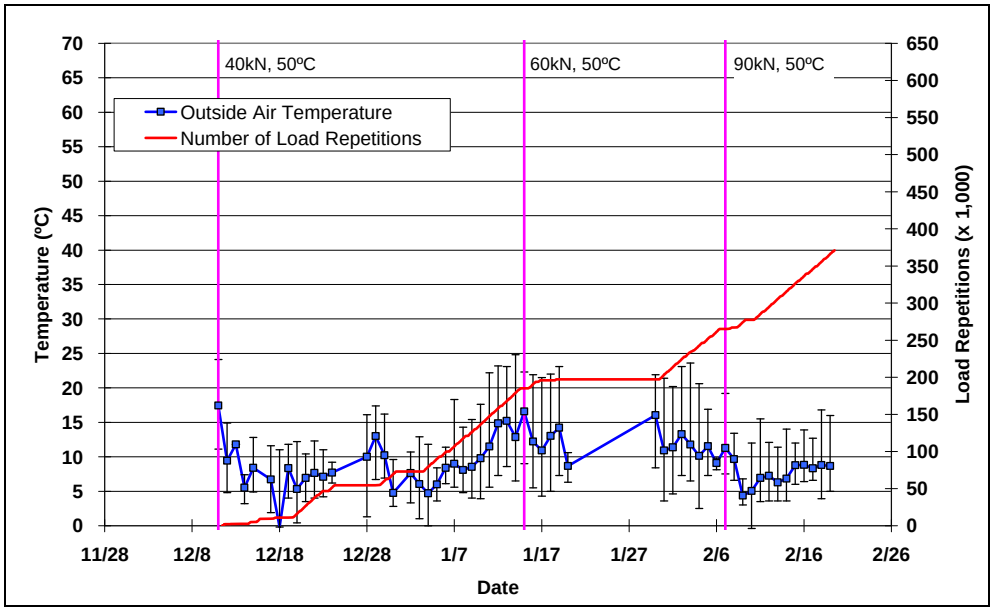

Figure 4.5: 604FD: Daily average outside air temperatures.

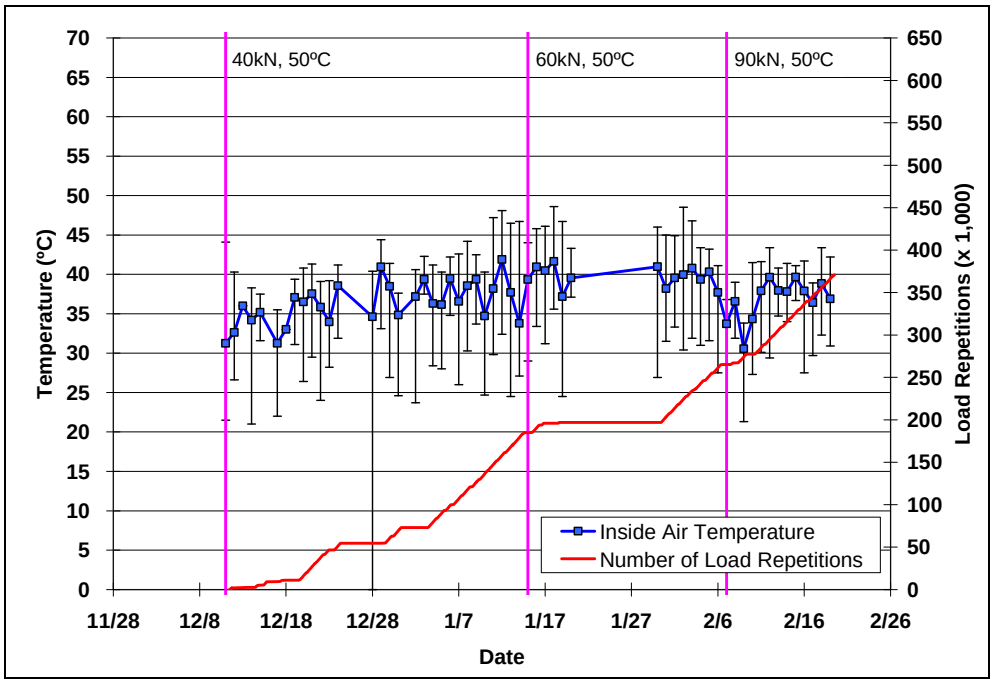

Figure 4.6: 604FD: Daily average inside air temperatures.

4.3.4 Temperatures in the Asphalt Concrete Layers

Daily averages of the surface and in-depth temperatures of the asphalt concrete layers are listed in Table 4.2 and shown in Figure 4.7. The target temperature of 50°C±4°C (122°F±7°F) could not be maintained due to the cold outside air and cold surrounding pavement temperatures. Pavement temperatures decreased slightly with increasing depth in the pavement, which was expected as there is usually a thermal gradient between the top and bottom of the asphalt concrete pavement layers.

Table 4.2: 604FD: Temperature Summary for Air and Pavement

Temperature	Average (°C)	Std Dev (°C)	Average (°F)	Std Dev (°F)
Pavement surface	42.6	4.9	108.7	8.8
- 25 mm below surface	39.9	4.9	103.8	8.8
- 50 mm below surface	39.2	5.1	102.6	9.2
- 90 mm below surface	37.9	5.0	100.2	9.0
- 120 mm below surface	36.4	5.1	97.5	9.2
Outside air	9.4	3.4	48.9	6.1
Inside air	37.3	2.7	99.1	4.9

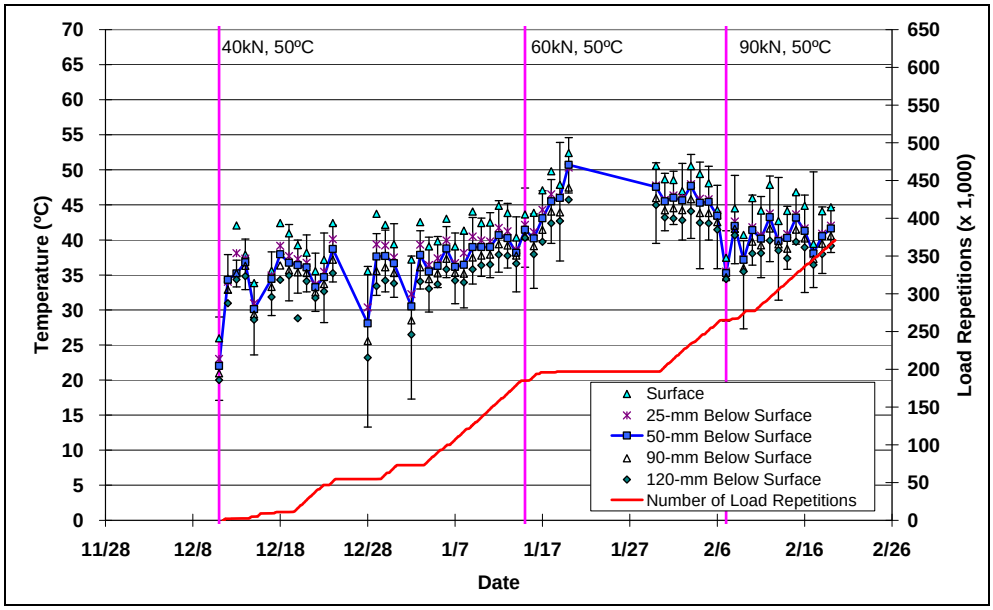

Figure 4.7: 604FD: Daily average temperatures at pavement surface and various depths.

4.3.5 Permanent Surface Deformation (Rutting)

Figure 4.8 shows the average transverse cross section measured with the Laser Profilometer at various stages of the test. This plot clearly shows the increase in rutting and deformation over the duration of the test. The average height of displaced material (i.e., above the pavement surface) was less than 5.0 mm (0.2 in.), while the depth of deformation (i.e., below the pavement surface) was about 10 mm (0.4 in.).

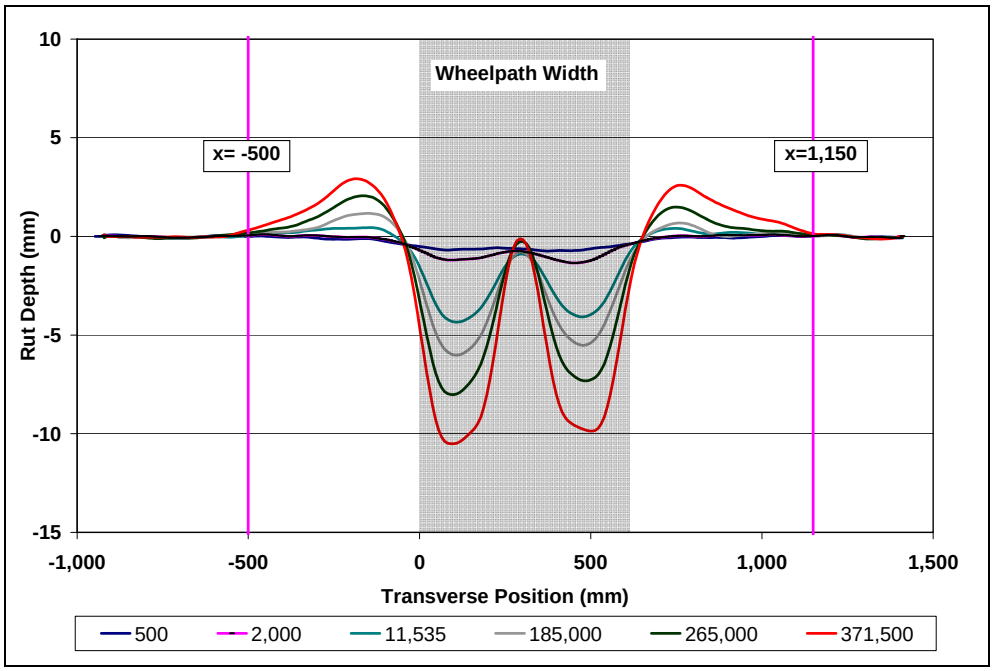

Figure 4.8: 604FD: Profilometer cross section at various load repetitions.

During HVS testing, rutting usually occurs at a high initial rate, and then it typically diminishes as trafficking progresses until reaching a steady state. This initial phase is referred to as the "embedment" phase. Figure 4.9 and Figure 4.10 show the development of permanent deformation (average maximum rut and average deformation, respectively) with load repetitions as measured with the Laser Profilometer for the test section. Data for the Phase 1 Control section are included for comparison. Embedment phases are apparent at the beginning of the experiment (i.e., first 25,000 repetitions) and at the two load changes. The initial embedment in terms of average maximum rut recorded during Phase 2 testing was less than that recorded during Phase 1 (approximately 2.0 mm [0.08 in.] less). However, embedment in terms of average deformation was slightly higher during Phase 2 than in Phase 1 (approximately 1.5 mm [0.06 in.] less) indicating less displacement on the surface in the later testing. The rate of rut progression during Phase 2 was also considerably slower compared to the rate during Phase 1 testing, despite presoaking and the addition of water during the test. The change in embedment and slower rutting rate were attributed to oxidation and consequent stiffening of the binder in the period between the two tests. The addition of water during the test did not appear to influence the performance of the pavement.

Error bars on the average readings indicate that there was little variation in rutting along the length of the section.

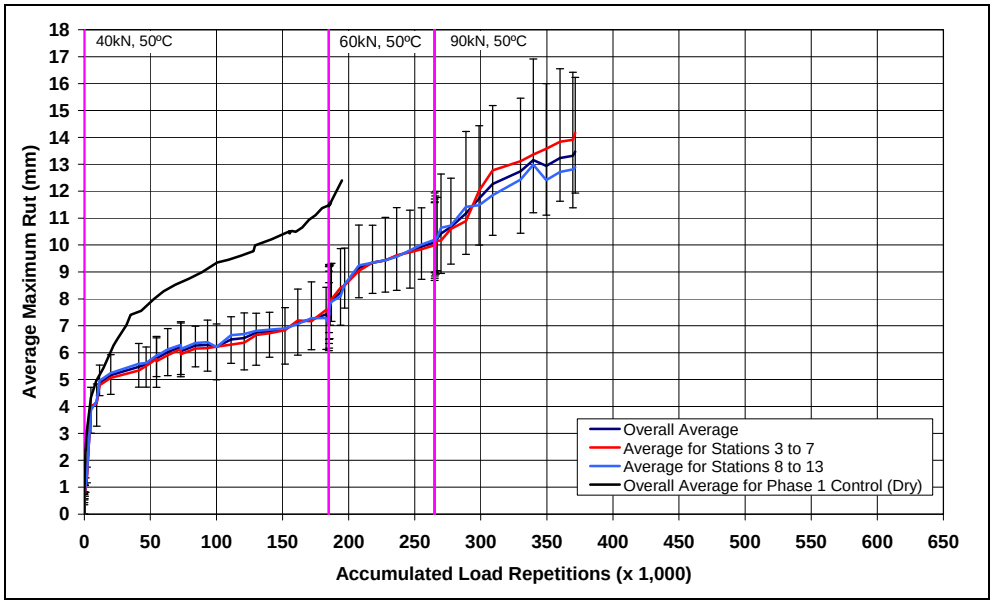

Figure 4.9: 604FD: Average maximum rut.

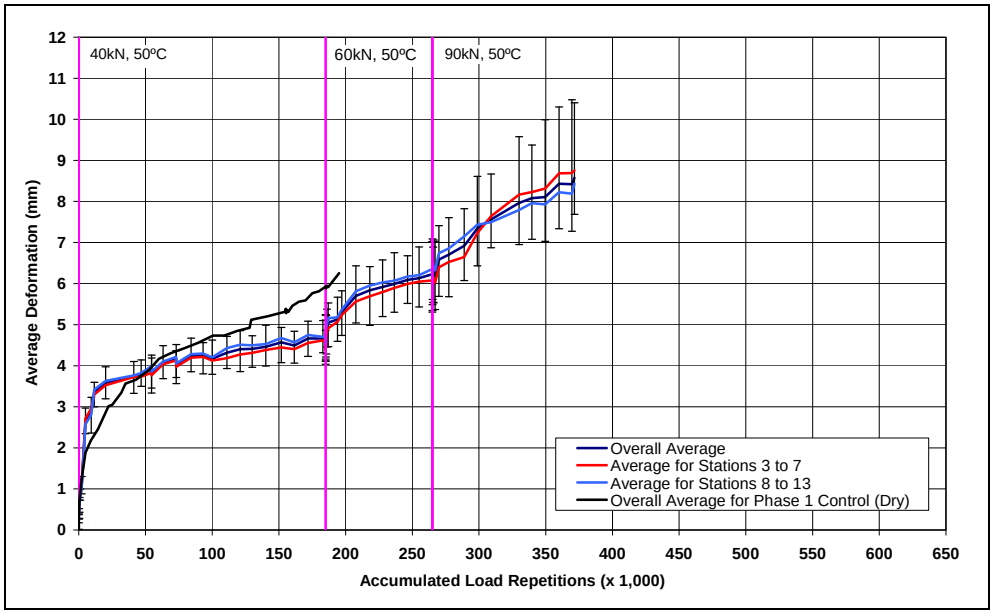

Figure 4.10: 604FD: Average deformation.

Figure 4.11 shows a contour plot of the pavement surface at the beginning (after 500 repetitions) and at the end of the test (371,000 repetitions), also indicating minimal variation along the section. After completion of trafficking, the average maximum rut depth and the average deformation were 13.5 mm (0.5 in.) and 8.6 mm (0.33 in.), respectively. The maximum rut depth measured on the section was 16.2 mm (0.64 in.), recorded at Station 6.

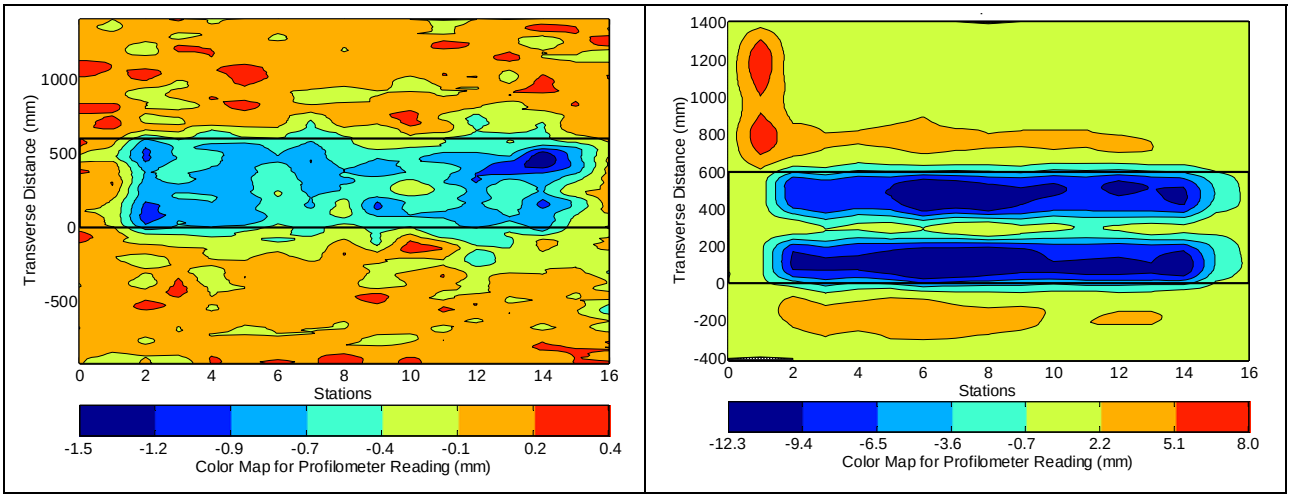

Figure 4.11: 604FD: Contour plot of permanent surface deformation at start and end of test.
(Note that scales are different.)

4.3.6 Asphalt Concrete Moisture Content

Moisture contents in the asphalt concrete were determined from 152 mm (6.0 in.) diameter cores removed immediately after testing from the centerline of the test section and from a line 1.0 m (3.3 ft) from the outside edge of the test section at Stations 4, 8 and 12 (Figure 4.12). The cores removed from within the test section were all separated at the bond between the two lifts. No debonding was noted on the cores removed from outside the test section. Photographs of the cores are shown in Figure 4.13.

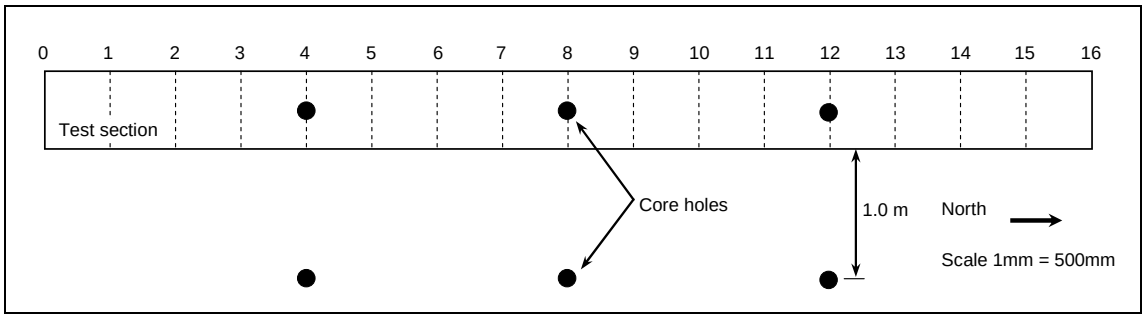

Figure 4.12: Location of cores for moisture content determination.

The results are summarized in Table 4.3 and indicate that some moisture (between 0.5 and 1.0 percent) infiltrated the surface of the test section during the course of the test.

Table 4.3: 604FD: Moisture Content after Testing

Station	Moisture Content (%)		
	Inside Test Section	Outside Test Section	Difference
4	0.82	0.35	0.47
8	1.21	0.35	0.86
12	1.40	0.35	1.05

Figure 4.13: 604FD: Cores for moisture content determination.

4.3.7 Visual Inspection

The test section was visually inspected during each data collection exercise. A more thorough examination of the test section was made after the HVS was removed at the end of the test. A forensic investigation of the section was undertaken on completion of all Phase 2 testing and is discussed in Chapter 5. A number of observations were made in the assessments during and after the test:

- Salts in the water flowing across the section crystallized along the edges of the wheelpaths soon after the start of the test and continued to accumulate throughout the test (Figure 4.14).
- Transverse cracks started to appear after about 200,000 load repetitions (i.e. after the 60 kN load change) (Figure 4.15). The final crack density was 4.98 m/m^2 (1.5 ft/ft^2) with a higher crack density between Stations 6 and 14 and relatively little cracking between Stations 2 and 6. Although most cracking was concentrated in the wheelpaths, some transverse cracking was noted between the wheelpaths. Longitudinal cracks were observed in the untrafficked area immediately adjacent to the outside edges of wheelpaths. The final crack pattern is illustrated in Figure 4.16.
- No pumping of fines was observed from the cracks, but some pumping was observed from the holes drilled for the presoak (Figure 4.17).
- The rutting pattern after completion of the test was typical of HVS rutting tests (Figure 4.18).
- Although some "wear" (attributed to the channelized traffic and constant water flow) was noted on the surface (Figure 4.18), no aggregate stripping, ravelling or other evidence of moisture damage was noted during or after the test.

Figure 4.14: 604FD: Crystallized salt on edges of wheelpaths during testing.

Figure 4.15: 604FD: Cracks in wheelpaths during testing.

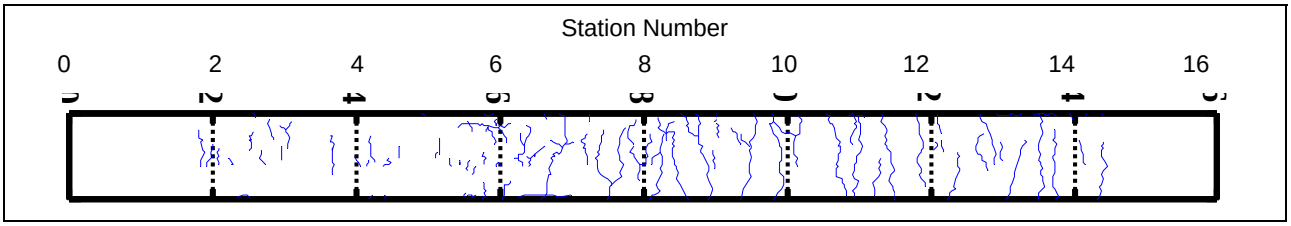

Figure 4.16: 604FD: Final crack pattern.

Figure 4.17: 604FD: Fines pumped from holes drilled for presoaking.

Figure 4.18: 604FD: Section photographs at test completion.

4.4 Section 605FD: Advera

4.4.1 Test Summary

No seepage was observed around the test section during presoaking.

Loading commenced on August 14, 2008, and ended on November 19, 2008. A total of 620,500 load repetitions were applied and 73 datasets were collected. Almost 250,000 more load repetitions were applied compared to the Control. In the interests of completing the project, testing was terminated prior to obtaining an average maximum rut depth of 12.5 mm (0.5 in.). The HVS loading history for Section 605FD is shown in Figure 4.19. Two breakdowns occurred during this test.

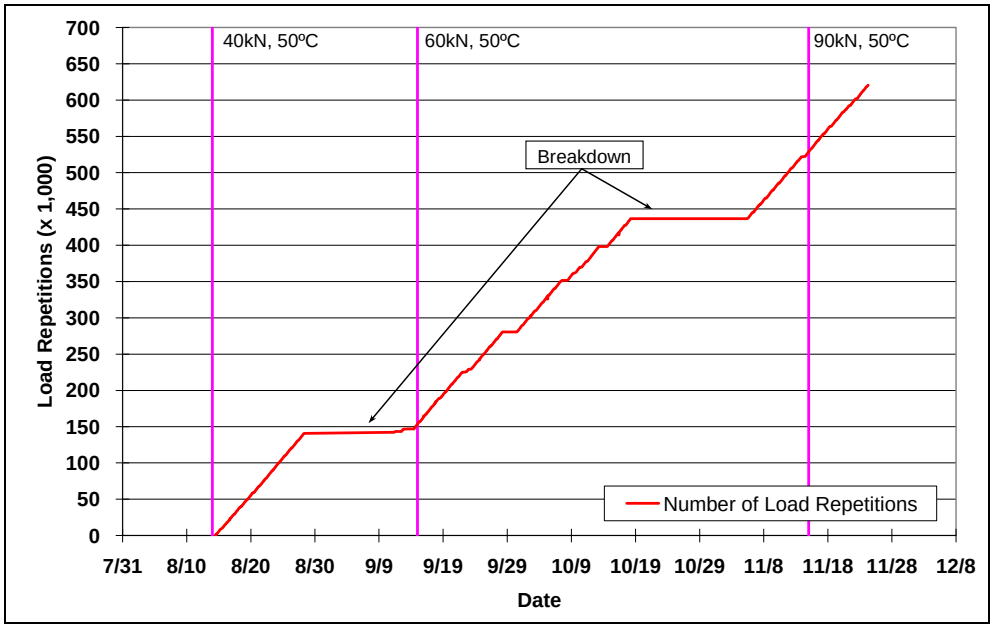

Figure 4.19: 605FD: Load history.

4.4.2 Outside Air Temperatures

Outside air temperatures are summarized in Figure 4.20. Vertical error bars on each point on the graph show the daily temperature range. Temperatures ranged from 3.7°C to 39.8°C (39°F to 104°F) during the course of HVS testing, with a daily average of 16.2°C (61°F), an average minimum of 10.8°C (51°F), and an average maximum of 25.9°C (79°F). Outside air temperatures were considerably warmer during testing of Section 605FD compared to the Control (Section 604FD) (daily average 6.8°C [12.2°F] warmer).

4.4.3 Air and Water Temperatures in the Temperature Control Unit

During the test, the measured air temperatures inside the temperature control chamber ranged from 16.4°C to 62.1°C (62°F to 144°F) with an average of 44.8°C (113°F) and standard deviation of 5.1°C (9.2°F). Temperatures were not maintained during breakdowns. The daily average air temperatures recorded in the temperature control unit, calculated from the hourly temperatures recorded during HVS operation, are shown in Figure 4.21. Vertical errors bars on each point on the graph show daily temperature range. Adjustments were made to maintain the pavement temperature at close to 50°C±4°C (122°F±7°F) at 50 mm depth.

Surface water temperature was maintained at 50°C±4°C (122°F±7°F) to prevent cooling of the pavement.

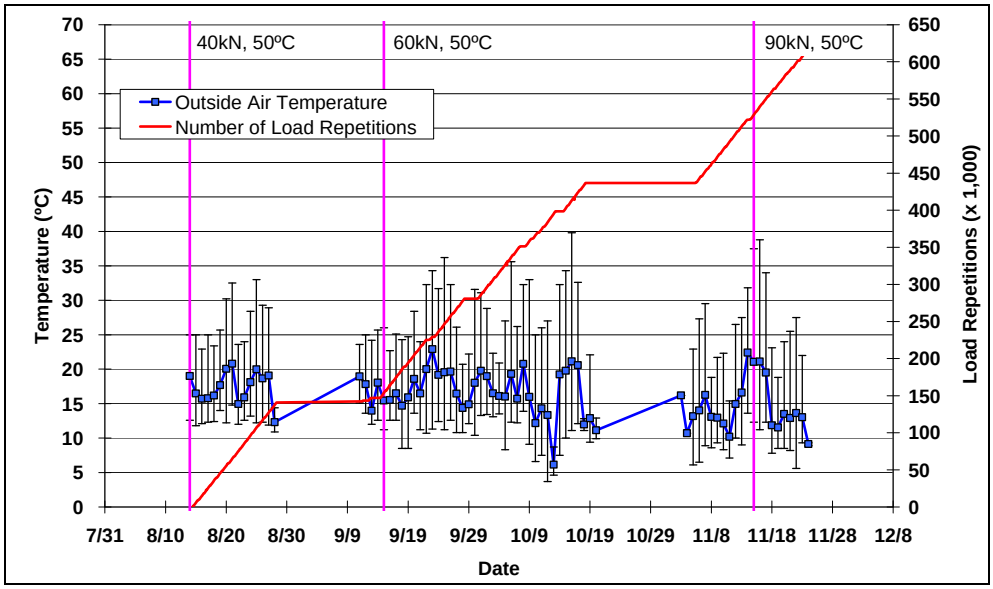

Figure 4.20: 605FD: Daily average outside air temperatures.

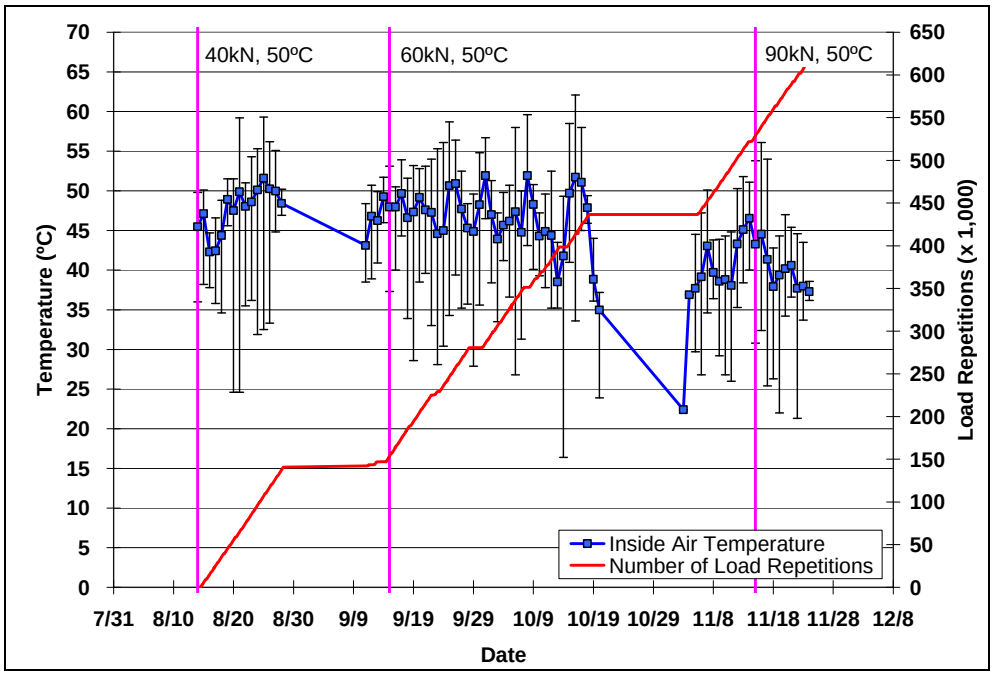

Figure 4.21: 605FD: Daily average inside air temperatures.

4.4.4 Temperatures in the Asphalt Concrete Layers

Daily averages of the surface and in-depth temperatures of the asphalt concrete layers are listed in Table 4.4 and shown in Figure 4.22. The target temperature of 50°C±4°C (122°F±7°F) could not be maintained due to the cold (but warmer than the Control) outside air and surrounding pavement

temperatures. However, average pavement temperatures at all depths of Section 605FD were about 5.0°C (9.0°F) higher than those recorded on the Control, which was attributed to higher average outside and surrounding pavement temperatures. Pavement temperatures decreased slightly with increasing depth in the pavement, as expected.

Table 4.4: 605FD: Temperature Summary for Air and Pavement

Temperature	605FD			604FD
	Average (°C)	Std Dev (°C)	Average (°F)	Average (°C)
Pavement surface	45.6	6.0	114.1	42.6
- 25 mm below surface	45.3	5.2	113.5	39.9
- 50 mm below surface	44.9	5.7	112.8	39.2
- 90 mm below surface	42.6	5.0	108.7	37.9
- 120 mm below surface	41.4	4.6	106.5	36.4
Outside air	16.2	3.4	61.2	9.4
Inside air	44.8	5.1	112.8	37.3

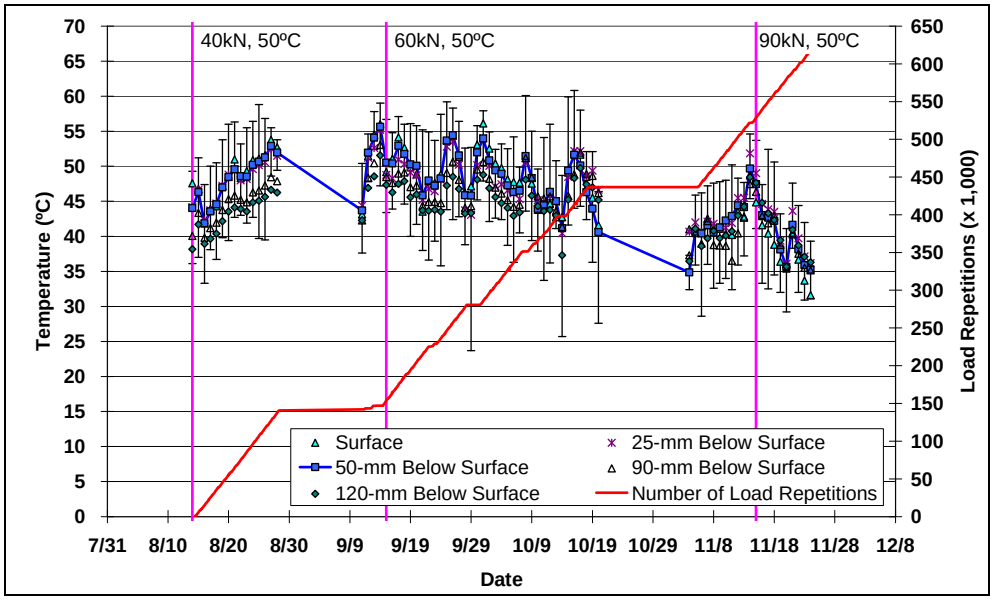

Figure 4.22: 605FD: Daily average temperatures at pavement surface and various depths.

4.4.5 Permanent Surface Deformation (Rutting)

Figure 4.23 shows the average transverse cross section measured with the Laser Profilometer at various stages of the test. This plot clearly shows the increase in rutting and deformation over the duration of the test. Note that HVS trafficking was halted after 620,500 repetitions, before the failure criterion of 12.5 mm (0.5 in.) was reached.

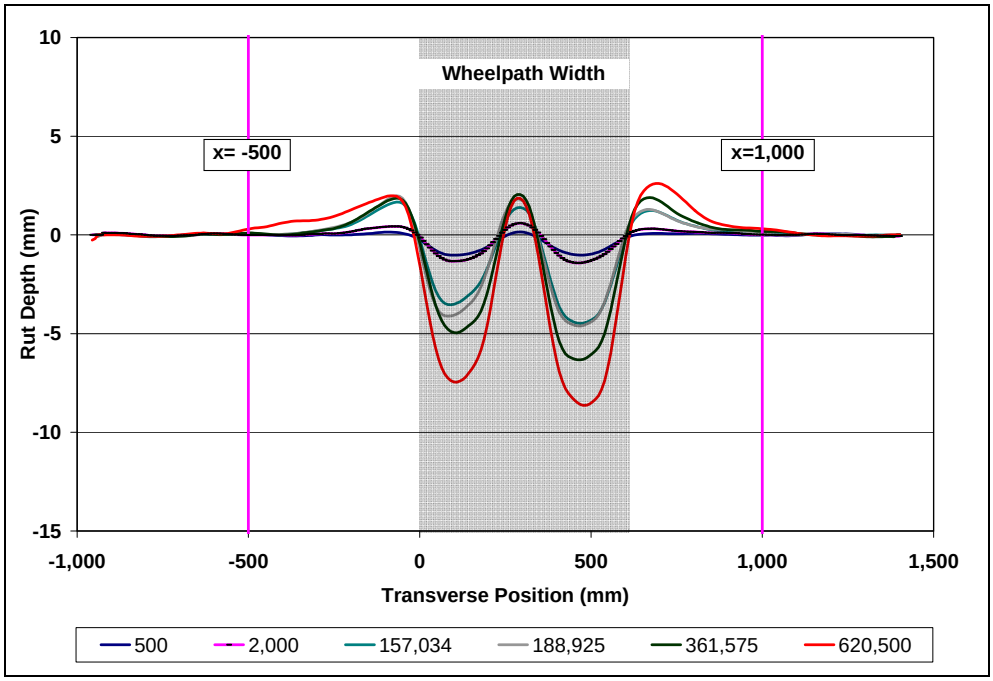

Figure 4.23: 605FD: Profilometer cross section at various load repetitions.

Figure 4.24 and Figure 4.25 show the development of permanent deformation (average maximum rut and average deformation, respectively) with load repetitions as measured with the Laser Profilometer for the test section. Results for the Control section (Section 604FD) and Phase 1 Advera test (Section 601FD) are also shown for comparative purposes. The embedment phase on Section 605FD was considerably shorter compared to the Control (±2.5 mm [0.1 in.] compared to ±5.0 mm [0.2 in.] on the Control) and compared to the Phase 1 testing (±2.5 mm [0.1 in.] compared to ±9.0 mm [0.35 in.]), when the Advera section had a longer embedment phase than the Control section *(2)*. The rate of rut-depth increase after embedment on Section 605FD was also significantly slower than the Control. It is not clear if this was a function of the warm-mix technology, or because Section 605FD received considerably more direct sunlight compared to Section 604FD, which was partially shaded by a shed. This additional sunlight would likely have caused a more rapid oxidation of the binder and consequent stiffening (see discussion in Section 4.7). Additional embedment phases were noted at the 60 kN and 90 kN load changes. The addition of water during the test did not appear to influence the performance of the pavement.

Error bars on the average reading indicate that there was very little variation along the length of the section. Figure 4.26 shows contour plots of the pavement surface at the beginning (after 500 repetitions) and at the end of the test (620,500 repetitions), also indicating minimal variation along the section.

After completion of trafficking, the average maximum rut depth and the average deformation were 11.5 mm (0.45 in.) and 6.1 mm (0.24 in.), respectively. The maximum rut depth measured on the section was 14.1 mm (0.56 in.) recorded at Station 13.

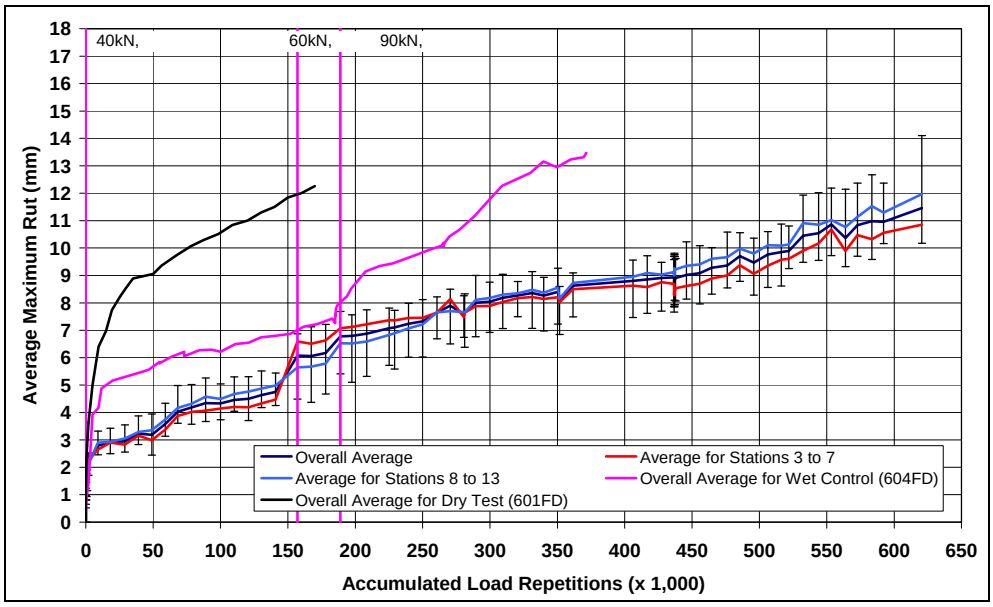

Figure 4.24: 605FD: Average maximum rut.

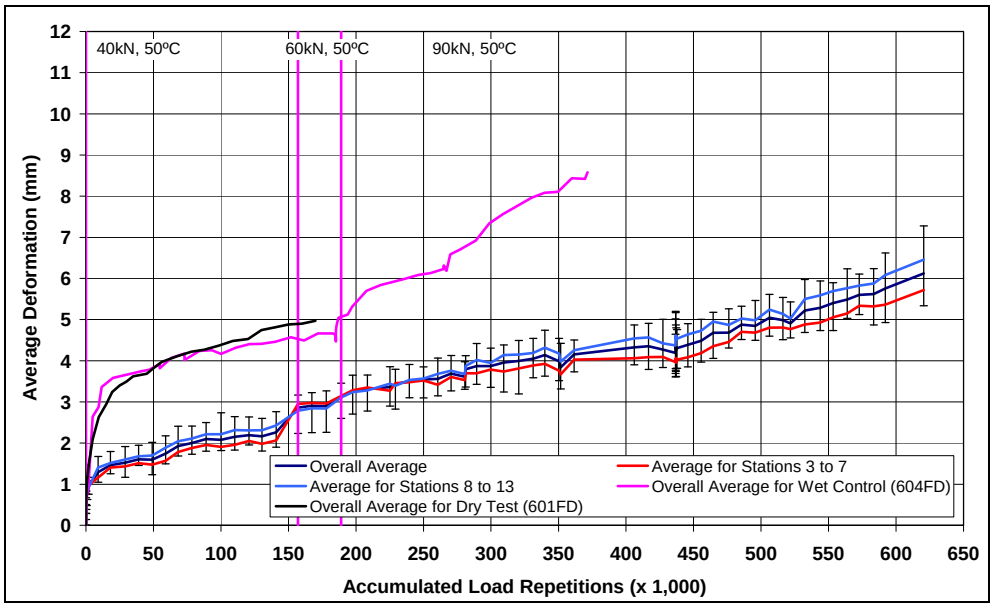

Figure 4.25: 605FD: Average deformation.

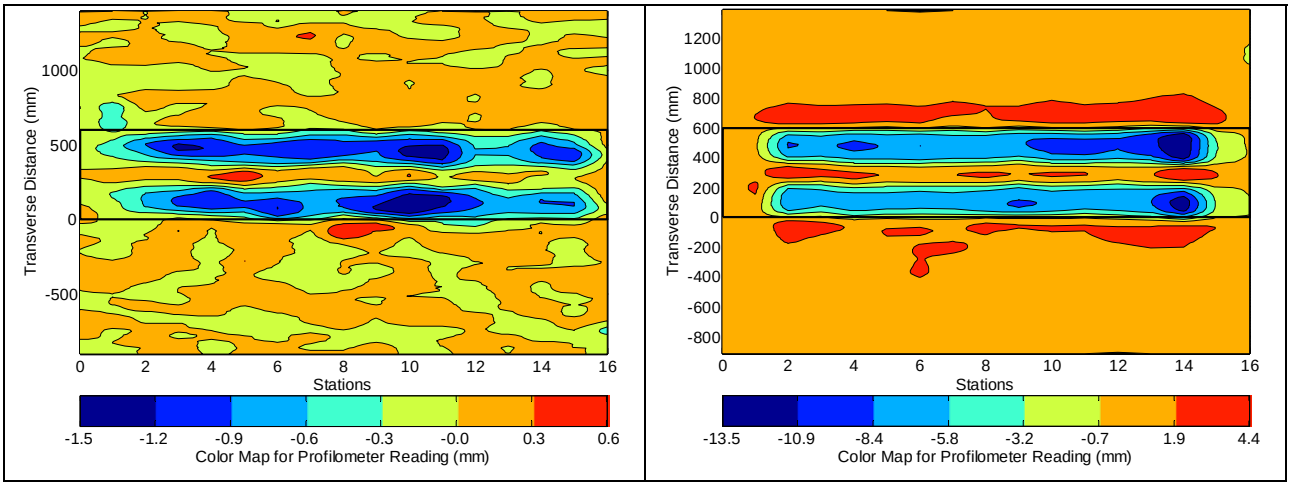

Figure 4.26: 605FD: Contour plot of permanent surface deformation at start and end of test.
(Note that scales are different.)

4.4.6 Asphalt Concrete Moisture Content

Moisture contents in the asphalt concrete were determined from 152 mm (6.0 in.) diameter cores removed immediately after testing from the same positions described in Section 4.3.6. No debonding was noted on any of the cores. Photographs of the cores are shown in Figure 4.27. The results are summarized in Table 4.5 and indicate that some moisture (between about 0.5 and 1.0 percent) infiltrated the surface of the test section during the course of the test.

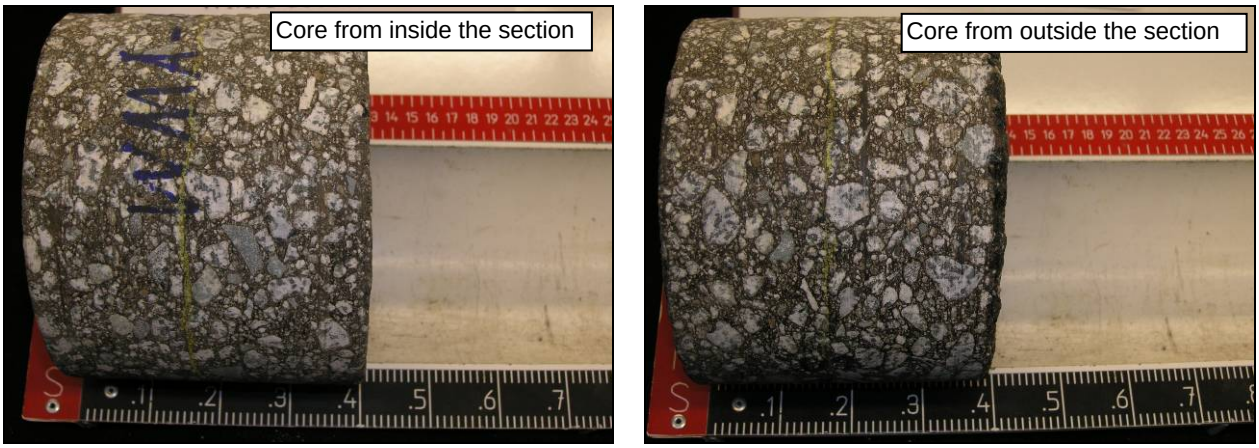

Figure 4.27: 605FD: Cores for moisture content determination.

Table 4.5: 605FD: Moisture Content after Testing

Station	Moisture Content (%)		
	Inside Test Section	Outside Test Section	Difference
4	1.63	0.69	0.94
8	1.03	0.60	0.43
12	1.44	0.62	0.82

4.4.7 Visual Inspection

The test section was visually inspected during each data collection exercise. A more thorough examination of the test section was made after the HVS was removed at the end of the test. A number of observations were made in the assessments during and after the test:

- Salt accumulations along the edges of the wheelpaths were similar to those described for the Control in Section 4.3.7. A photograph of the accumulations is provided in Figure 4.28.
- Transverse cracks started to appear after about 200,000 load repetitions (i.e., after the 60 kN load change), similar to those described for the Control (Figure 4.29). The final crack density was 3.52 m/m^2 (1.07 ft/ft^2) with cracking relatively evenly distributed along the length of the section, but with a slightly higher density between Stations 8 and 16 compared to that between Stations 0 and 8. Although most cracking was concentrated in the wheelpaths, some transverse cracking was also noted between the wheelpaths. Longitudinal cracks were observed in the untrafficked area immediately adjacent to the outside edges of wheelpaths. The final crack pattern is illustrated in Figure 4.30.
- No pumping of fines was observed from the cracks, but some pumping was observed from the holes drilled for the presoak (Figure 4.31). The quantity of material pumped from Section 605FD was considerably less than that observed on the Control.
- The rutting pattern after completion of the test was typical of HVS rutting tests (Figure 4.32) and similar to that observed on the Control.
- Although some "wear" was noted on the surface (Figure 4.32), no aggregate stripping, ravelling or other evidence of moisture damage was noted during or after the test.

Figure 4.28: 605FD: Crystallized salt on edges of wheelpaths during early testing.

Figure 4.29: 605FD: Cracks in wheelpaths during testing.

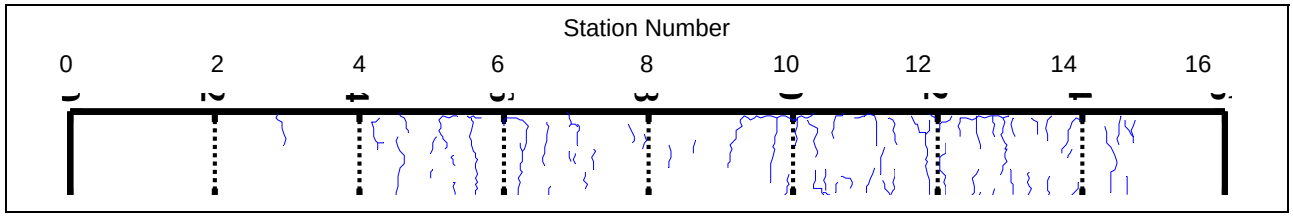

Figure 4.30: 605FD: Final crack pattern.

Figure 4.31: 605FD: Fines pumped from holes drilled for presoaking.

Figure 4.32: 605FD: Section photographs at test completion.

4.5 Section 606FD: Evotherm

4.5.1 Test Summary

No seepage was observed around the test section during presoaking.

Loading commenced on March 07, 2009 and ended on April 24, 2009. A total of 352,020 load repetitions were applied and 58 datasets were collected. The number of load repetitions applied was very similar to the Control section. The HVS loading history for Section 606FD is shown in Figure 4.33. Two breakdowns occurred during this test.

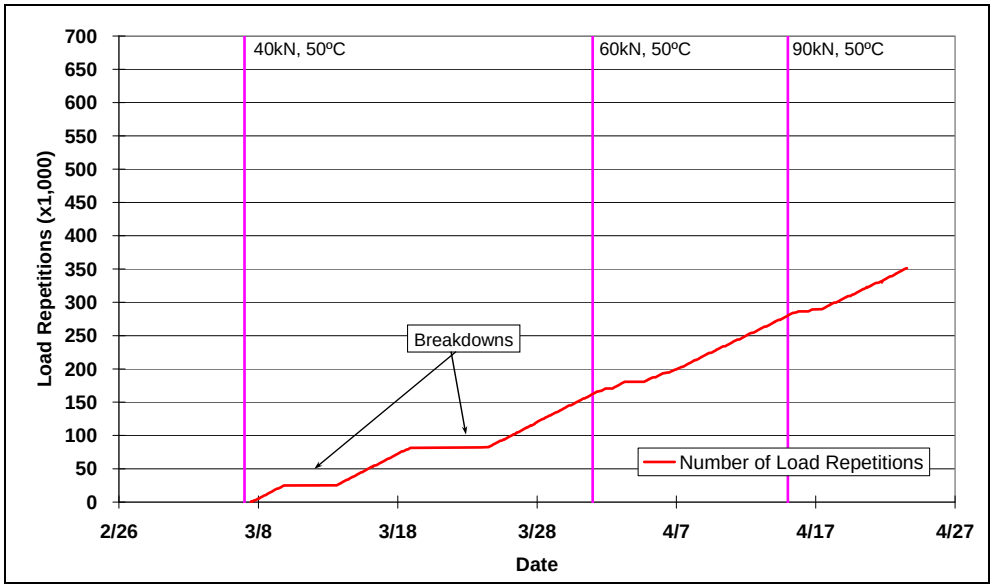

Figure 4.33: 606FD: Load history.

4.5.2 Outside Air Temperatures

Outside air temperatures are summarized in Figure 4.34. Vertical error bars on each point on the graph show the daily temperature range. Temperatures ranged from 2.4°C to 35.5°C (36°F to 96°F) during the course of HVS testing, with a daily average of 16.2°C (61°F), an average minimum of 7.2°C (45°F), and an average maximum of 23.4°C (74°F). Outside air temperatures were considerably warmer during testing of Section 606FD compared to those during testing of the Control (Section 604FD) (daily average 6.8°C [12°F] warmer). Maximum temperatures varied considerably during the test (between 13.8°C and 35.5°C [57°F and 96°F]).

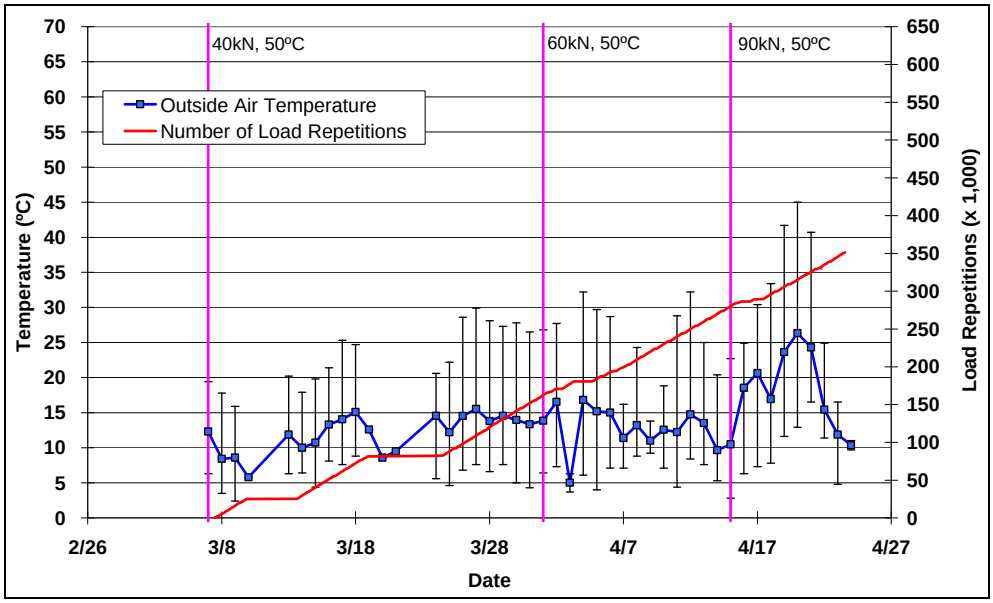

Figure 4.34: 606FD: Daily average outside air temperatures.

4.5.3 Air and Water Temperatures in the Temperature Control Unit

During the test, air temperatures inside the temperature control chamber ranged from 19.0°C (during breakdown) to 58.1°C (66°F to 136°F) with an average of 38.7°C (102°F) and standard deviation of 4.5°C (8.1°F). The air temperature was adjusted to maintain a pavement temperature of 50°C±4°C (122°F±7°F). The daily average air temperatures recorded in the temperature control unit, calculated from the hourly temperatures recorded during HVS operation, are shown in Figure 4.35. Vertical errors bars on each point on the graph show the daily temperature range.

Surface water temperature was maintained at 50°C±4°C (122°F±7°F) to prevent cooling of the pavement.

4.5.4 Temperatures in the Asphalt Concrete Layers

Daily averages of the surface and in-depth temperatures of the asphalt concrete layers are listed in Table 4.6 and shown in Figure 4.36. Pavement temperatures decreased slightly with increasing depth in the pavement, as expected. Average pavement temperatures at all depths of Section 606FD were slightly higher than those recorded on the Control, which was attributed to the warmer outside temperatures measured during the test. However, the target temperature of 50°C±4°C (122°F±7°F) could not be maintained due to the cool outside air and surrounding pavement temperatures.

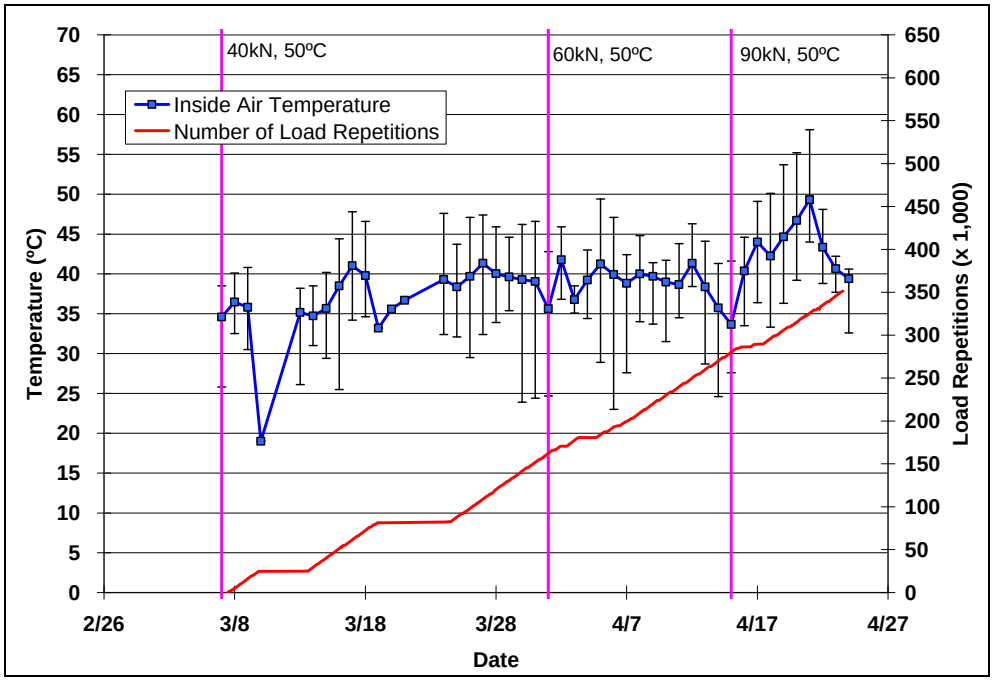

Figure 4.35: 606FD: Daily average inside air temperatures.

Table 4.6: 606FD: Temperature Summary for Air and Pavement

Temperature	606FD			604FD
	Average (°C)	Std Dev (°C)	Average (°F)	Average (°C)
Pavement surface	47.8	5.3	118	42.6
- 25 mm below surface	46.1	5.1	115	39.9
- 50 mm below surface	44.6	4.8	112	39.2
- 90 mm below surface	43.1	4.6	110	37.9
- 120 mm below surface	41.2	4.6	106	36.4
Outside air	16.2	4.3	61	9.4
Inside air	38.7	4.5	102	37.3

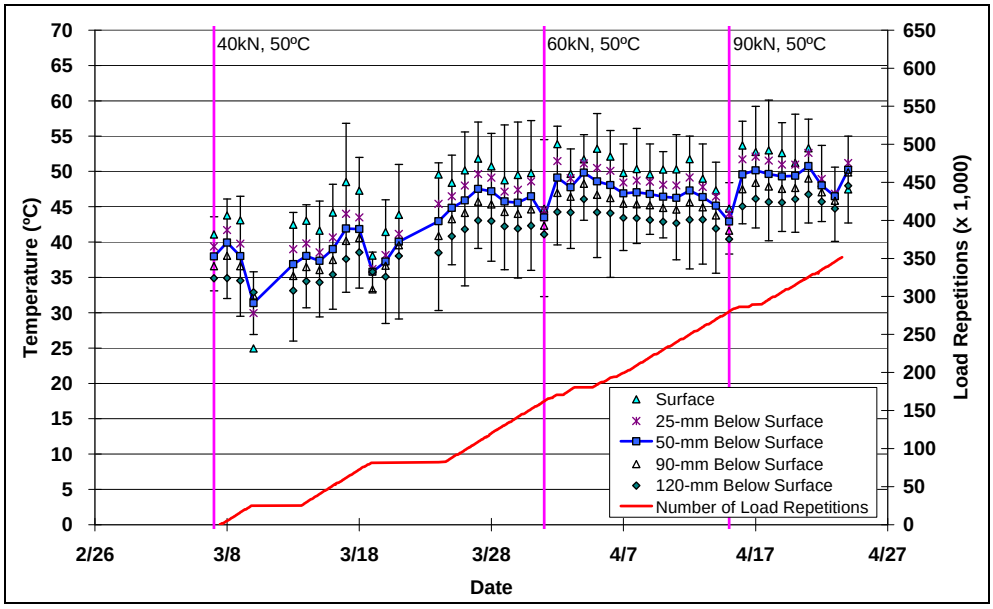

Figure 4.36: 606FD: Daily average temperatures at pavement surface and various depths.

4.5.5 Permanent Surface Deformation (Rutting)

Figure 4.37 shows the average transverse cross section measured with the Laser Profilometer at various stages of the test. This plot clearly shows the increase in rutting and deformation over the duration of the test.

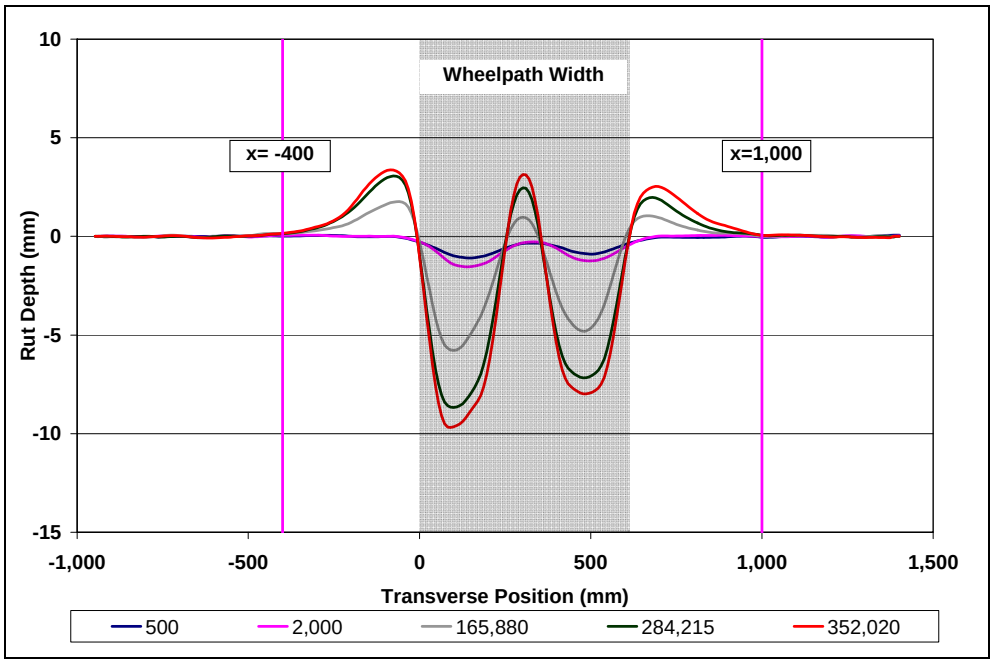

Figure 4.37: 606FD: Profilometer cross section at various load repetitions.

Figure 4.38 and Figure 4.39 show the development of permanent deformation (average maximum rut and average deformation, respectively) with load repetitions as measured with the Laser Profilometer for the test section. Results for the Control section (Section 604FD) and Phase 1 Evotherm test (Section 602FD) are also shown for comparative purposes.

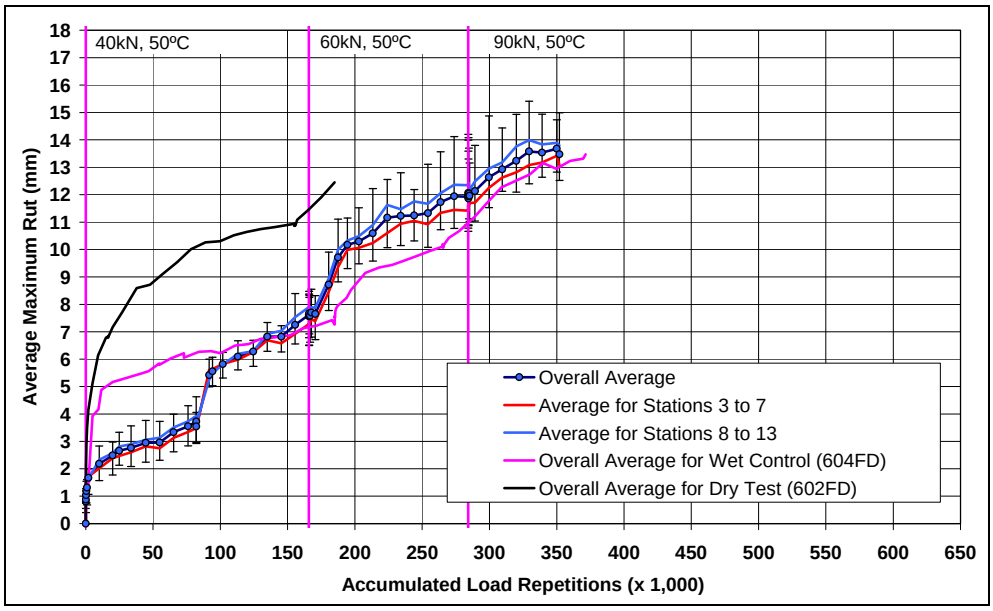

Figure 4.38: 606FD: Average maximum rut.

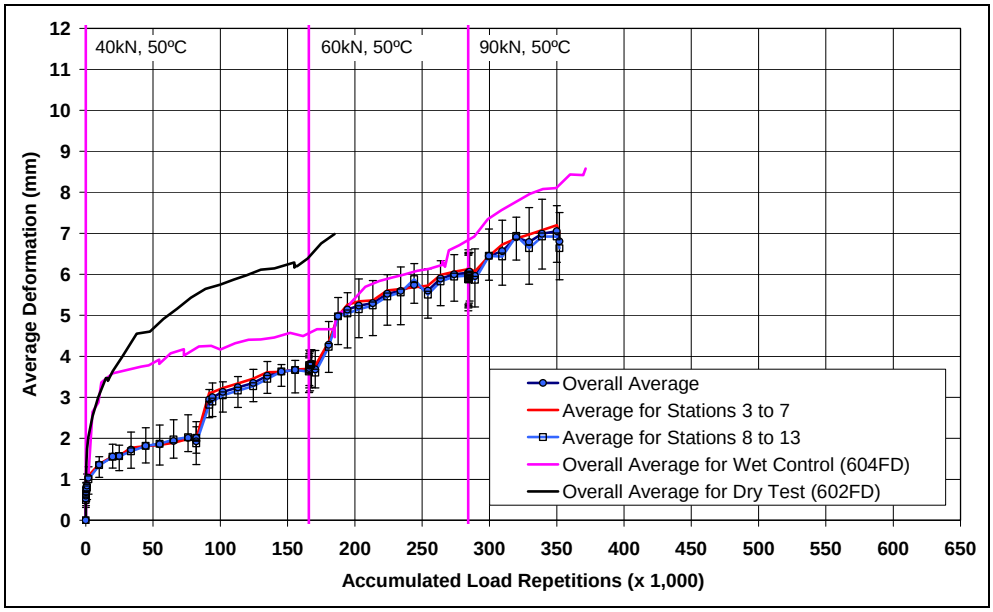

Figure 4.39: 606FD: Average deformation.

The initial embedment phase on Section 606FD was considerably shorter compared to the Control (±2.5 mm [0.1 in.] compared to ±5.0 mm [0.2 in.] on the control), and compared to the Phase 1 testing (±2.5 mm [0.1 in.] compared to ±8.5 mm [0.33 in.]), when the Evotherm section had a longer embedment phase than the Control section *(2)*. The Evotherm mix appeared more sensitive to load increases than the Control mix, with longer embedment phases than the Control after the 60 kN and 90 kN load changes. This could be attributed to the higher air-void contents measured on the Evotherm test track *(2)*. However, the rate of rut depth increase after the load change embedment phases was similar to the Control, resulting in the two sections reaching the failure criteria after a similar number of load repetitions. The addition of water during the test did not appear to influence the performance of the pavement.

Error bars on the average reading indicate that there was very little variation along the length of the section. Figure 4.40 shows contour plots of the pavement surface at the beginning (after 500 repetitions) and at the end of the test (352,000 repetitions), also indicating minimal variation along the section.

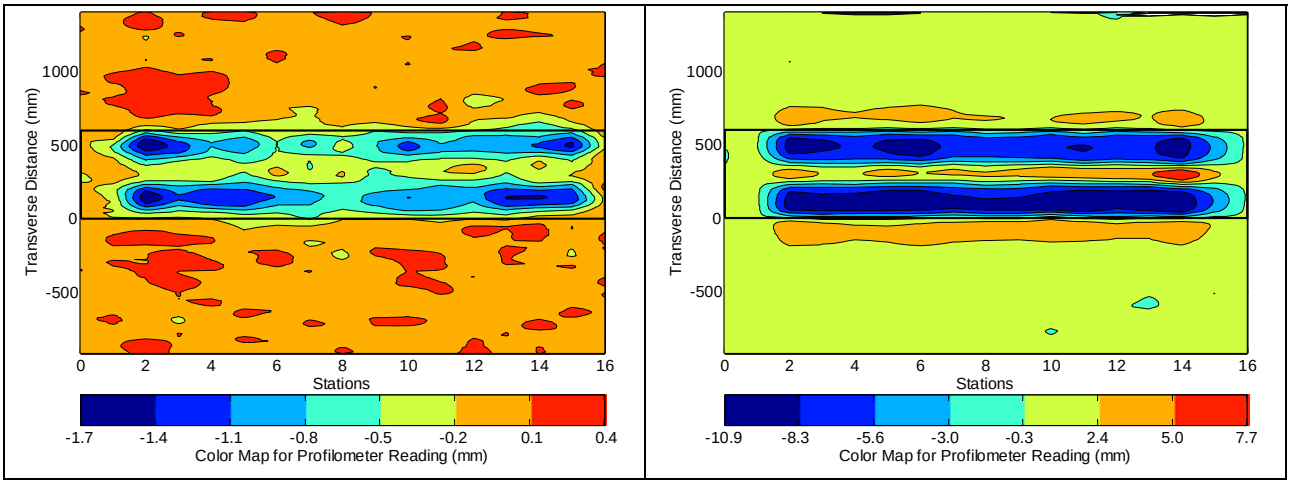

Figure 4.40: 606FD: Contour plot of permanent surface deformation at start and end of test.
(Note that scales are different.)

After completion of trafficking, the average maximum rut depth and the average deformation were 13.9 mm (0.55 in.) and 7.1 mm (0.28 in.), respectively. The maximum rut depth measured on the section was 14.1 mm (0.56 in.) recorded at Station 11.

4.5.6 Asphalt Concrete Moisture Content

Moisture contents in the asphalt concrete were determined from 152 mm (6.0 in.) diameter cores removed immediately after testing from the same positions described in Section 4.3.6. No debonding was noted on any of the cores. Photographs of the cores are shown in Figure 4.41.

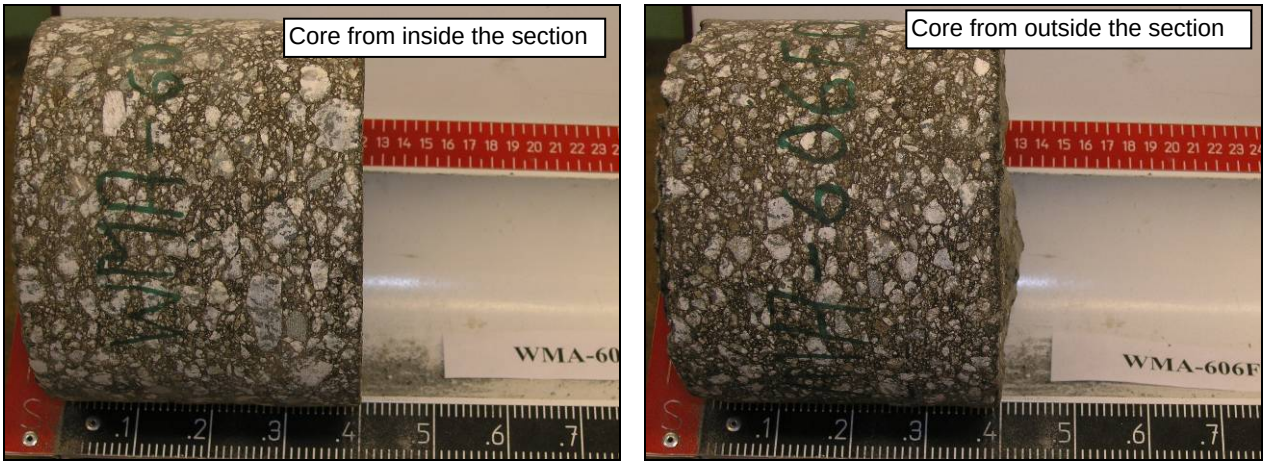

Figure 4.41: 606FD: Cores for moisture content determination.

The results are summarized in Table 4.7. There was a notable difference in the moisture content along the test section. At Station 4 and Station 8, the difference in moisture content of the cores taken from within the test section compared to those taken outside was negligible (± 0.2 percent). At Station 12, the difference was much higher (1.7 percent), which was attributed to the higher crack density in this part of the test section.

Table 4.7: 606FD: Moisture Content after Testing

Station	Moisture Content (%)		
	Inside Test Section	Outside Test Section	Difference
4	0.64	0.47	0.17
8	0.98	0.75	0.23
12	2.03	0.36	1.67

4.5.7 Visual Inspection

The test section was visually inspected during each data collection exercise. A more thorough examination of the test section was made after the HVS was removed at the end of the test. A number of observations were made in the assessments during and after the test:

- Salt accumulations along the edges of the wheelpaths were similar to those described for the Control in Section 4.3.7.
- Transverse cracks started to appear after about 200,000 load repetitions (i.e., after the 60 kN load change), similar to those described for the Control (Figure 4.29). The final crack density was 4.51 m/m^2 (1.38 ft/ft^2) with cracking relatively evenly distributed along the length of the section, but with a slightly higher density between Stations 4 and 8 compared to the rest of the test section. Although most cracking was concentrated in the wheelpaths, some transverse cracking was also noted between the wheelpaths. Longitudinal cracks were observed in the untrafficked area immediately adjacent to the outside edges of wheelpaths. The final crack pattern is illustrated in Figure 4.42.
- No pumping of fines was observed from the cracks, but some pumping was observed from the holes drilled for the presoak, similar to that described for the Advera section (see Figure 4.31). The

quantity of material pumped from Section 606FD was considerably less than that observed on the Control.

- The rutting pattern after completion of the test was typical of HVS rutting tests (Figure 4.43) and similar to that observed on the Control.
- Although some "wear" was noted on the surface (Figure 4.43), no aggregate stripping, ravelling or other evidence of moisture damage was noted during or after the test.

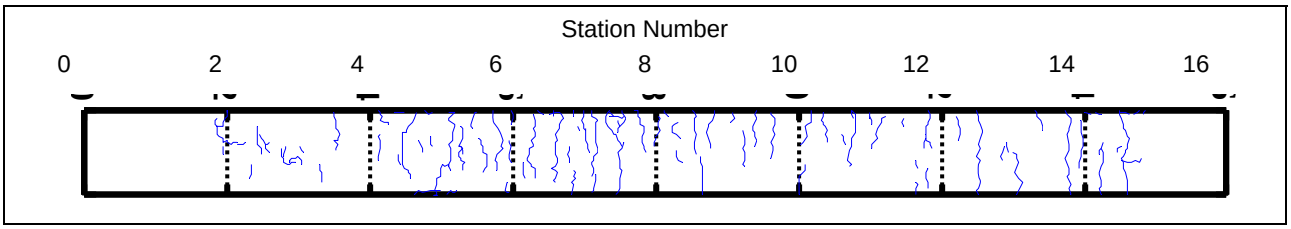

Figure 4.42: 606FD: Final crack pattern.

Figure 4.43: 606FD: Section photographs at test completion.

4.6 Section 607FD: Sasobit

4.6.1 Test Summary

No seepage was observed around the test section during presoaking.

Loading commenced on April 05, 2009, and ended on June 18, 2009. A total of 464,275 load repetitions were applied and 68 datasets were collected. Considerably more load repetitions (90,000) were applied to Section 607FD compared to the Control; however, the failure criterion of 12.5 mm (0.5 in.) was not reached and testing was halted in the interest of completing the project. The high rut resistance was probably attributable in part to the lower binder content of the mix used in this test section, discussed in the Phase 1 report *(2)* and therefore direct performance comparisons between the Control and this test section are not possible. The HVS loading history for Section 607FD is shown in Figure 4.44. Three breakdowns occurred during testing.

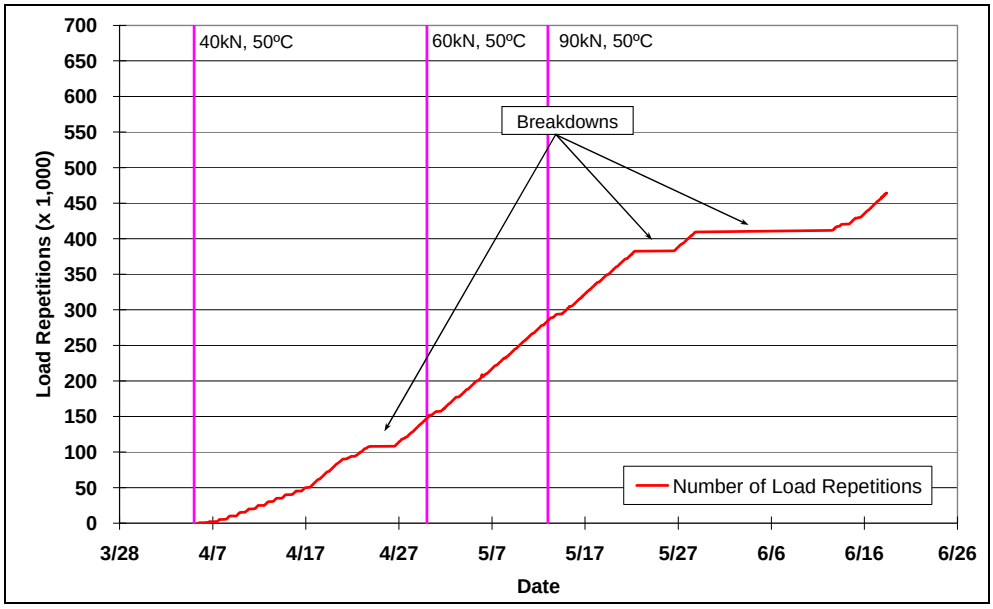

Figure 4.44: 607FD: Load history.

4.6.2 Outside Air Temperatures

Outside air temperatures are summarized in Figure 4.45. Vertical error bars on each point on the graph show the daily temperature range. Temperatures ranged from 2.9°C to 35.5°C (37°F to 96°F) during the course of HVS testing, with a daily average of 14.1°C (57°F), an average minimum of 8.9°C (48°F), and an average maximum of 26.9°C (80°F), all higher than those recorded on the Control.

4.6.3 Air and Water Temperatures in the Temperature Control Unit

During the test, air temperatures inside the temperature control chamber ranged from 27.2°C to 45.8°C (65°F to 148°F) with an average of 36.6°C (122°F) and standard deviation of 4.8°C (8.6°F). The air temperature was adjusted to maintain a pavement temperature of 50°C±4°C (122°F±7°F). The daily average air temperatures recorded in the temperature control unit, calculated from the hourly temperatures

recorded during HVS operation, are shown in Figure 4.46. Vertical errors bars on each point on the graph show daily temperature range.

Surface water temperature was maintained at 50°C±4°C (122°F±7°F) to prevent cooling of the pavement.

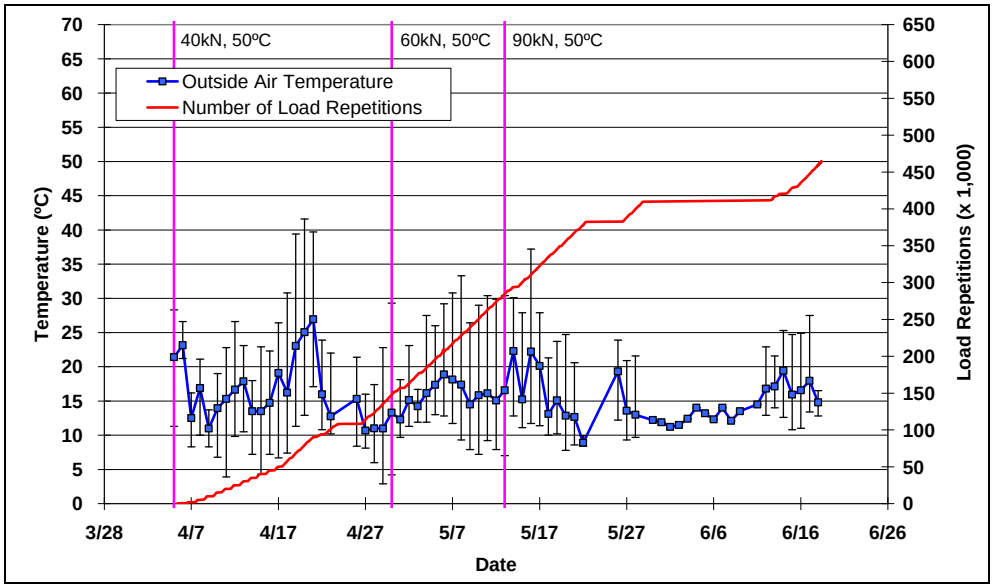

Figure 4.45: 607FD: Daily average outside air temperatures.

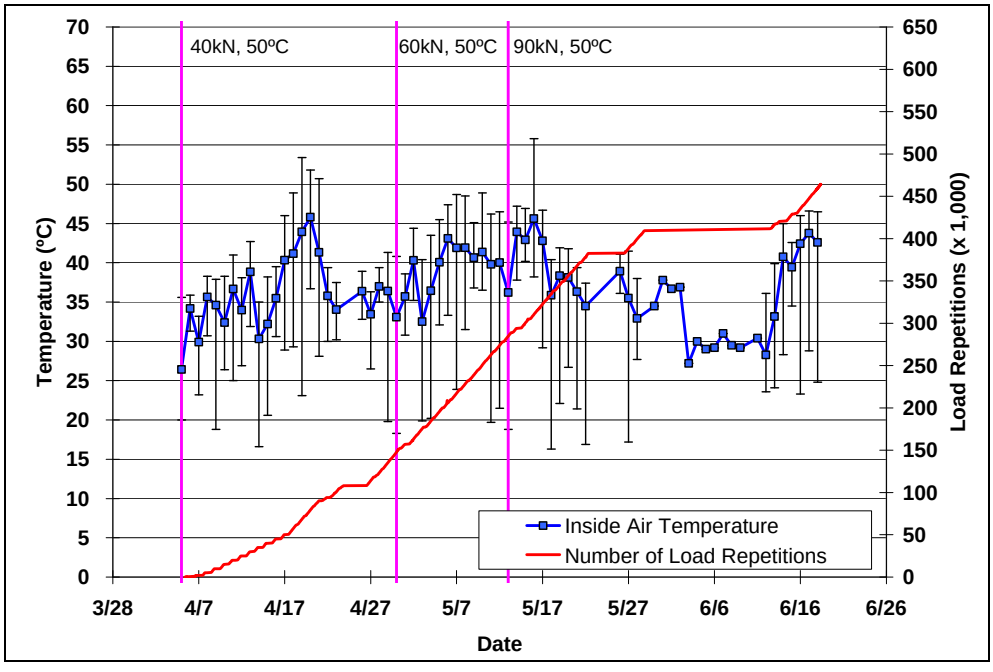

Figure 4.46: 607FD: Daily average inside air temperatures.

4.6.4 Temperatures in the Asphalt Concrete Layers

Daily averages of the surface and in-depth temperatures of the asphalt concrete layers are listed in Table 4.8 and shown in Figure 4.47. Pavement temperatures decreased slightly with increasing depth in the pavement, as expected. Average pavement temperatures at all depths of Section 607FD were considerably higher than those recorded on the Control (but still lower than the target as on the other sections), which was attributed in part to the warmer outside temperatures and in part to the better insulation of the temperature chamber used on this test.

Table 4.8: 607FD: Temperature Summary for Air and Pavement

Temperature	607FD			604FD
	Average (°C)	Std Dev (°C)	Average (°F)	Average (°C)
Pavement surface	48.6	6.7	120	42.6
- 25 mm below surface	46.0	5.6	115	39.9
- 50 mm below surface	45.3	5.2	114	39.2
- 90 mm below surface	43.3	4.3	110	37.9
- 120 mm below surface	42.7	3.8	109	36.4
Outside air	14.1	5.2	57	9.4
Inside air	36.6	4.8	98	37.3

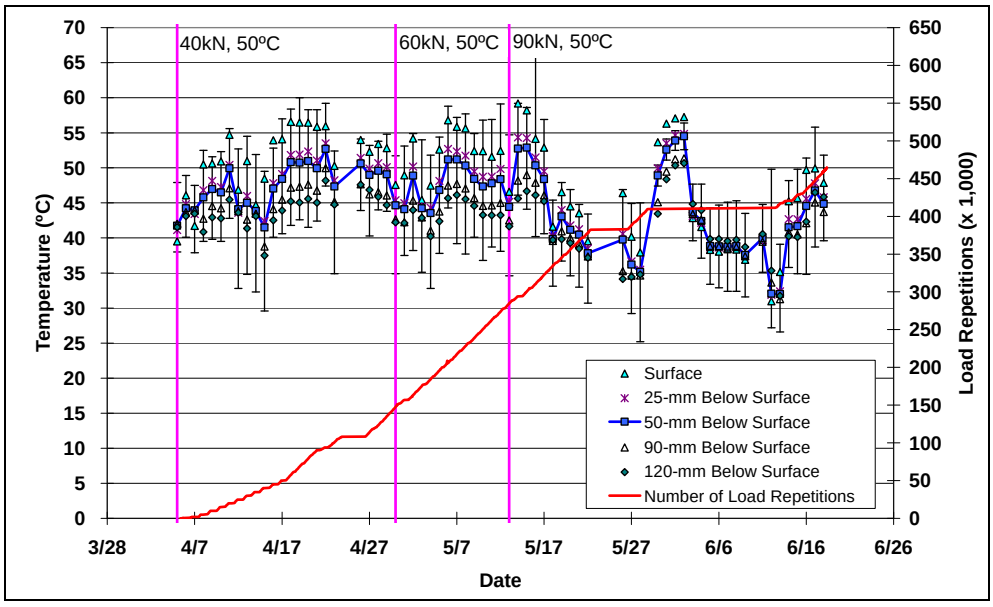

Figure 4.47: 607FD: Daily average temperatures at pavement surface and various depths.

4.6.5 Permanent Surface Deformation (Rutting)

Figure 4.48 shows the average transverse cross section measured with the Laser Profilometer at various stages of the test. This plot clearly shows the increase in rutting and deformation over the duration of the test.

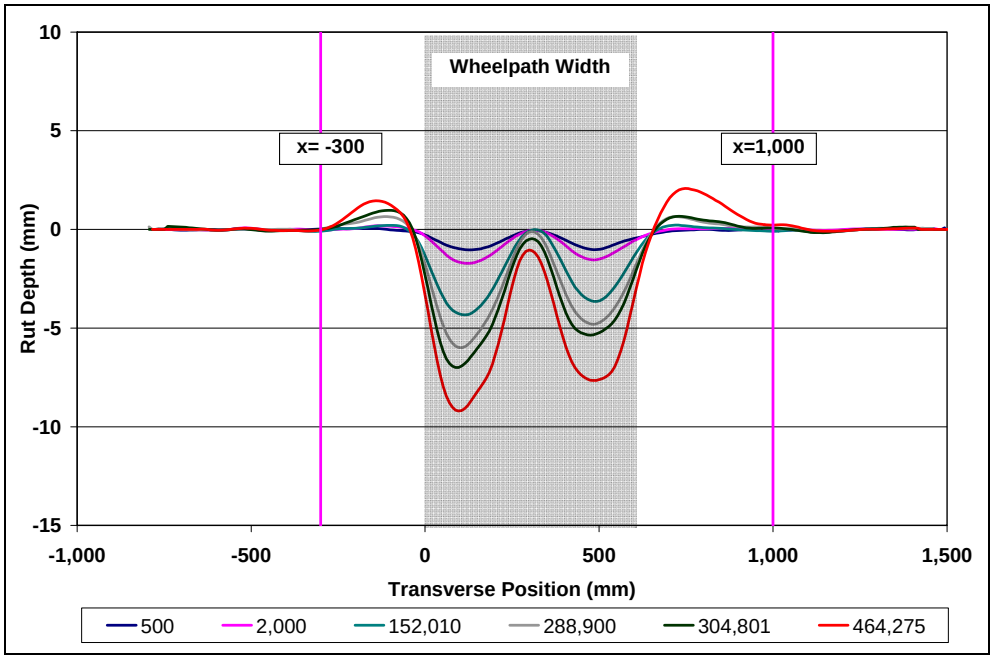

Figure 4.48: 607FD: Profilometer cross section at various load repetitions.

Figure 4.49 and Figure 4.50 show the development of permanent deformation (average maximum rut and average deformation, respectively) with load repetitions as measured with the Laser Profilometer for the test section. Results for the Control section (Section 604FD) and Phase 1 Sasobit test (Section 603FD) are also shown for general comparative purposes, although no direct comparisons to the Control can be made given the difference in binder content between the two sections. The embedment phase on Section 607FD was considerably shorter compared to the Control (±2.5 mm [0.1 in.] compared to ±5.0 mm [0.2 in.] on the control) and slightly shorter compared to the Phase 1 testing (±2.5 mm [0.1 in.] compared to ±3.5 mm [0.14 in.]) *(2)*. The rate of rut depth increase after embedment on Section 607FD was similar to the Phase 1 testing, but significantly slower than the Control. It is not clear if this difference between the Control and Sasobit sections was a function of the warm-mix technology, the lower binder content, or because Section 607FD received considerably more direct sunlight compared to Section 604FD, which was partially shaded by a shed. This additional sunlight would likely have caused a more rapid oxidation of the binder and consequent stiffening (see discussion in Section 4.7). A small embedment phase was noted at the 60 kN load change, while a more substantial embedment phase was noted at the 90 kN load change. The addition of water during the test did not appear to influence the performance of the pavement.

Error bars on the average reading indicate that there was very little variation along the length of the section. Figure 4.51 shows contour plots of the pavement surface at the beginning (after 500 repetitions) and at the end of the test (464,275 repetitions), also indicating minimal variation along the section.

After completion of trafficking, the average maximum rut depth and the average deformation were 10.8 mm (0.43 in.) and 8.5 mm (0.34 in.), respectively. The maximum rut depth measured on the section was 12.4 mm (0.5 in.) recorded at Station 5.

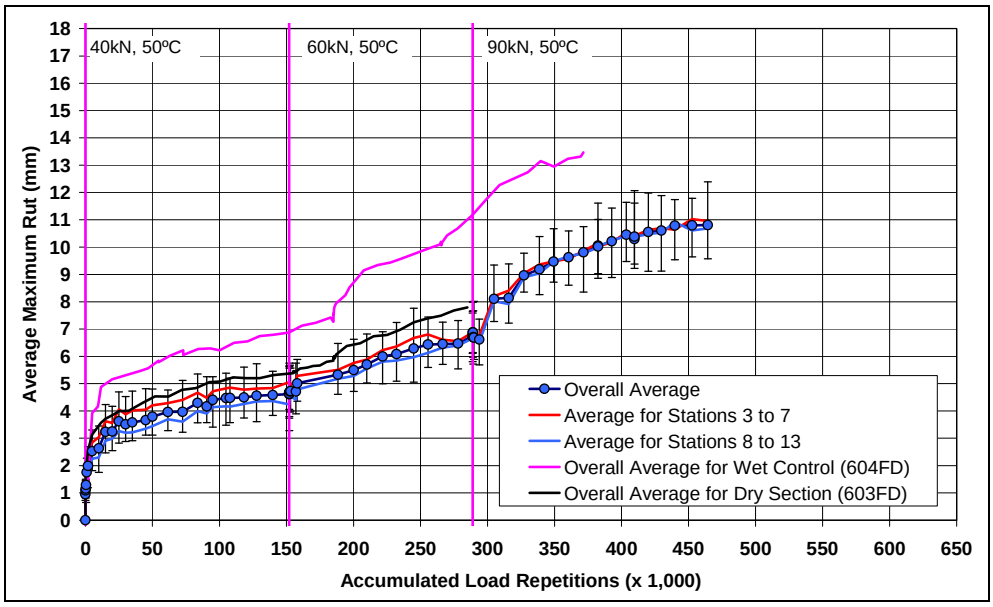

Figure 4.49: 607FD: Average maximum rut.

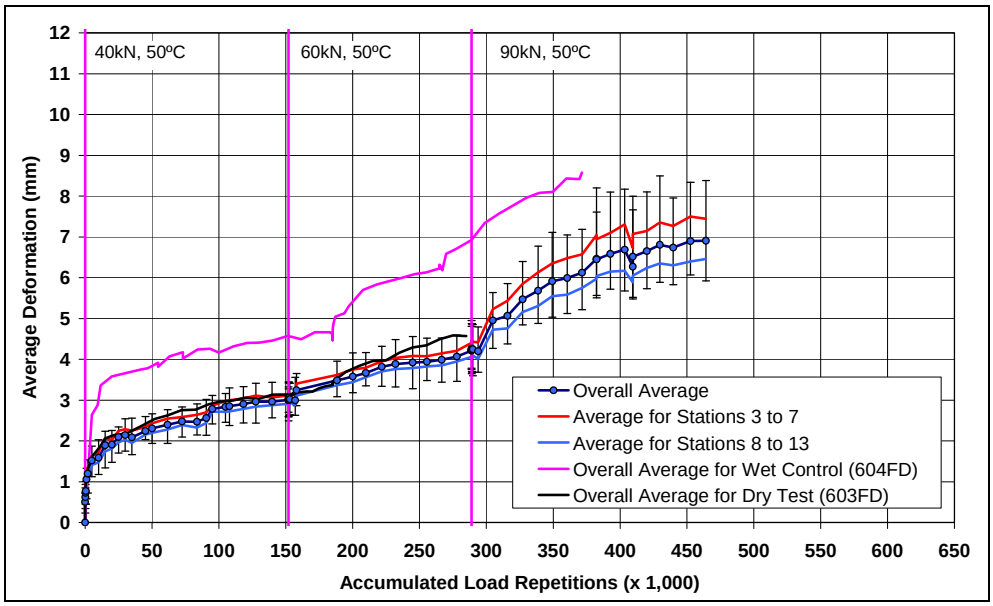

Figure 4.50: 607FD: Average deformation.

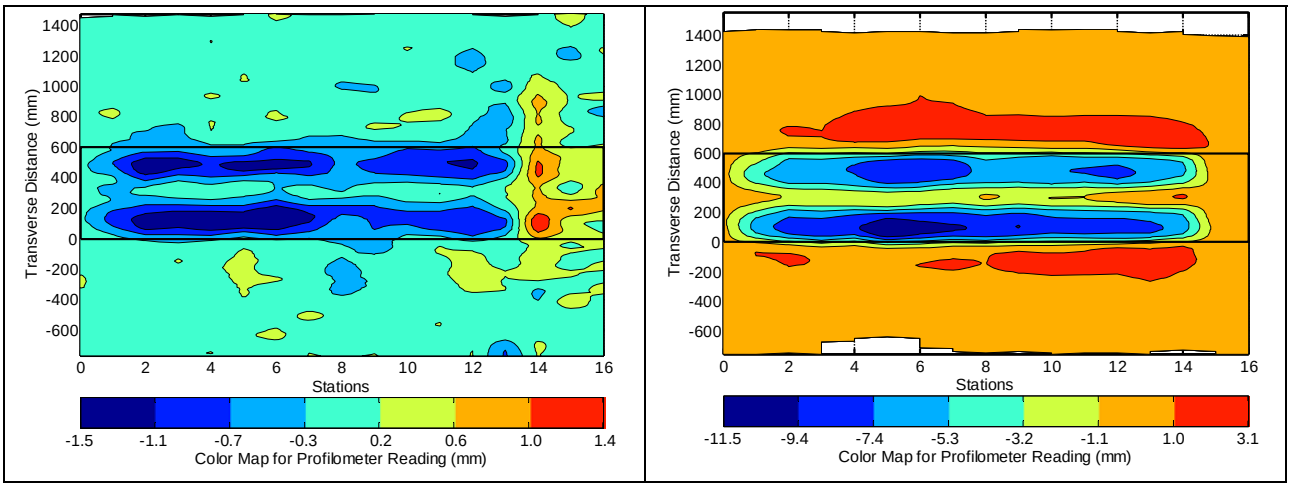

Figure 4.51: 607FD: Contour plot of permanent surface deformation at start and end of test.
(Note that scales are different)

4.6.6 Asphalt Concrete Moisture Content

Moisture contents in the asphalt concrete were determined from 152 mm (6.0 in.) diameter cores removed immediately after testing from the same positions described in Section 4.3.6. No debonding was noted on any of the cores. Photographs of the cores are shown in Figure 4.52.

The results are summarized in Table 4.9 and indicate that some moisture (between about 0.3 and 0.9 percent) infiltrated the surface of the test section during the course of the test.

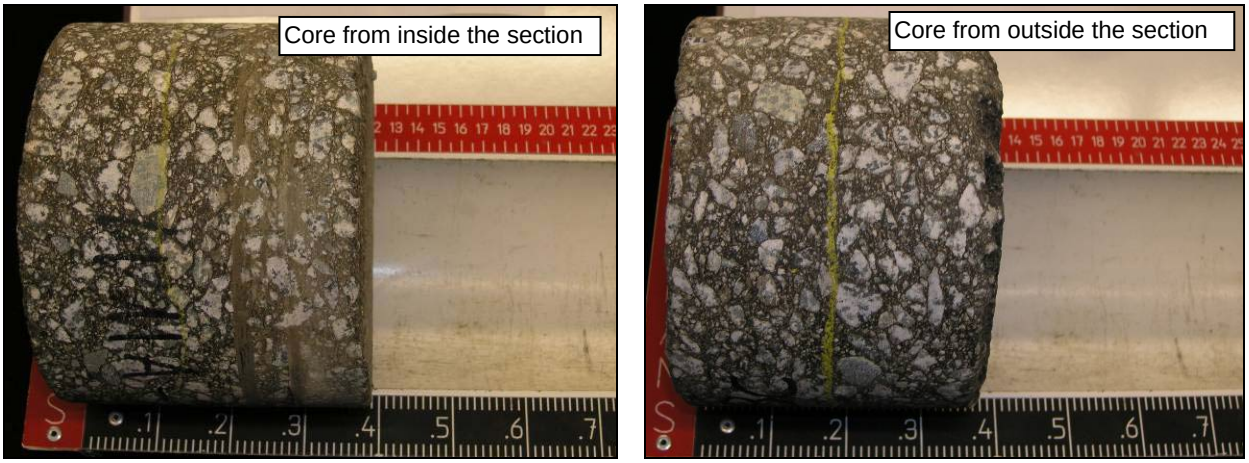

Figure 4.52: 607FD: Cores for moisture content determination.

Table 4.9: 607FD: Moisture Content after Testing

Station	Moisture Content (%)		
	Inside Test Section	Outside Test Section	Difference
4	0.59	0.34	0.25
8	0.74	0.30	0.44
12	1.15	0.27	0.88

4.6.7 Visual Inspection

The test section was visually inspected during each data collection exercise. A more thorough examination of the test section was made after the HVS was removed at the end of the test. A number of observations were made in the assessments during and after the test:

- Salt accumulations along the edges of the wheelpaths were similar to those described for the Control in Section 4.3.7.
- Transverse cracks started to appear after about 200,000 load repetitions (i.e., after the 60 kN load change), similar to those described for the Control (Figure 4.29). The final crack density was 7.44 m/m^2 (2.33 ft/ft^2), somewhat higher than the other sections, and with cracking evenly distributed along the length of the section. Although most cracking was concentrated in the wheelpaths, some transverse cracking was also noted between the wheelpaths. Longitudinal cracks were observed in the untrafficked area immediately adjacent to the outside edges of wheelpaths. The final crack pattern is illustrated in Figure 4.53.
- No pumping of fines was observed from the cracks, but some pumping was observed from the holes drilled for the presoak, similar to that described for the Advera section (see Figure 4.31). The quantity of material pumped from Section 607FD was considerably less than that observed on the Control.
- The rutting pattern after completion of the test was typical of HVS rutting tests (Figure 4.54) and similar to that observed on the Control.
- Although some "wear" was noted on the surface (Figure 4.54), no aggregate stripping, ravelling or other evidence of moisture damage was noted during or after the test.

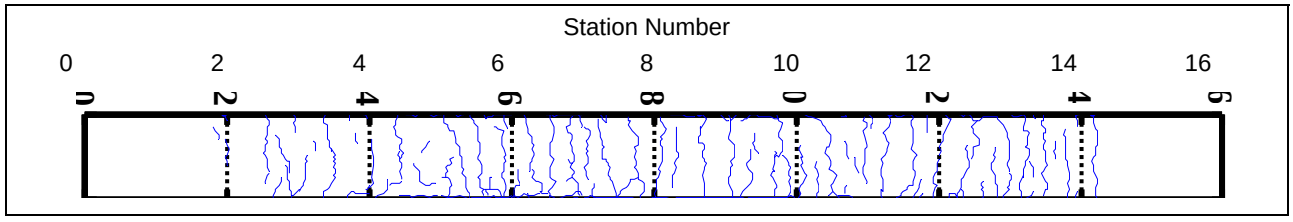

Figure 4.53: 607FD: Final crack pattern.

Figure 4.54: 607FD: Section photographs at test completion.

4.7 Test Summary and Discussion

Testing on the four sections was started in late summer of 2008 and ended in early summer of 2009. The duration of the tests varied from 352,000 load repetitions (Evotherm) to 620,500 load repetitions (Advera). A range of daily average temperatures was experienced during the course of testing; however, the pavement temperatures remained constant throughout HVS trafficking.

Rutting behavior for the four sections is compared in Figure 4.55 (average maximum rut) and Figure 4.56 (average deformation). HVS trafficking on each of the four sections revealed that the duration and rut depths of the embedment phases (high early-rutting phase of typical two-phase rutting processes) on the warm-mix sections were approximately half that of the Control, a trend opposite that observed in Phase 1 (discussed in Section 4.8). This indicates that the effects of oxidation of the binder at lower production temperatures may only influence rutting performance in the first few months after construction.

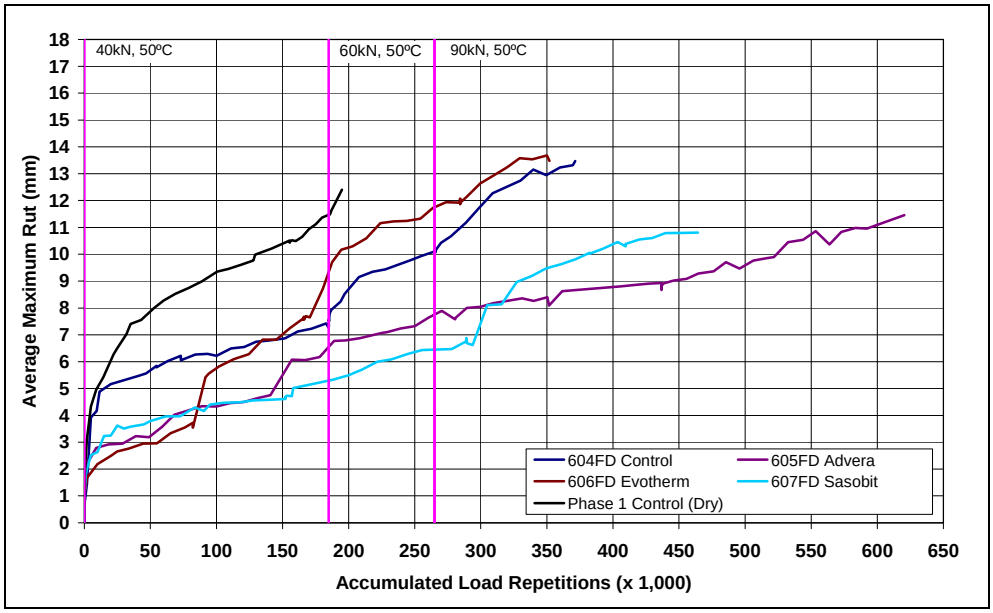

Figure 4.55: Comparison of average maximum rut.

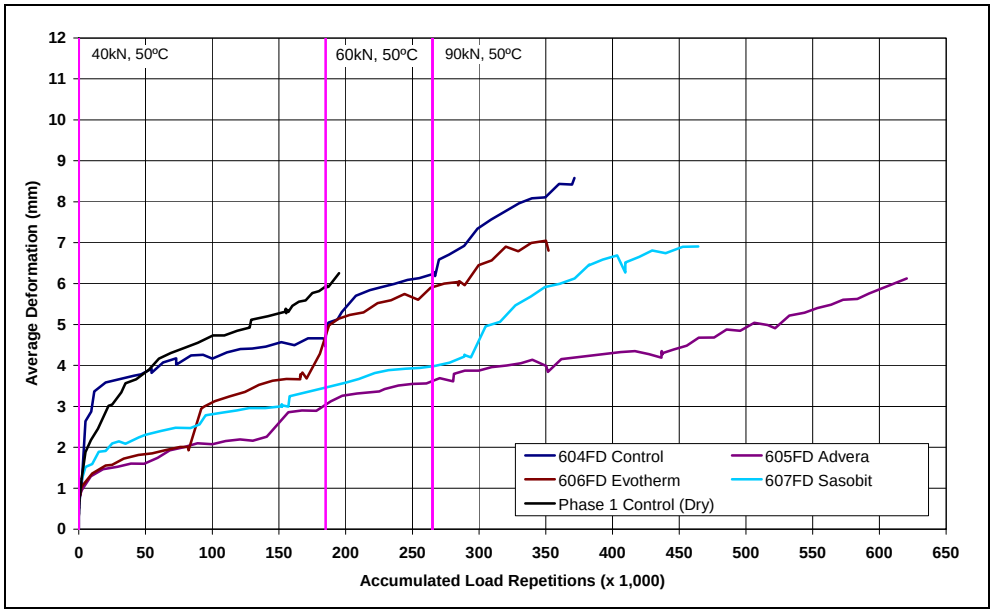

Figure 4.56: Comparison of average deformation.

The rutting behavior of Section 604FD (Control) and Section 606FD (Evotherm) differed significantly from that of Section 605FD (Advera) and Section 607FD (Sasobit) after the embedment phase. This was attributed to the Control and Evotherm sections being predominantly in the shade of an adjacent shed for most of the day, while the Advera and Sasobit sections were predominantly in the sun for most of the day (Figure 4.57). Consequently the binder in the mixes may have oxidized more rapidly on the Advera and

Sasobit sections in the year since construction, leading to potentially a higher stiffness and consequent better rutting performance. This is being investigated in a separate study, and those results will be presented with the Phase 3 laboratory and HVS test results (on rubberized asphalt) when that testing is complete.

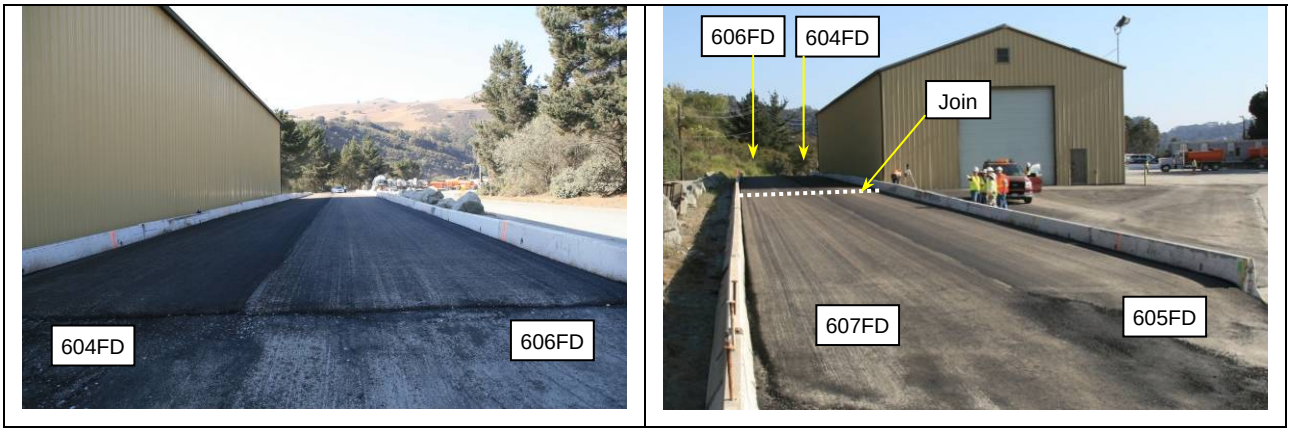

Figure 4.57: Afternoon shade from the shed on Sections 604FD and 606FD.

The Control and Evotherm tests (both predominantly in the shade) followed similar trends after the first 80,000 HVS load repetitions and reached the 12.5 mm (0.5 in.) failure point at about 300,000 load repetitions. The Advera and Sasobit tests (both predominantly in the sun) also followed similar trends with a very slow increase in rut depth after the short embedment phase. In the interests of completing this phase of the study, the Advera test was terminated after 625,000 repetitions when the rut depth was 11.5 mm (i.e., before the failure point of 12.5 mm), while the Sasobit test was terminated after 420,000 repetitions when the rut depth was 9.9 mm.

Although some top-down cracking was noted on all four sections, there was no evidence of moisture damage on any of the sections.

These results further support the findings from the Phase 1 HVS testing in that the use of any of the three warm-mix asphalt additives tested in this experiment and subsequent compaction of the mix at lower temperatures will not significantly influence the rutting performance of the mix in the longer term. The results also indicate that, provided aggregate and mix moisture contents are within specified limits and specified compaction requirements are met, the warm-mix asphalt additives tested in this experiments are unlikely to increase the moisture sensitivity of the mix.

4.8 Comparison of Phase 1 and Phase 2 HVS Test Results

The average maximum rut progression for both phases is shown in Figure 4.58. The plot clearly shows the difference in the embedment phases in terms of duration (number of repetitions) and rut depth and in terms of the difference between the Control and warm-mix sections. In Phase 1, the embedment phases of the warm-mix sections were similar to the Control, but the rut depths were deeper. In Phase 2, the duration of the embedment phase on all sections was again similar; however the rut depth was notably less on the warm-mix sections compared to the Control. The plot also clearly shows the difference in the number of repetitions required to reach an average maximum rut depth of 12.5 mm (0.5 in.), with the Phase 2 sections requiring significantly more repetitions. A significant proportion of the later trafficking on each section in Phase 2 was undertaken at higher wheel loads (60 kN and 90 kN [13,500 lb and 20,250 lb]) than those used in Phase 1.

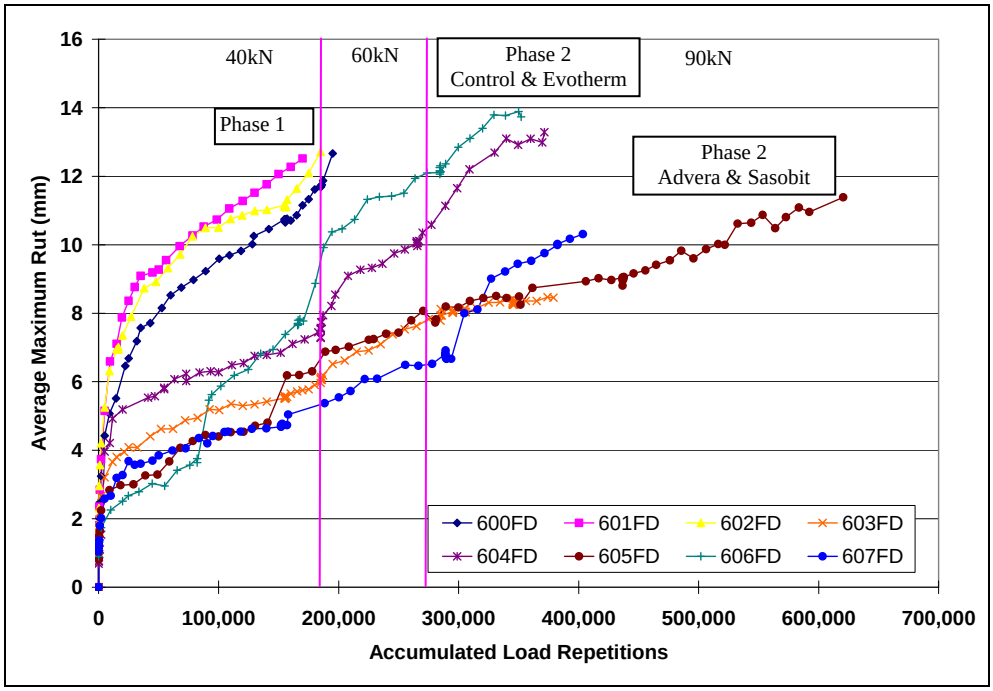

Figure 4.58: Comparison of Phase 1 and Phase 2 rutting performance.

Visual assessments after Phase 1 testing indicated that the only distress evident on the sections was the deformation. After Phase 2 testing, top-down cracking was evident on all sections along with some stone loss attributed to channelized trafficking and the constant presence of water in the wheelpath. There was no significant difference in the crack patterns, crack length, crack density, or stone loss among the sections.

Based on the comparison of performance between the two phases, it can be concluded that the effect on rutting performance of reduced binder aging attributed to lower mix production temperatures appear to be of relatively limited duration. It can therefore be concluded, based on the limited testing undertaken to date, that equal performance will be obtained in the longer term from the hot and warm mixes tested in this study. This will need to be verified in full-scale field testing.

4.9 Fatigue Performance Testing

The work plan for this study *(1)* included a fatigue performance testing phase. However, based on the very long testing programs required to achieve failure in the rutting experiments (attributed to the very stiff pavement and proximity of the bedrock to the surface), it was concluded that a significant number of HVS load repetitions (more than one million) would be required to induce fatigue cracking on the test sections, and consequently the testing was not undertaken.

5 FORENSIC INVESTIGATION

5.1 Introduction

A forensic investigation was carried out after completion of all HVS testing to compare the condition of the asphalt concrete layers within and outside the HVS trafficked area, and to remove samples for laboratory testing.

5.2 Forensic Investigation Procedure

The forensic investigation included the following tasks:

1. Demarcate core and test pit locations;
2. Drill, remove, seal, and label cores;
3. Saw the asphalt concrete;
4. Remove the slab and inspect surfacing/base bond;
5. Determine the wet density of the base (nuclear density gauge);
6. Determine the in situ strength of the base and subgrade (Dynamic Cone Penetrometer);
7. Remove the base material;
8. Sample material from the top 200 mm of the base for moisture content determination;
9. Measure asphalt concrete layer thicknesses;
10. Describe the profile;
11. Photograph the profile;
12. Sample additional material from the profile if required, and
13. Reinstate the pit.

The following additional information is relevant to the investigation:

- The procedures for HVS test section forensic investigations, detailed in the document entitled *Quality Management System for Site Establishment, Daily Operations, Instrumentation, Data Collection and Data Storage for APT Experiments (3)* were followed.
- The saw cuts were made at least 50 mm into the base to ensure that the slab could be removed from the pit without breaking.
- Nuclear density measurements were taken between the test section centerline and the inside (caravan side) edge of the test section. Two readings were taken: the first with the gauge aligned with the direction of trafficking and the second at 90° to the first measurement (Figure 5.1).
- DCP measurements were taken between the test section centerline and inside (caravan side) edge of the test section, and between the outside edge of the test section and the edge of the test pit on the traffic side (Figure 5.1). A third DCP measurement was taken between these two points if inconsistent readings were obtained.
- Layer thicknesses were measured from a leveled reference straightedge above the pit. This allowed the crossfall of the section to be included in the profile. Measurements were taken across the pit at 50-mm intervals.

5.3 Coring and Test Pit Excavation

Twelve cores were extracted from a line approximately 1.0 m (3.3 ft) from the edge of the test section, as shown in Figure 5.1. These were used to check layer thickness and to extract binder to quantify any effects of aging. An additional six cores were removed from within the test section to study crack behavior. A total of eight test pits were excavated for the study, one test pit on each HVS test section (between Stations 9 and 11 [see Figure 5.1]). The Station 9 test pit face was evaluated.

5.4 Core Evaluation

Average measurements for the 12 cores removed from a line adjacent to each test section are summarized in Table 5.1.

Table 5.1: Average Asphalt Concrete Thicknesses from Cores

Phase	Section	Average (mm)	Std. Deviation (mm)
1	600FD	130	4
	601FD	116	3
	602FD	117	3
	603FD	124	1
2	604FD	135	3
	605FD	130	1
	606FD	122	4
	607FD	119	4

The measurements from each set of cores show that the asphalt concrete thickness consistency along the length of each test section was good based on the low standard deviations recorded. The average core thickness varied between 116 mm (4.6 in.) on Section 601FD and 135 mm (5.3 in.) on Section 604FD indicating that there was some variation along the length of the test track.

Six cores were sampled from the trafficked area on each section to assess cracking (crack initiation, crack path, and crack termination), debonding, and any moisture related damage. Each core was cleaned and then scrutinized for any distresses. Photographs of the cores from each section are shown in Figure 5.2 through Figure 5.9. Apart from the debonding between lifts on the Phase 2 Control, no evidence of moisture damage was noted. Top-down cracks in the top lift were observed on all Phase 2 cores.

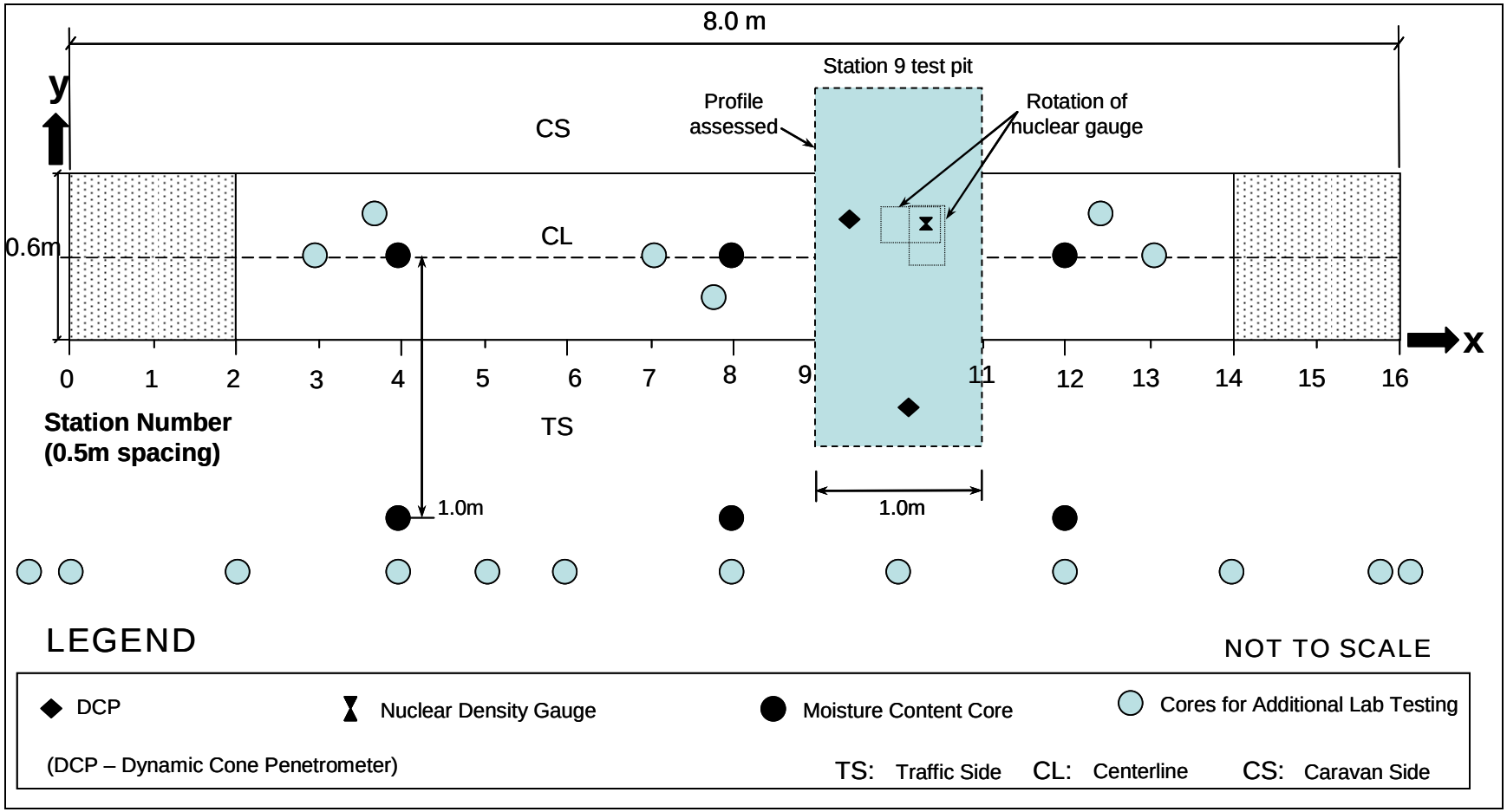

Figure 5.1: Test pit layout.

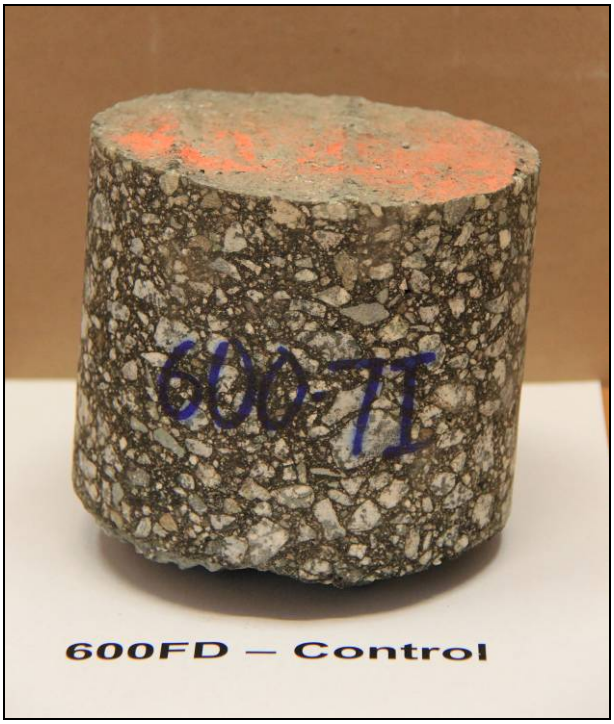

Figure 5.2: 600FD: Core from Trafficked Area.

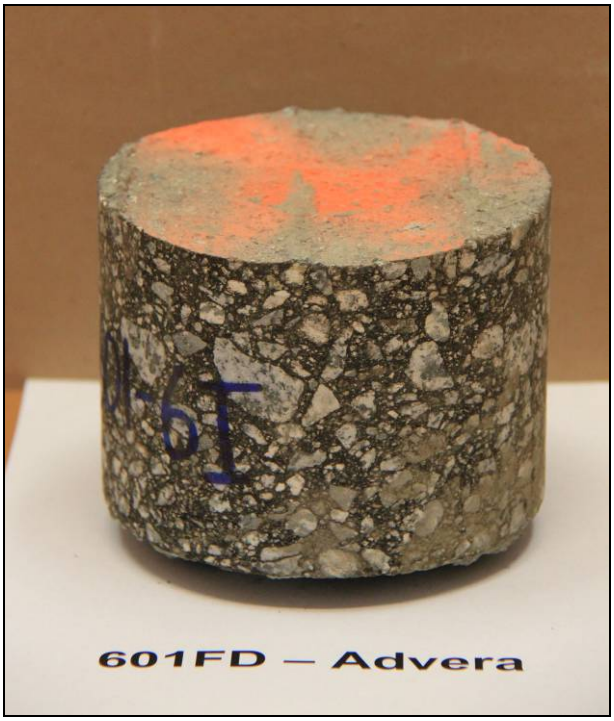

Figure 5.3: 601FD: Core from Trafficked Area.

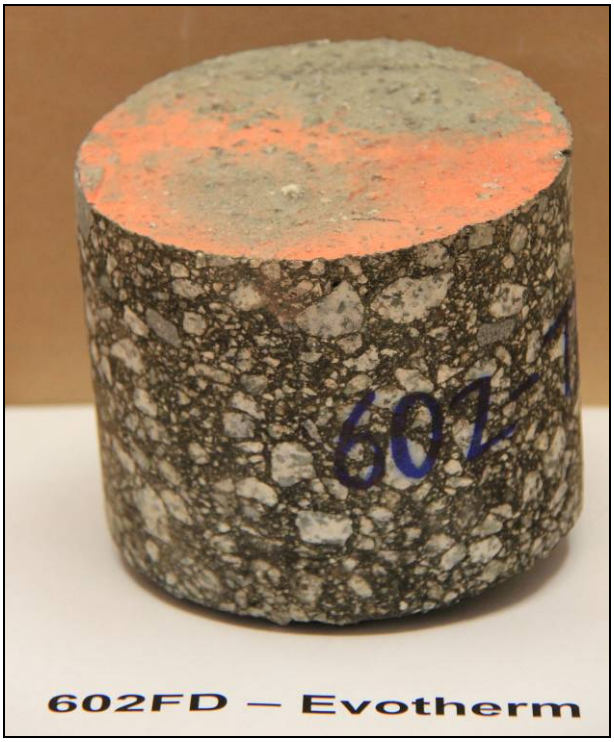

Figure 5.4: 602FD: Core from Trafficked Area.

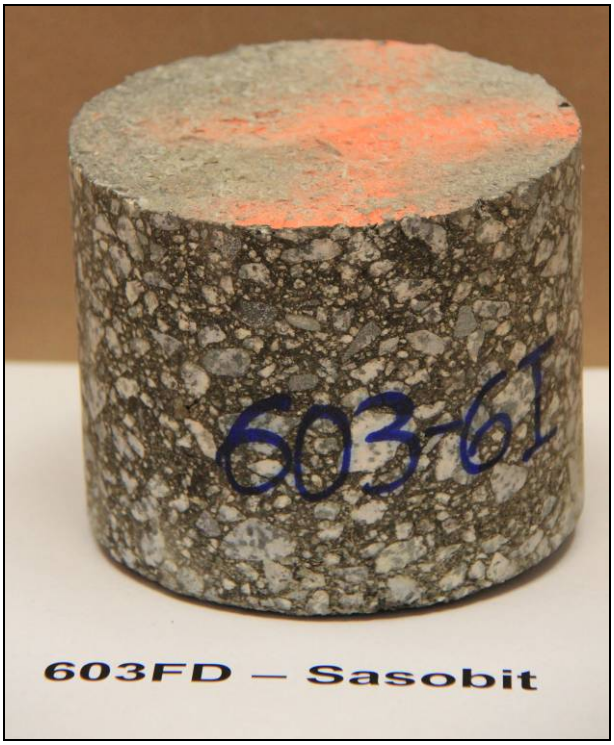

Figure 5.5: 603FD: Core from Trafficked Area.

Figure 5.6: 604FD: Core from Trafficked Area.

Figure 5.7: 605FD: Core from Trafficked Area.

Figure 5.8: 606FD: Core from Trafficked Area.

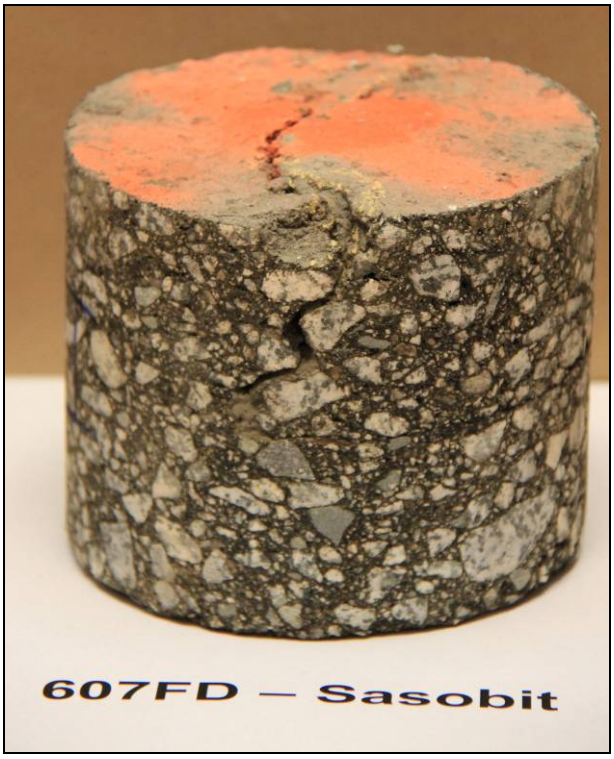

Figure 5.9: 607FD: Core from Trafficked Area.

5.5 Test Pit Profiles and Observations

Test pit profile illustrations are provided in Appendix A. Average measurements for each profile at Station 9 are listed in Table 5.2. The average thickness includes the wheelpaths and adjacent bulge. Minimum thickness measurements were always recorded in one of the wheelpaths, while maximum thickness measurements were always recorded in one of the adjacent bulges.

Table 5.2: Average Asphalt Concrete Thicknesses from Test Pit Profiles (Station 9).

	Section	Layer	Average (mm)	Std. Deviation (mm)	Minimum (mm)	Maximum (mm)
Phase 1	600FD	AC – top	55	5	46	60
		AC – bottom	71	4	65	77
		AC – total	126	6	116	135
		Base	300	4	294	307
	601FD	AC – top	68	5	60	76
		AC – bottom	49	1	46	52
		AC – total	117	5	109	124
		Base	301	2	297	305
	602FD	AC – top	66	9	53	80
		AC – bottom	53	4	47	60
		AC – total	119	6	108	128
		Base	304	1	301	306
	603FD	AC – top	57	2	52	60
		AC – bottom	64	2	62	67
		AC – total	120	3	116	127
		Base	303	1	301	305
Phase 2	604FD	AC – top	68	4	61	73
		AC – bottom	70	2	66	74
		AC – total	138	5	128	147
		Base	301	3	297	307
	605FD	AC – top	62	4	56	70
		AC – bottom	66	4	60	75
		AC – total	127	5	120	135
		Base	305	2	302	308
	606FD	AC – top	63	4	55	67
		AC – bottom	61	3	56	66
		AC – total	124	5	115	130
		Base	307	1	303	309
	607FD	AC – top	57	4	49	63
		AC – bottom	57	2	55	61
		AC – total	114	4	106	119
		Base	304	1	301	307

The measurements from each test pit show that layer thickness consistency on each test section was good based on the low standard deviations recorded. The average base thickness varied between 300 mm (11.8 in.) on Section 600FD and 307 mm (12.1 in.) on Section 606FD, while the combined asphalt concrete thickness varied between 114 mm (4.5 in.) on Section 607FD and 138 mm (5.4 in.) on Section 604FD. Average asphalt concrete thicknesses measured in the test pits were consistent with the

measurements from cores. A discussion of the observations from each test pit is provided in the following sections.

5.5.1 Section 600FD: Phase 1 Control

Observations from the Section 600FD test pit (Figure 5.10) include:

- The average thickness of the bottom lift of asphalt concrete was thicker (71 mm [2.8 in.]) than the design thickness (60 mm [2.4 in.]), while the average top lift thickness, which includes rut and bulge measurements, was slightly thinner (55 mm [2.2 in.]) than the design. The average combined thickness was slightly thicker (126 mm [5.0 in.]) than the design (120 mm [4.7 in.]).
- Rutting was restricted to the upper region of the top lift of asphalt. No rutting was noted in the bottom lift, base, or subgrade. Some displacement was recorded on either side of the trafficked area.
- The two asphalt concrete layers were well bonded to each other and well bonded to the aggregate base. The precise location of the bond between the two lifts was difficult to determine.
- Apart from rutting, no other distresses were noted in the asphalt layers.
- Base thickness showed very little variation across the profile. The material was well graded, no oversize material was observed, and the properties appeared to be very consistent. Material consistency was rated as very hard throughout the layer. No organic matter was observed.
- Moisture content in the base was rated as dry. There appeared to be little variation in moisture content through the depth of the base layer. There was no indication of higher moisture content at the interface between the base and asphalt concrete layers.
- The layer definition between the base and subgrade was clear. No punching of the base into the subgrade was noted.
- The subgrade was damp, crushed granite, similar to the base material. Consistency was rated as very hard. No organic matter was noted.

5.5.2 Section 601FD: Phase 1 Advera

Observations from the Section 601FD test pit (Figure 5.11) include:

- The average thickness of the bottom lift of asphalt concrete was thinner (49 mm [2.0 in.]) than the design thickness (60 mm [2.4 in.]), while the average top lift thickness, which includes rut and bulge measurements, was slightly thicker (68 mm [2.7 in.]) than the design. The average combined thickness was slightly thinner (117 mm [4.6 in.]) than the design (120 mm [4.7 in.]).
- Rutting was restricted to the upper region of the top lift of asphalt. No rutting was noted in the bottom lift, base, or subgrade. Some displacement was recorded on either side of the trafficked area.
- The two asphalt concrete layers were well bonded to each other and well bonded to the aggregate base. The precise location of the bond between the two lifts was difficult to determine.
- Apart from rutting, no other distresses were noted in the asphalt layers.
- The base and subgrade descriptions were consistent with those of the Control.

5.5.3 Section 602FD: Phase 1 Evotherm

Observations from the Section 602FD test pit (Figure 5.12) include:

- The average thickness of the bottom lift of asphalt concrete was slightly thinner (53 mm [2.1 in.]) than the design thickness (60 mm [2.4 in.]), while the average top lift thickness, which includes rut and bulge measurements, was slightly thicker (66 mm [2.6 in.]) than the design. The average combined thickness equaled the design (120 mm [4.7 in.]) thickness.

- Rutting was restricted to the upper region of the top lift of asphalt. No rutting was noted in the bottom lift, base, or subgrade. Some displacement was recorded on either side of the trafficked area.
- The two asphalt concrete layers were well bonded to each other and well bonded to the aggregate base. The precise location of the bond between the two lifts was very difficult to determine.
- Apart from rutting, no other distresses were noted in the asphalt layers.
- The base and subgrade descriptions were consistent with those of the Control.

5.5.4 Section 603FD: Phase 1 Sasobit

Observations from the Section 603FD test pit (Figure 5.13) include:

- The average thickness of the bottom lift of asphalt concrete was slightly thicker (64 mm [2.5 in.]) than the design thickness (60 mm [2.4 in.]), while the average top lift thickness, which includes rut and bulge measurements, was slightly thinner (57 mm [2.2 in.]) than the design. The average combined thickness equaled the design (120 mm [4.7 in.]) thickness.
- Rutting was restricted to the upper region of the top lift of asphalt. No rutting was noted in the bottom lift, base, or subgrade. Some displacement was recorded on either side of the trafficked area.
- The two asphalt concrete layers were well bonded to each other and well bonded to the aggregate base. The precise location of the bond between the two lifts was difficult to determine.
- Apart from rutting, no other distresses were noted in the asphalt layers.
- The base and subgrade descriptions were consistent with those of the Control.

5.5.5 Section 604FD: Phase 2 Control

Observations from the Section 604FD test pit (Figure 5.14) include:

- The average thickness of the bottom and top lifts of asphalt concrete were both thicker (70 mm [2.8 in.] and 68 mm [2.7 in.] respectively) than the design thickness (60 mm [2.4 in.]). The average combined thickness was considerably thicker (138 mm [5.4 in.]) than the design (120 mm [4.7 in.]).
- Rutting was restricted to the upper region of the top lift of asphalt. No rutting was noted in the bottom lift, base, or subgrade. Some displacement was recorded on either side of the trafficked area.
- The two asphalt concrete layers were debonded with some evidence of moisture at the interface.
- Apart from rutting, one top-down crack was observed in the profile. No evidence of moisture-related damage (e.g., stripping, ravelling) or other distresses were noted in the asphalt layers.
- The base and subgrade descriptions were consistent with those of the Phase 1 Control.

5.5.6 Section 605FD: Phase 2 Advera

Observations from the Section 605FD test pit (Figure 5.15) include:

- The average thickness of the bottom and top lifts of asphalt concrete were both slightly thicker (66 mm [2.6 in.] and 62 mm [2.4 in.] respectively) than the design thickness (60 mm [2.4 in.]). The average combined thickness was thus also slightly thicker (127 mm [5.0 in.]) than the design (120 mm [4.7 in.]).
- Rutting was restricted to the upper region of the top lift of asphalt. No rutting was noted in the bottom lift, base, or subgrade. Some displacement was recorded on either side of the trafficked area.
- The two asphalt concrete layers were well bonded to each other and well bonded to the aggregate base. The precise location of the bond between the two lifts was difficult to determine.
- One top-down crack was observed in the profile. No evidence of moisture-related damage (e.g., stripping, ravelling) or other distresses were noted in the asphalt layers. Although some stone plucking was evident on the surface of the section, no loose stones were observed in the profile.

- The base and subgrade descriptions were consistent with those of the Phase 1 Control.

5.5.7 Section 606FD: Phase 2 Evotherm

Observations from the Section 606FD test pit (Figure 5.16) include:

- The average thickness of the bottom and top lifts of asphalt concrete were both slightly thicker (61 mm [2.4 in.] and 63 mm [2.5 in.] respectively) than the design thickness (60 mm [2.4 in.]). The average combined thickness was thus also slightly thicker (124 mm [4.9 in.]) than the design (120 mm [4.7 in.]).
- Rutting was restricted to the upper region of the top lift of asphalt. No rutting was noted in the bottom lift, base, or subgrade. Some displacement was recorded on either side of the trafficked area.
- The two asphalt concrete layers were well bonded to each other and well bonded to the aggregate base. The precise location of the bond between the two lifts was difficult to determine.
- Top-down cracking was observed in the profile. No evidence of moisture-related damage (e.g., stripping, ravelling) or other distresses were noted in the asphalt layers. Although some stone plucking was evident on the surface of the section, no loose stones were observed in the profile.
- The base and subgrade descriptions were consistent with those of the Phase 1 Control.

5.5.8 Section 607FD: Phase 2 Sasobit

Observations from the Section 607FD test pit (Figure 5.17) include:

- The average thicknesses of the bottom and top lifts of asphalt concrete were both slightly thinner (both 57 mm [2.2 in.]) than the design thickness (60 mm [2.4 in.]). The average combined thickness was thus also thinner (114 mm [4.5 in.]) than the design (120 mm [4.7 in.]).
- Rutting was restricted to the upper region of the top lift of asphalt. No rutting was noted in the bottom lift, base, or subgrade. Some displacement was recorded on either side of the trafficked area.
- The two asphalt concrete layers were debonded in the untrafficked area of the test pit, but not in the trafficked area. Some evidence of moisture at the interface was noted in the debonded areas. The asphalt concrete layers were well bonded to the aggregate base.
- Top-down cracking was observed in the profile. No evidence of moisture-related damage (e.g., stripping, ravelling) or other distresses were noted in the asphalt layers. Although some stone plucking was evident on the surface of the section, no loose stones were observed in the profile.
- The base and subgrade descriptions were consistent with those of the Phase 1 Control.

Figure 5.10: 600FD: Test pit photographs.

Figure 5.11: 601FD: Test pit photographs.

Figure 5.12: 602FD: Test pit photographs.

Figure 5.13: 603FD: Test pit photographs.

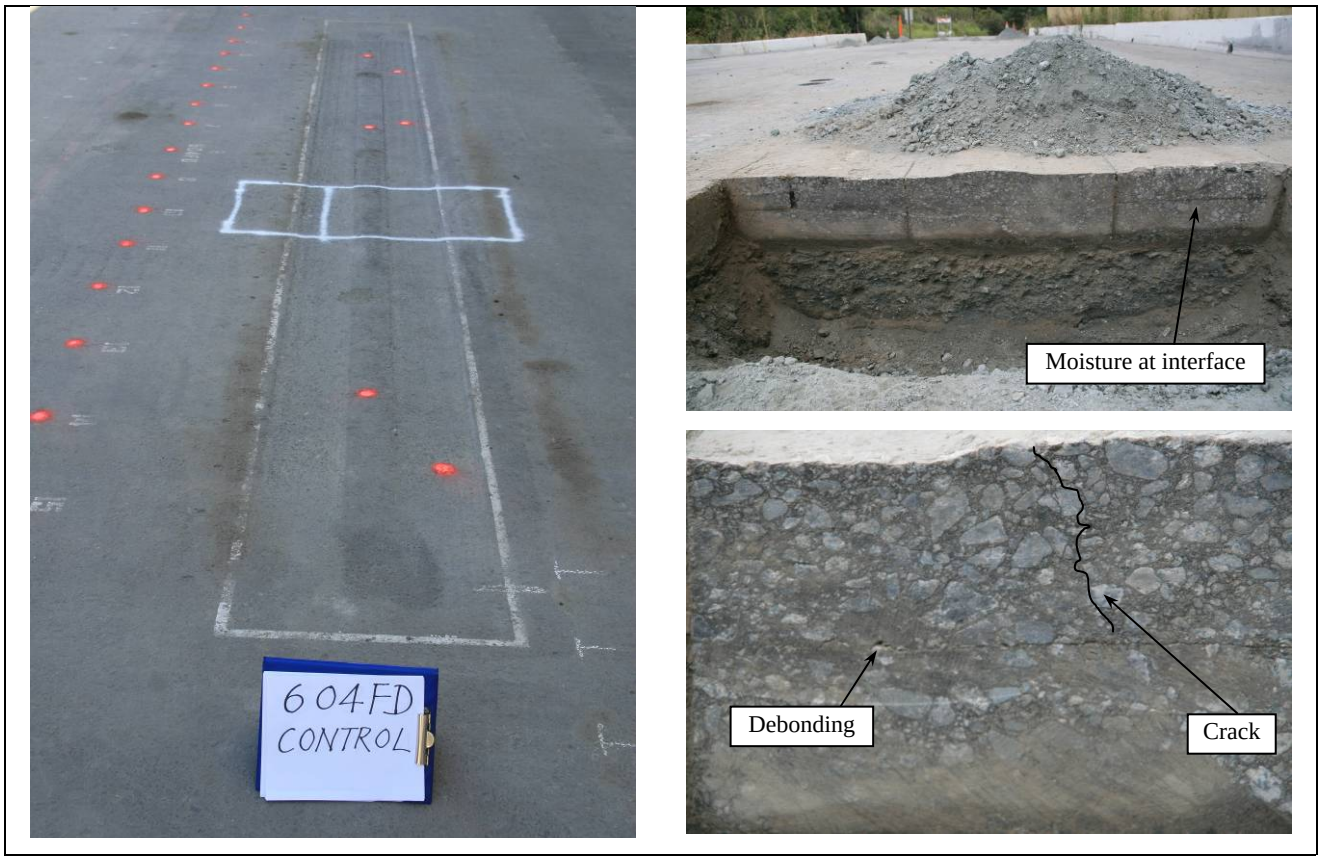

Figure 5.14: 604FD: Test pit photographs.

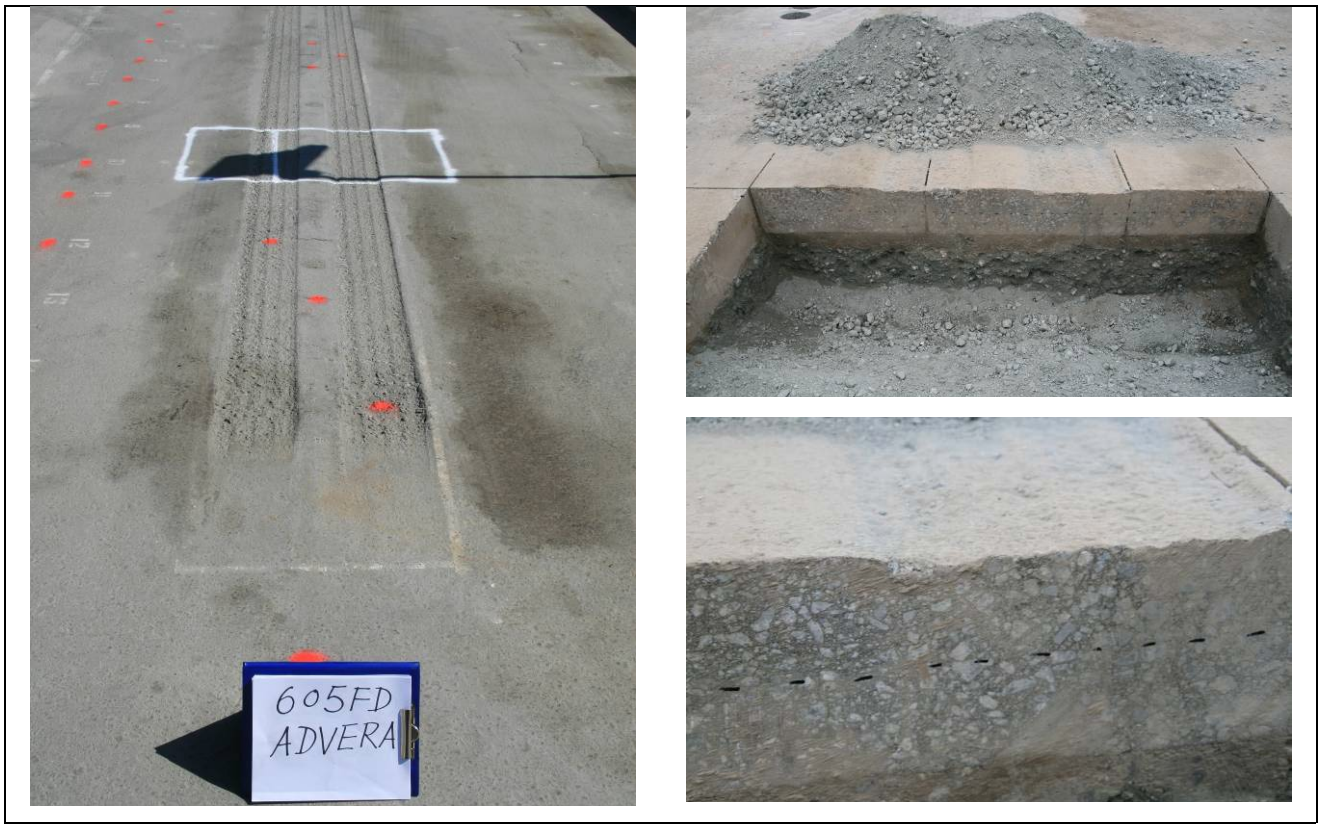

Figure 5.15: 605FD: Test pit photographs.

Figure 5.16: 606FD: Test pit photographs.

Figure 5.17: 607FD: Test pit photographs.

5.6 Base-Course Density and Moisture Content

Table 5.3 summarizes the base-course density and moisture content measurements on each section. The table includes the wet and dry density and moisture content of the base in the HVS wheelpath and in the adjacent untrafficked area (see Figure 5.1). Measurements were taken with a nuclear gauge. Laboratory-determined gravimetric moisture contents of the base material (average of two samples from the top and bottom of the excavated base) and recalculated dry densities of the base (using the average gauge-determined wet density and laboratory-determined gravimetric moisture content) are also provided. Each gauge measurement is an average of two readings taken at each location in the pit (gauge perpendicular to wheelpath and parallel to wheelpath as shown in Figure 5.1). Subgrade densities and moisture contents were not measured.

Table 5.3: Summary of Base Course Density and Moisture Content Measurements

Phase	Section	Depth	Nuclear Gauge						Laboratory	
			Wheelpath			Untrafficked				
			Wet Density (kg/m^3)	Moisture (%)	Dry Density (kg/m^3)	Wet Density (kg/m^3)	Moisture (%)	Dry Density (kg/m^3)	Base Moisture (%)	Dry Density* (kg/m^3)
1	600FD (Control)	50	2,146	6.5	2,016	2,302	6.1	2,169	4.2	2,227
		100	2,259	6.3	2,126	2,382	6.0	2,247		
		150	2,334	6.3	2,195	2,427	6.0	2,291		
		200	2,370	5.8	2,242	2,460	5.6	2,330		
	601FD (Advera)	50	2,220	7.4	2,067	2,352	5.8	2,222	4.1	2,346
		100	2,382	6.7	2,232	2,401	5.9	2,266		
		150	2,463	6.6	2,311	2,422	5.8	2,302		
		200	2,483	5.8	2,347	2,466	5.5	2,337		
	602FD (Evotherm)	50	2,194	5.5	2,080	2,210	5.5	2,095	3.5	2,271
		100	2,262	5.6	2,143	2,347	5.1	2,235		
		150	2,378	5.4	2,257	2,401	4.9	2,289		
		200	2,413	5.1	2,295	2,439	4.8	2,323		
	603FD (Sasobit)	50	2,360	5.9	2,229	2,360	7.1	2,204	4.0	2,401
		100	2,451	5.2	2,318	2,441	6.7	2,288		
		150	2,510	5.6	2,378	2,492	6.5	2,340		
		200	2,531	5.6	2,395	2,502	6.3	2,354		
2	604FD (Control)	50	2,376	6.0	2,242	2,288	6.6	2,146	4.0	2,391
		100	2,444	5.8	2,309	2,385	6.4	2,245		
		150	2,498	5.6	2,365	2,446	6.3	2,299		
		200	2,517	5.6	2,379	2,457	5.9	2,335		
	605FD (Advera)	50	2,348	6.7	2,201	2,397	6.2	2,257	3.8	2,391
		100	2,443	6.6	2,292	2,485	6.0	2,343		
		150	2,495	6.3	2,347	2,520	5.8	2,381		
		200	2,507	6.6	2,353	2,528	5.7	2,392		
	606FD (Evotherm)	50	2,403	6.0	2,267	2,396	6.0	2,259	4.0	2,412
		100	2,475	5.7	2,343	2,464	5.8	2,328		
		150	2,518	5.8	2,380	2,500	5.8	2,362		
		200	2,533	5.6	2,399	2,517	6.0	2,374		
	607FD (Sasobit)	50	2,380	6.1	2,244	2,352	6.4	2.211	3.8	2,367
		100	2,423	5.8	2,291	2,400	6.4	2.257		
		150	2,466	5.6	2,336	2,447	6.2	2.280		
		200	2,481	5.6	2,348	2,482	6.2	2.336		

* Recalculated dry density using nuclear gauge wet density and laboratory gravimetric moisture content.

The following observations were made:

- Densities increased with increasing depth, following a similar pattern to the densities measured after construction of the test track *(2)*.
- Densities were consistent throughout the section and there was very little difference between the densities measured in the trafficked and untrafficked areas. Nuclear gauge–determined dry densities of the base at the four depths measured ranged between 2,126 kg/m^3 ([132.7 lb/ft^3] on Section 600FD) and 2,399 kg/m^3 ([149.8 lb/ft^3] on Section 606FD) for the eight test pits. The average dry density for the eight test pits was 2,311 kg/m^3 (144.3 lb/ft^3), (standard deviation 60 kg/m^3 [3.7 lb/ft^3]), which corresponds with the average dry density of 2,297 kg/m^3 (143.4 lb/ft^3) recorded after construction, indicating that the base density did not increase under trafficking. The average nuclear gauge–determined wet density was 2,447 kg/m^3 (152.8 lb/ft^3) with a standard deviation of 63 kg/m^3 (3.9 lb/ft^3).
- Nuclear gauge–determined moisture contents of the eight test pits, measured at three intervals (100 mm, 150 mm and 200 mm) in the top 200 mm of the base, ranged between 4.8 percent and 6.6 percent with an average of 5.9 percent (standard deviation of 0.5 percent), very similar to the measurements recorded after construction. Moisture contents at the top of the base were generally slightly higher compared to those in the lower regions of the base and may have been influenced by the water from the saw cutting. The optimum moisture content of the base material, determined by Graniterock Company prior to placing the asphalt concrete, was 6.5 percent.
- Laboratory-determined gravimetric moisture contents varied between 3.5 percent and 4.2 percent, with an average of 3.9 percent and standard deviation of 0.2 percent. The laboratory-determined moisture contents were on average 2.0 percent lower than those recorded by the nuclear gauge, and appeared more consistent with visual evaluations of the test pit face, and more representative of typical dry back conditions in base materials. The higher moisture contents determined with the nuclear gauge could be associated with the presence of some excess moisture from the saw cutting operation during pit excavation. Recalculated dry densities, determined using the gauge wet density and gravimetric moisture content, were therefore slightly higher than the gauge-determined dry densities.

5.7 Dynamic Cone Penetrometer

Dynamic Cone Penetrometer (DCP) measurements were attempted in each test pit, both in the trafficked and untrafficked areas. Full-depth penetrations were not possible in any of the test pits, with penetration stopping (i.e., penetration of less than 1.0 mm in 25 blows) at between 140 mm (Section 605FD after 110 blows) and 237 mm (Section 602FD after 130 blows). DCP measurements are typically taken to 800 mm in order to determine a valid DCP structure number and to allow calculation of California Bearing Ratio, unconfined compressive strength, and modulus values. This inability to penetrate the material is indicative of a very strong, well-compacted base (observed), well-graded but stony material (observed), and/or cementation in the base (not observed during the test pit assessment). A summary of the measurements is provided in Table 5.4. The results show some variation; however, this is attributed to the stony nature of the material and not to differences in strength/stiffness.

Table 5.4: Summary of Dynamic Cone Penetrometer Measurements

Phase	Section	No. of Blows		Penetration Depth		mm/Blow	
		Trafficked	Untrafficked	Trafficked	Untrafficked	Trafficked	Untrafficked
1	600FD	175	95	209	192	1.2	2.0
	601FD	155	120	202	205	1.3	1.7
	602FD	160	130	224	237	1.4	1.8
	603FD	160	130	209	211	1.3	1.6
2	604FD	160	140	168	172	1.1	1.2
	605FD	110	145	140	172	1.3	1.2
	606FD	185	170	192	190	1.0	1.1
	607FD	90	130	184	220	2.0	1.7

5.8 Forensic Investigation Summary

A forensic investigation of all test sections indicated that the rutting was confined to the upper lift of the asphalt concrete. No evidence of moisture damage was noted on any of the sections, although some evidence of debonding between the two lifts of asphalt was noted on the Control section. All sections had some top-down cracking in the top lift of the asphalt concrete.

6 PHASE 2a LABORATORY TEST DATA SUMMARY

6.1 Introduction

This chapter discusses laboratory testing on field-mixed, laboratory-compacted (FMLC) specimens, designated as Phase 2a laboratory testing. Laboratory testing on laboratory-mixed, laboratory-compacted (LMLC) specimens (designated as Phase 2b laboratory testing) was delayed due to project administration constraints and will be discussed in a separate report.

6.1.1 Specimen Preparation

Specimens were prepared at the same time as construction of the test track. Each mix was sampled from the truck before it was tipped into the paver. Samples of each mix were weighed out according to the theoretical maximum specific gravity (RICE) values (Table 6.1) provided by the Graniterock laboratory, and then compacted into ingots using a rolling wheel compactor *(2)*. The target air-void content for all mixes was set at 6.0 percent. The ingots were then transported to the UCPRC's Richmond Field Station, where they were cored (for shear testing) and sawn into beams (for beam fatigue testing).

Table 6.1: Theoretical Maximum Specific Gravity (RICE) Values

Mix	RICE Value
Control	2.5757
Advera	2.5958
Evotherm	2.5893
Sasobit	2.5979

6.2 Experiment Design

Phase 2a laboratory testing included a limited number of shear and fatigue tests following a reduced experiment matrix based on the Phase 1 laboratory testing *(2)*.

6.2.1 Shear Testing

Test Method

The AASHTO T-320 Permanent Shear Strain and Stiffness Test was used for shear testing in this study. In the standard fatigue test methodology, cylindrical test specimens 150 mm in diameter and 50 mm thick (6.0 in. by 2.0 in.) are subjected to repeated loading in shear using a 0.1-second haversine waveform followed by a 0.6-second rest period. Three different shear stresses are applied while the permanent (unrecoverable) and recoverable shear strains are measured. The permanent shear strain versus applied repetitions is normally recorded up to a value of five percent although 5,000 repetitions are called for in

the AASHTO procedure. A constant temperature is maintained during the test (termed the *critical temperature)*, representative of the local environment. Shear Frequency Sweep Tests are used to establish the relationship between complex modulus and load frequency. The same loading is used at frequencies of 15, 10, 5, 2, 1, 0.5, 0.2, 0.1, 0.05, 0.02, and 0.01 Hz.

Number of Tests

Due to the limited number of specimens available for testing, the experimental matrix used in the Phase 1 testing was reduced for the Phase 2a testing from 18 to eight shear tests on each mix (total of 32 tests for the four mixes) as follows. No frequency sweep tests were carried out.

- Standard test
  - Two temperatures: 45°C and 55°C (113°F and 131°F)
  - Two stresses: 70 kPa and 130 kPa (10.2 and 18.9 psi)
  - Two replicates.

6.2.2 Fatigue Testing

Test Method

The AASHTO T-321 Flexural Controlled-deformation Fatigue Test method was followed. In the standard test, three replicate beam test specimens, 50 mm thick by 63 mm wide by 380 mm long (2.0 x 2.5 x 15 in.), are subjected to four-point bending using a sinusoidal waveform at a loading frequency of 10 Hz. Testing is usually performed in both dry and wet condition at two different strain levels and at three different temperatures. Flexural Controlled-deformation Frequency Sweep Tests are used to establish the relationship between complex modulus and load frequency. The same sinusoidal waveform is used in a controlled deformation mode and at frequencies of 15, 10, 5, 2, 1, 0.5, 0.2, 0.1, 0.05, 0.02, and 0.01 Hz. The upper limit of 15 Hz is a constraint imposed by the capabilities of the test machine. To ensure that the specimen is tested in a nondestructive manner, the frequency sweep test is conducted at a small strain amplitude level, proceeding from the highest frequency to the lowest in the sequence noted above.

The wet specimens used in the fatigue and frequency sweep tests were conditioned following the beam-soaking procedure described in Appendix B. In this procedure, the beam is first vacuum-saturated to ensure a saturation level greater than 70 percent, and then placed in a water bath at 60°C (140°F) for 24 hours, followed by a second water bath at 20°C (68°F) for two hours. The beams are then wrapped with Parafilm™ and tested within 24 hours after soaking.

Number of Tests

Due to the limited number of specimens available for testing, the experimental matrix used in the Phase 1 testing was reduced for the Phase 2a testing from 36 to 12 fatigue tests on each mix (total of 48 tests for the four mixes) and from 12 to 6 frequency sweep tests as follows:

- Standard test:
  - Two conditions (wet and dry)
  - One temperature, namely, 20°C (68°F)
  - Two strains: 200 microstrain and 400 microstrain
  - Three replicates.
- Frequency sweep test:
  - Two conditions (wet and dry)
  - Three temperatures: 10°C, 20°C, and 30°C (50°F, 68°F, and 86°F)
  - One strain: 100 microstrain
  - One replicate.

6.3 Test Results

6.3.1 Shear Tests

The shear test results are summarized in Table 6.2 and illustrated and discussed in more detail in the following sections.

Air-Void Content

Air-void contents were measured using the modified Parafilm™ method (AASHTO T-275A). Table 6.3 summarizes the air-void distribution categorized by mix type, test temperature, and test shear stress level. Figure 6.1 presents the summary boxplots of air-void content based on additive type. Although there was considerable difference in the air-void contents of the individual specimens, the average air-void contents between the four mixes was similar. The warm mixes had a lower variation in air-void content compared to the Control mix. The air-void contents of the FMLC specimens were significantly lower than those of the Phase 1 FMFC specimens.

Table 6.2: Summary of Shear Test Results on FMLC Specimens

Mix	Specimen No.	Air-Voids (%)	Temperature (°C)	Shear Stress Level (kPa)	Shear Modulus (kPa)	PSS at 5,000 cycles[1]	Cycles to 5% PSS
Control	1	6.8	45.0	70	189.4	0.015878	286,495*
	2	7.5	44.9	71	192.5	0.011991	597,608*
	3	3.6	44.9	131	247.4	0.024681	46,916*
	4	3.7	44.8	130	236.3	0.022555	56,065*
	5	5.2	54.9	61	83.4	0.032776	21,496
	6	4.7	54.8	60	89.3	0.026029	43,603*
	7	5.6	55.1	60	85.5	0.034883	11,933
	8	6.1	54.8	91	90.2	0.052875	4,375
	9	4.0	54.7	93	98.3	0.040178	12,501*
	10	6.1	54.9	93	93.0	0.058405	3,823
	11	4.8	54.8	123	86.2	0.051428	4,781
	12	4.7	54.9	126	103.5	0.065251	3,139
Advera	1	5.5	44.9	70	189.4	0.013489	22,935,445*
	2	6.8	44.8	70	192.9	0.016504	1,237,272*
	3	4.9	44.9	124	180.0	0.026592	31,909*
	4	5.1	44.9	123	190.0	0.023857	45,937*
	5	5.6	54.8	66	86.1	0.031308	211,407*
	6	5.2	55.2	67	85.1	0.027886	47,278*
	7	5.4	54.9	124	94.5	0.048764	5,211
Evotherm	1	4.6	44.9	69	225.4	0.011129	207,760,118*
	2	4.3	44.9	75	196.3	0.011507	4,191,724*
	3	5.8	44.9	134	254.9	0.026413	17,893
	4	4.6	44.9	129	235.4	0.023137	71,429*
	5	5.7	54.9	61	86.5	0.027876	38,138*
	6	4.9	55.0	62	94.6	0.024007	201,284*
	7	4.9	55.0	128	101.9	0.064182	2,953
	8	5.2	55.3	128	95.7	0.094737	1,619
	9	5.0	55.2	127	85.4	0.079373	2,593
Sasobit	1	5.3	45.0	70	404.3	0.006411	3.86004E+11*
	2	5.3	45.0	75	398.5	0.011527	1,228,791,460*
	3	5.6	45.0	136	387.6	0.017129	980,387*
	4	5.8	45.0	132	398.4	0.015306	2,284,025*
	5	5.6	55.0	72	170.1	0.013162	14,736,351*
	6	5.3	55.0	74	146.8	0.018936	129,352*
	7	5.8	55.0	127	155.6	0.038227	8,781
	8	5.5	54.9	126	141.9	0.031892	18,169

[1] Permanent Shear Strain * Values extrapolated

Table 6.3: Summary of Air-Void Contents of FMLC Shear Test Specimens

Temperature		Stress Level (kPa)	Air Void Content							
			Control		Advera		Evotherm		Sasobit	
°C	°F		Mean	SD[1]	Mean	SD	Mean	SD	Mean	SD
45	113	70	7.2	0.5	6.2	1.0	4.5	0.2	5.3	0.0
		130	3.7	-.1	5.0	0.2	5.2	0.9	5.7	0.2
55	131	70	5.2	0.5	5.4	0.3	5.3	0.6	5.5	0.2
		130	4.6	0.2	5.4	0.0	5.0	0.2	5.7	0.2
Overall			5.2	1.2	5.5	0.6	5.0	0.5	5.5	0.2
Overall for Phase 1			6.8	0.7	8.4	0.7	8.8	0.7	8.1	0.6

[1] SD: Standard deviation.

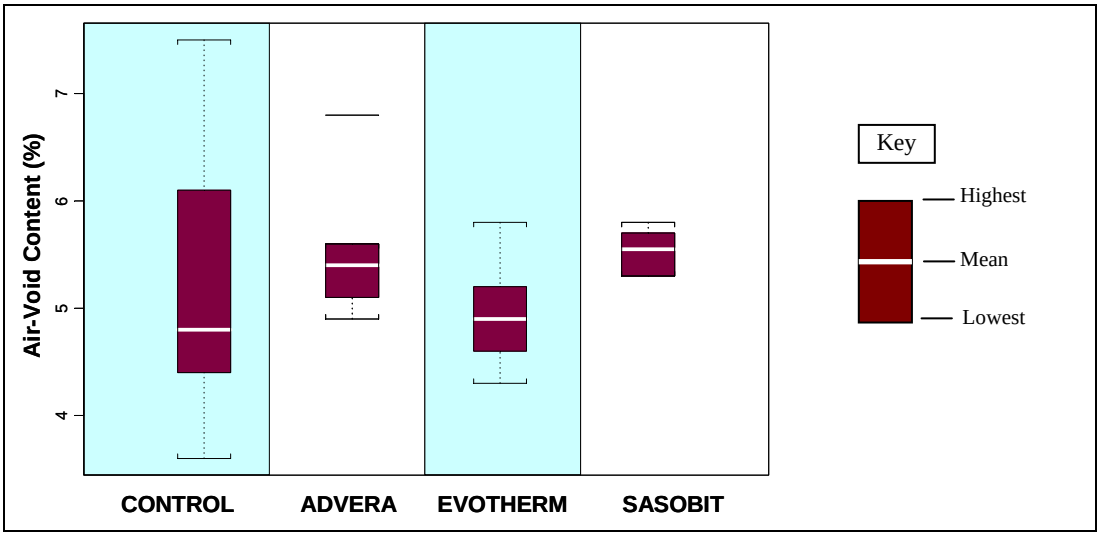

Figure 6.1: Air-void contents of FMLC shear specimens.

6.3.2 Resilient Shear Modulus (*G*)

The resilient shear modulus results for the four mixes are presented in Table 6.2 and summarized in Figure 6.2. The results indicate that:

- The resilient shear modulus was influenced by temperature, with the modulus increasing with decreasing temperature.
- Resilient shear modulus was not influenced by stress.
- The variation of resilient shear moduli at 45°C was greater compared to the results at 55°C.
- The Sasobit specimens had the highest resilient shear modulus of the four mixes at both temperatures (significantly higher at 45°C and marginally higher at 55°C), as expected given the lower binder content.
- At the higher testing temperature (i.e., mix will be more susceptible to rutting), all mixes had essentially the same shear modulus indicating that the use of the additives and lower production and compaction temperatures did not significantly influence the performance of the mixes in this test.

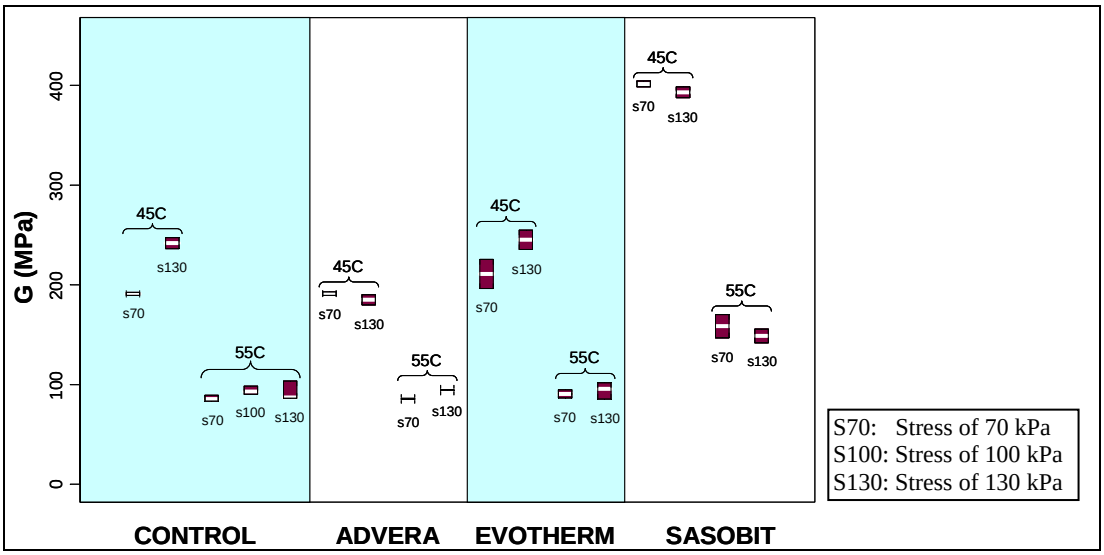

Figure 6.2: Summary boxplots of resilient shear modulus.

Cycles to Five Percent Permanent Shear Strain

The number of cycles to five percent permanent shear strain provides an indication of the rut-resistance of an asphalt mix, with higher numbers of cycles implying better rut-resistance. Figure 6.3 summarizes the shear test results in terms of the natural logarithm of this parameter. The results indicate that:

- The rut-resistance capacity decreased with increasing temperature and stress level, as expected.
- The warm-mixes had higher numbers of cycles to five percent permanent shear strain than the Control (Sasobit, followed by Evotherm and Advera) at 70 kPa at both temperatures.
- There was no significant difference in performance between the mixes at the higher stress level at both temperatures.
- At the higher stress and testing temperature, all mixes had essentially the same number of cycles to five percent permanent shear strain, indicating that the use of the additives and lower production and compaction temperatures did not significantly influence the performance of the mixes in this test.

Permanent Shear Strain at 5,000 Cycles

The measurement of permanent shear strain (PSS) accumulated after 5,000 cycles provides an alternative indication of the rut-resistance capacity of an asphalt mix. The smaller the permanent shear strain the better the mix's rut-resistance capacity. Figure 6.4 summarizes the rutting performance of the four mixes in terms of the natural logarithm of this parameter (i.e., increasingly negative values represent smaller cumulative permanent shear strain.). The results indicate the following:

- The effect of shear stress level was significant at both temperatures.
- The higher the temperature and stress level the larger the cumulative permanent shear strain.
- In general, and as expected, the Sasobit mix accumulated the least permanent shear strain when compared with the other mixes at the same stress level and temperature. The other three mixes did not appear to have obvious differences per stress level and per test temperature.

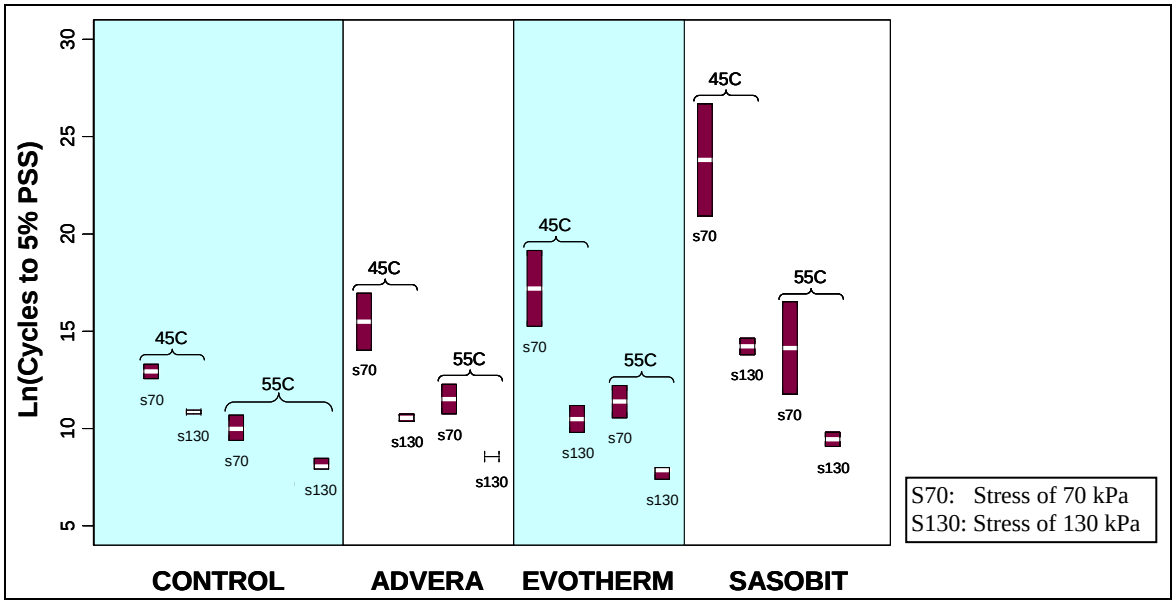

Figure 6.3: Summary boxplots of cycles to 5% permanent shear strain.

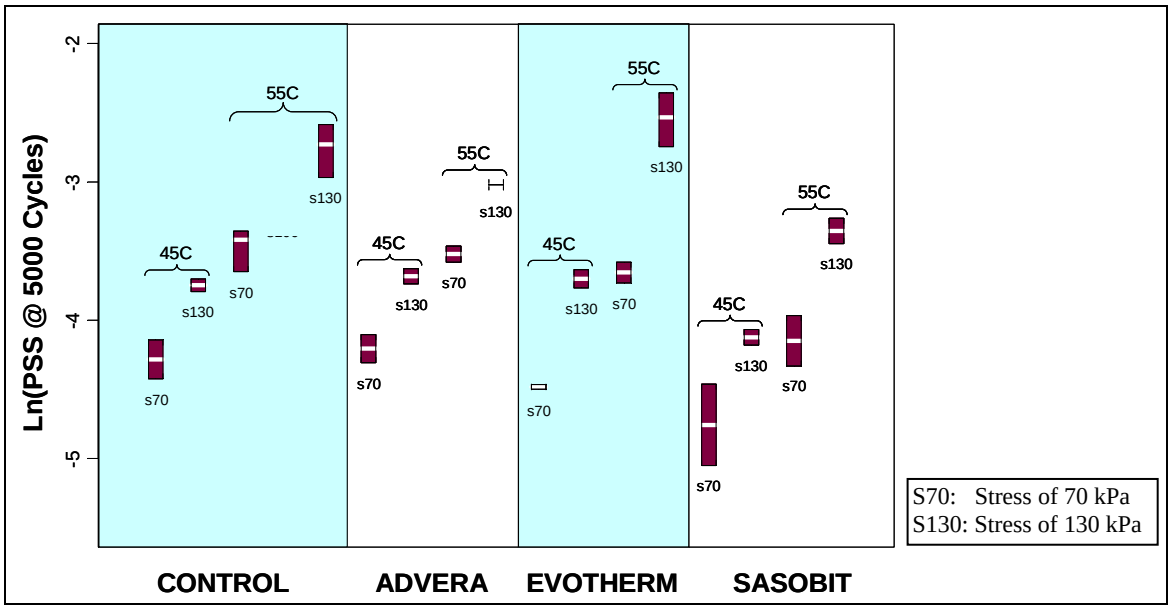

Figure 6.4: Summary boxplots of cumulative permanent shear strain at 5,000 cycles.

Figure 6.5 shows a plot of the number of cycles to five percent permanent shear strain against the permanent shear strain accumulated after 5,000 load repetitions for each of the tests. The results show that the permanent shear strain accumulated after 5,000 load repetitions is highly negative-correlated with the cycles to five percent permanent shear strain, as expected.

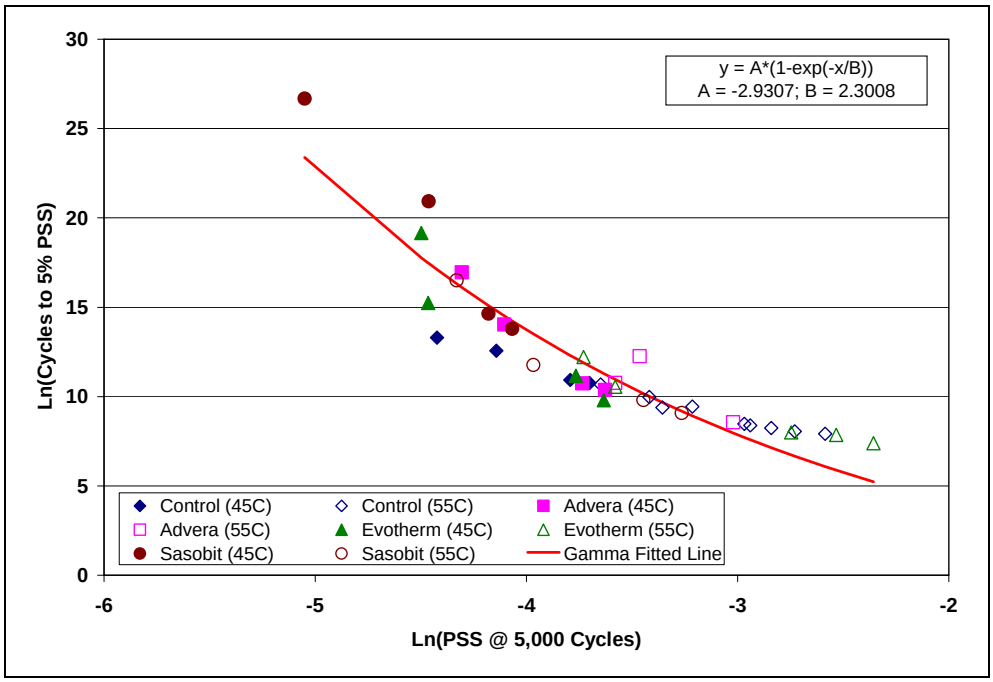

Figure 6.5: Cycles to 5% permanent shear strain versus permanent shear strain after 5,000 cycles.
(Double natural logarithm scale)

6.3.3 Fatigue Beam Tests

Fatigue beam test results are summarized in Table 6.4. The results of each test are discussed in the following sections.

Air-Void Content

Air-void contents were measured using the modified Parafilm™ method (AASHTO T-275A). Table 6.5 and Table 6.6 summarize the air-void distribution categorized by mix type, test temperature, and test tensile strain level for the fatigue beam and frequency sweep specimens, respectively. Figure 6.6 and Figure 6.7 present the summary boxplots of air-void content for the wet and dry fatigue beam and flexural frequency sweep specimens, respectively. There was no significant difference in air-void content between the dry and wet specimens, but significant differences among the four mixes. The Control specimens had the lowest mean air-void content, followed by the Evotherm, Sasobit and Advera mix specimens. The differences between the mixes were factored into the analysis of the results. The air-void contents of the FMLC specimens were significantly lower than those on the Phase 1 FMFC specimens.

Table 6.4: Summary of Fatigue Beam Test Results on FMLC Specimens

Mix	Specimen No.	Air-Voids[1] (%)	Temperature (°C)	Strain Level (microstrain)	Initial Phase Angle (Deg.)	Initial Stiffness (MPa)	Fatigue Life (Nf)
Control	1	3.7	19.61	202	28.69	5,138	7,668,551*
	2	3.8	19.21	200	19.92	5,444	42,607,441*
	3	4.5	20.07	201	28.59	5,165	7,801,703*
	4	3.4	20.19	413	30.81	4,936	78,192
	5	3.5	20.18	402	29.43	5,609	18,093
	6	3.6	19.57	399	31.04	5,086	20,022
Advera	1	7.5	20.15	0.000213	32.19	3,436	2,558,313
	2	8.2	20.11	0.000207	32.17	2,677	113,782
	3	6.1	20.25	0.000411	33.48	3,366	12,068
	4	6.8	19.60	0.000404	31.30	4,357	66,793
Evotherm	1	4.4	20.16	0.000210	28.86	5,056	15,918,352*
	2	5.6	20.16	0.000202	30.10	5,020	22,421,167*
	3	4.8	19.65	0.000200	27.30	5,291	30,456,475*
	4	4.7	20.29	0.000421	30.83	4,748	86,618
	5	5.1	20.17	0.000400	28.97	5,339	33,930
	6	4.4	20.39	0.000419	30.13	4,873	145,595
Sasobit	1	5.6	19.23	0.000207	22.53	5,195	1,855,302
	2	5.2	20.16	0.000203	26.23	4,773	3,001,302
	3	5.4	19.60	0.000203	27.02	4,438	758,483
	4	6.9	20.44	0.000415	30.47	3,615	9,887
	5	6.1	20.29	0.000404	28.29	4,285	27,506
	6	6.9	19.85	0.000407	23.85	5,049	18,204

Notes:

*: Extrapolated values.

[1] RICE values for air-void content calculation: Control (2.5757), Advera (2.5958), Evotherm (2.5893), and Sasobit (2.5979).

Table 6.5: Summary of Air-Void Contents of Fatigue Beam Specimens

Condition	Strain (μstrain)	Temp.		Control		Advera		Evotherm		Sasobit	
		°C	°F	Mean	SD[1]	Mean	SD	Mean	SD	Mean	SD
Dry	200	20	68	4.7	0.4	6.9	2.1	5.1	0.7	6.4	0.9
	400			3.6	0.2	6.3	1.1	5.3	1.4	5.8	0.4
	Overall			4.2	0.7	6.6	1.4	5.2	1.0	6.1	0.7
	Overall for Phase 1			7.1	0.6	7.6	1.1	8.1	1.0	6.9	0.6
Wet	200	20	68	4.0	0.4	7.9	0.5	4.9	0.6	5.4	0.2
	400			3.5	0.1	6.5	0.6	4.7	0.4	6.6	0.5
	Overall			3.8	0.4	7.2	0.9	4.8	0.5	6.0	0.8
	Overall for Phase 1			7.1	0.7	7.5	0.9	8.6	0.7	6.7	0.4

[1] SD: Standard deviation.

Table 6.6: Summary of Air-Void Contents of Flexural Frequency Sweep Specimens

Condition	Control		Advera		Evotherm		Sasobit	
	Mean	SD[1]	Mean	SD	Mean	SD	Mean	SD
Dry	3.7	0.4	6.9	1.3	4.8	0.6	5.7	0.3
Wet	5.4	0.4	5.9	0.2	4.8	0.2	6.1	0.7

[1] SD: Standard deviation.

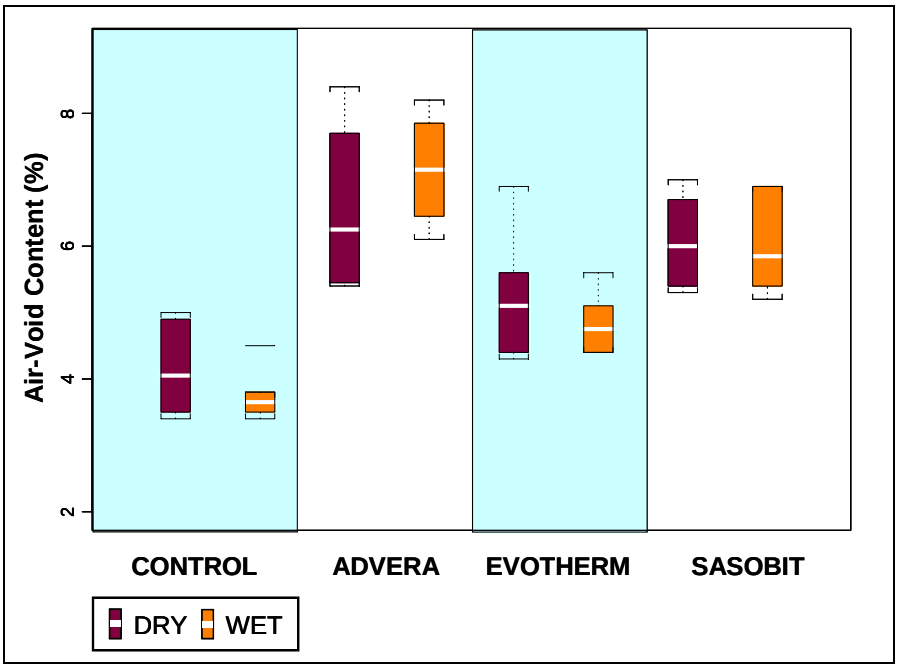

Figure 6.6: Air-void contents of fatigue beam specimens (dry and wet).

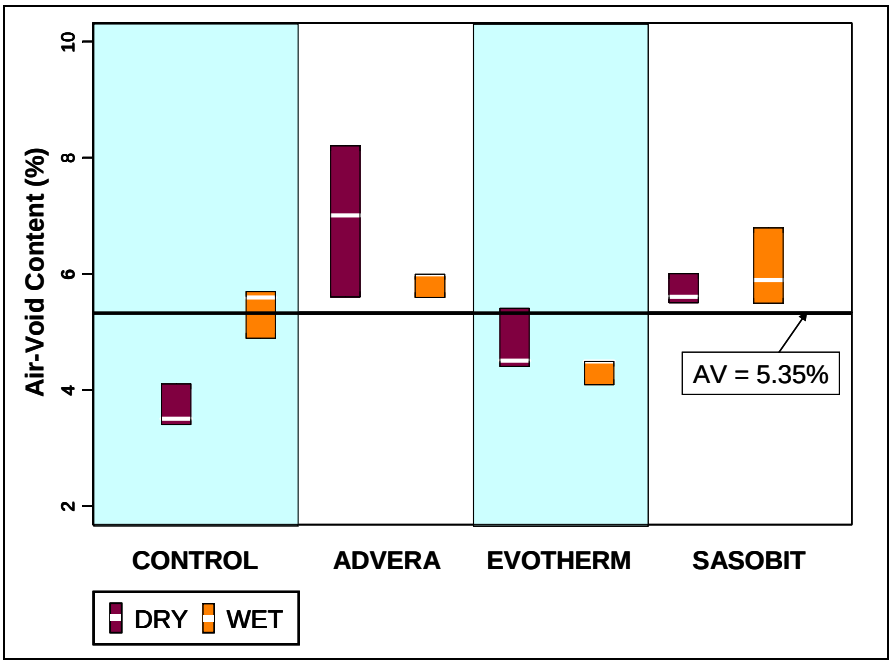

Figure 6.7: Air-void contents of flexural frequency sweep specimens (dry and wet).

Initial Stiffness

Figure 6.8 illustrates the initial stiffness comparison at various strain levels and conditioning for the different mix types. Only one test temperature (20°C [68°F]) was used. The following observations were made:

- Initial stiffness was generally strain-independent for both the dry and wet tests.
- A reduction of initial stiffness due to soaking was apparent for each mix type indicating a potential loss of structural capacity due to moisture damage.
- The reduction in initial stiffness appeared to be highly dependent on air-void content and not additive type. The ranking of degree of initial stiffness reduction in the four mixes, from highest to lowest, was Advera, Sasobit, Evotherm, and Control. This is the same ranking as highest to lowest air-void content. This implies that any moisture damage is more likely to be attributed to compaction problems (i.e., high air-void contents) than to choice of warm-mix asphalt technology.

Initial Phase Angle

The initial phase angle can be used as an index of mix viscosity properties, with higher phase angles corresponding to more viscous and less elastic properties. Figure 6.9 illustrates the side-by-side phase angle comparison of dry and wet tests for the four mixes. The following observations were made:

- The initial phase angle appeared to be strain-independent.
- Soaking appeared to increase the phase angle slightly. The range in phase angle between the specimens in each mix varied considerably among the mixes.
- There was no significant difference between the four mixes in terms of initial phase angle, indicating that the addition of the additives and lower production and compaction temperatures did not significantly influence the performance of the mixes in terms of this parameter.

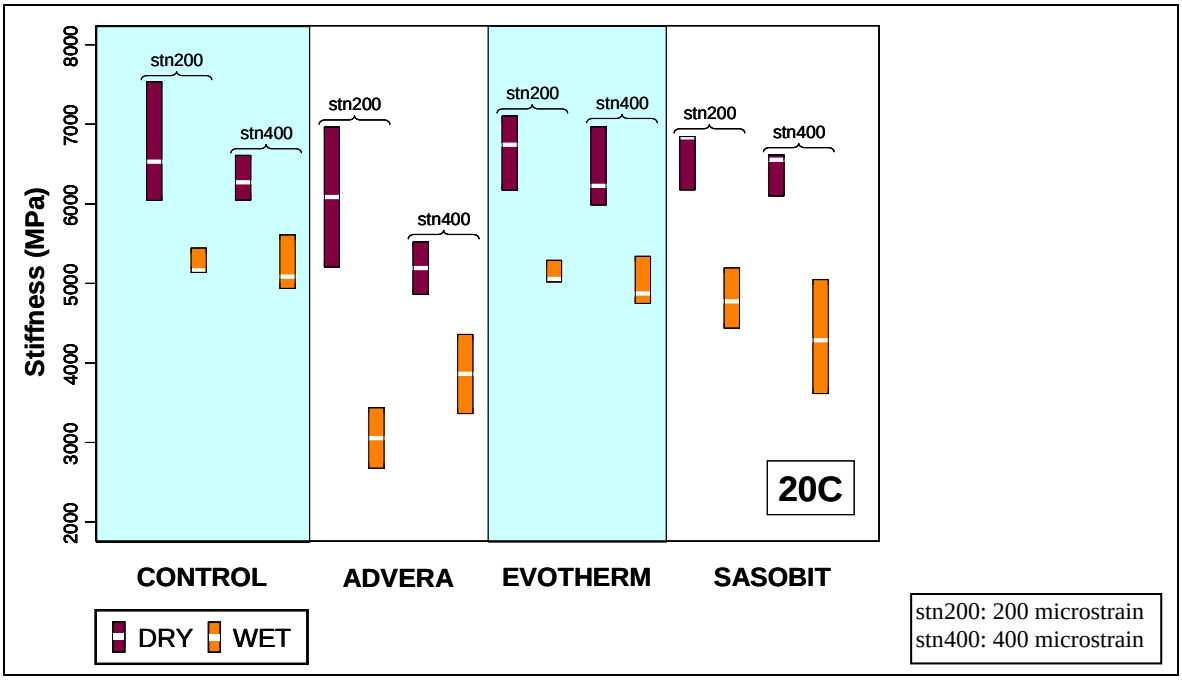

Figure 6.8: Summary boxplots of initial stiffness.

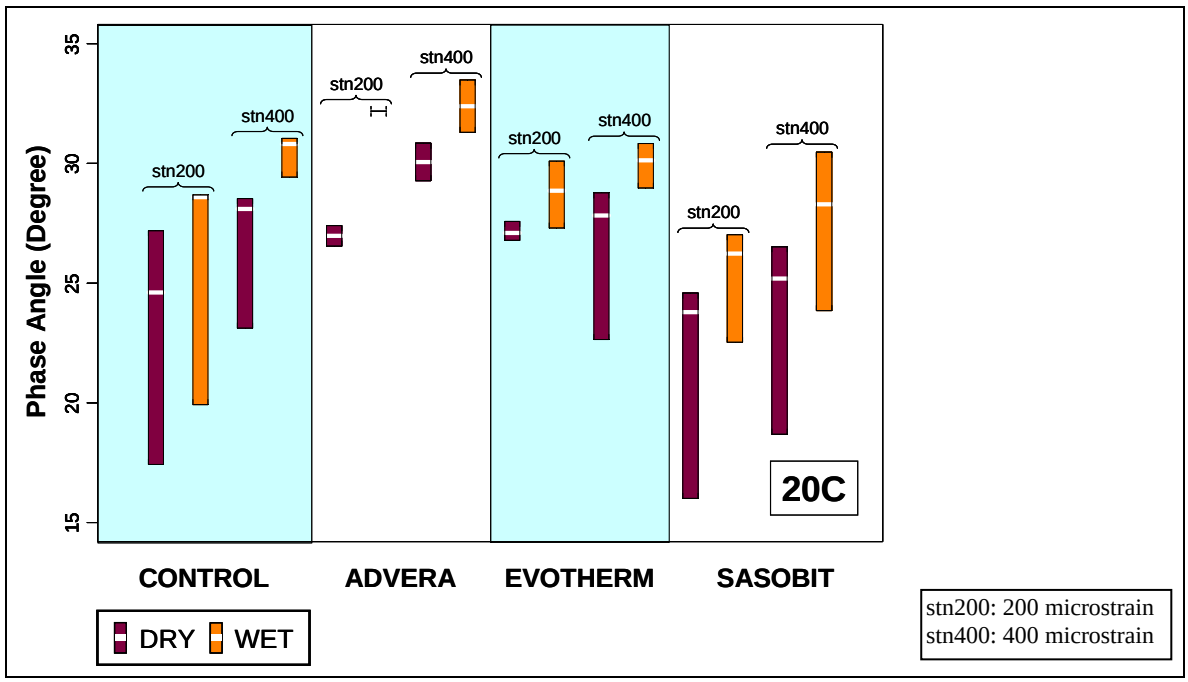

Figure 6.9: Summary boxplots of initial phase angle.

- The initial phase angle was highly negative-correlated with initial stiffness. Figure 6.10 shows a plot of these two parameters (using arithmetic scales). The negative-correlated trend between initial stiffness and phase angle is apparent; however, the dispersion of data is also observable. The dry

test specimens generally had higher initial stiffness and smaller phase angle compared with the wet test specimens. On average, the Sasobit mix had the highest stiffness and the smallest phase angle.

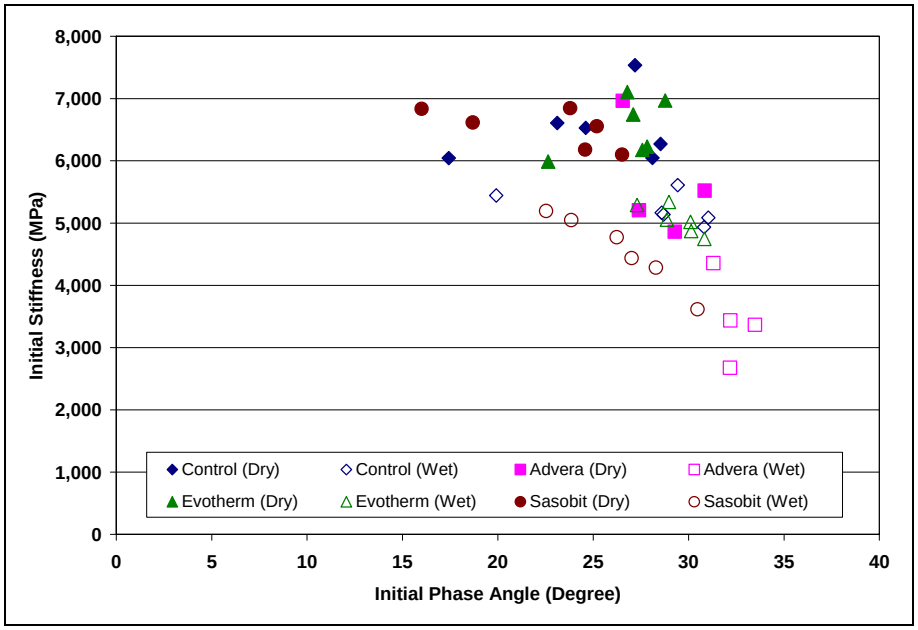

Figure 6.10: Initial stiffness versus phase angle for fatigue beam specimens.

Fatigue Life at 50 Percent Stiffness Reduction

Mix stiffness decreased with increasing test-load repetitions. Conventional fatigue life is defined as the number of load repetitions when 50 percent stiffness reduction has been reached. A high fatigue life implies a slow fatigue damage rate and consequently higher fatigue-resistance. The side-by-side fatigue life comparison of dry and wet tests is plotted in Figure 6.11. The following observations were made:

- Fatigue life was strain-dependent. In general, lower strains resulted in higher fatigue life.
- Soaking generally resulted in a lower fatigue life compared to the unsoaked specimens. Inconsistent results were obtained across the mixes at the lower strain level, specifically for the Control and Evotherm mixes. It is not clear why this occurred, although the lower air-void contents measured on these specimens may have had some influence on performance.
- There was no significant difference among the four mixes in terms of fatigue life at 50 percent stiffness reduction, indicating that the addition of any one of the additives and lower production and compaction temperatures did not significantly influence the performance of the mixes in this test.

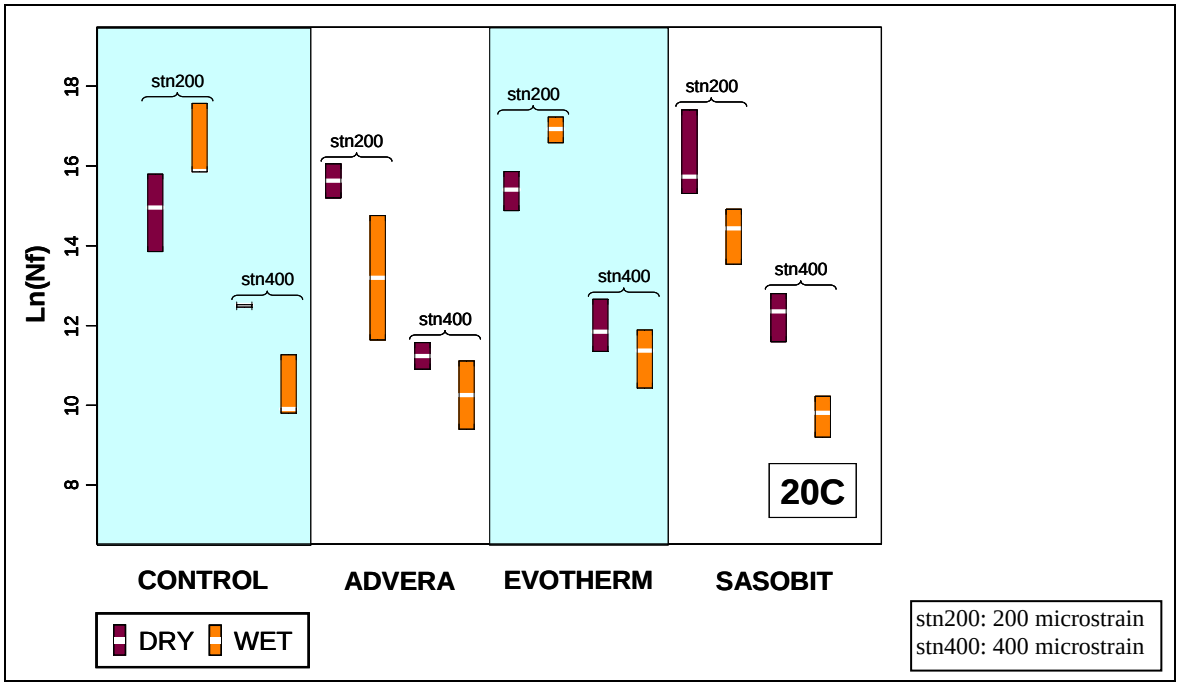

Figure 6.11: Summary boxplots of fatigue life.

Flexural Frequency Sweep

The average stiffness values of each specimen (no replicates due to limited specimen numbers) tested at the three temperatures were used to develop the flexural complex modulus (E^*) master curve. This is considered a useful tool for characterizing the effects of loading frequency (or vehicle speed) and temperature on the initial stiffness of an asphalt mix (i.e., before any fatigue damage has occurred). The shifted master curve with minimized residual-sum-of-squares derived using a genetic algorithm approach can be appropriately fitted with the following modified Gamma function (Equation 6.1):

$$E^* = D + A \cdot \left(1 - \exp\left(-\frac{(x-C)}{B}\right) \cdot \sum_{m}^{n-1} \frac{(x-C)^m}{B^m m!}\right) \quad \textbf{(6.1)}$$

where: E^* = flexural complex modulus (MPa);
$x = \ln freq + \ln aT$ = is the loading frequency in Hz and $\ln aT$ can be obtained from the temperature-shifting relationship (Equation 6.2);
A, B, C, D, and n are the experimentally determined parameters.

$$\ln aT = A \cdot \left(1 - \exp\left(-\frac{T - Tref}{B}\right)\right) \quad \textbf{(6.2)}$$

where: $lnaT$ = is a horizontal shift to correct the temperature effect with the same unit as ln $freq$,
T = is the temperature in °C,
$Tref$ = is the reference temperature, in this case, $Tref$ = 20°C
A and B are the experimentally determined parameters.

The experimentally determined parameters of the modified Gamma function for each mix type are listed in Table 6.7, together with the parameters in the temperature-shifting relationship.

Figure 6.12 and Figure 6.13 show the shifted master curves with Gamma-fitted lines and the temperature-shifting relationships, respectively, for the dry frequency sweep tests. The temperature-shifting relationships were obtained during the construction of the complex modulus master curve and can be used to correct the temperature effect on initial stiffness. Note that a positive lnaT value needs to be applied when the temperature is lower than the reference temperature, while a negative lnaT value needs to be used when the temperature is higher than the reference temperature.

The following observations were made from the dry frequency sweep test results:

- There was no apparent difference between the complex modulus master curves of the Control, Evotherm, and Sasobit mixes. The curve for the Advera mix was below those of the other three mixes. This was attributed to the higher air-void contents of the tested Advera beams.
- The temperature-shifting relationships indicate that the Sasobit mix was the most temperature-sensitive in extreme temperatures and the least temperature-sensitive at the higher temperatures. Higher temperature-sensitivity implies that a per unit change of temperature will cause a larger change of stiffness (i.e., larger change of lnaT).

Figure 6.14 and Figure 6.15 respectively show the shifted master curves with Gamma-fitted lines and the temperature-shifting relationships for the wet frequency sweep tests. The comparison of dry and wet complex modulus master curves is shown in Figure 6.16 for each mix type. The following observations were made with regard to the wet frequency sweep tests results:

- The complex modulus curves of all the mixes were essentially the same.
- There were no apparent temperature-sensitivity differences among the four mixes at higher temperatures (i.e., higher than 20°C). At lower temperatures (i.e., lower than 20°C), there was some variation in the mixes, with the Advera mix specimens showing the least temperature sensitivity of the four mixes and the Sasobit mix the highest temperature sensitivity. The difference between the Advera and Sasobit mixes was, however, not significant.
- A loss of stiffness attributed to moisture damage was apparent in all four mixes.
- There was less variation in the master curves of the soaked specimens compared to the dry specimens.

Table 6.7: Summary of Master Curves and Time-Temperature Relationships

Mix	Conditioning	Master Curve					Time-Temperature Relationship	
		N	A	B	C	D	A	B
Control	Dry	3	21,080.86	4.2285	-6.3543	444.4376	8.1156	-27.912
Advera		3	10,352.90	12.3972	-8.8686	269.9997	-1.5963	6.883
Evotherm		3	57,323.54	8.7227	-5.7172	236.3571	-8.6155	27.287
Sasobit		3	22,482.76	4.5928	-5.7820	370.4686	0.9082	-7.007
Control	Wet	3	20,751.28	4.8594	-5.3548	365.5347	-9.4381	31.022
Advera		3	50,720.39	27.1786	-8.7953	133.9993	154.5040	-557.646
Evotherm		3	28,559.86	6.2285	-5.5522	290.2198	-15.2794	51.129
Sasobit		4	19,804.97	4.4906	-5.5004	362.5876	-9.6926	28.037

Notes:

1. The reference temperature is 20°C.
2. The wet test specimens were soaked at 60°C.
3. Master curve Gamma-fitted equations:

   If $n = 3$, $E^* = D + A \cdot \left(1 - \exp\left(-\frac{(x-C)}{B}\right)\right) \cdot \left(1 + \frac{x-C}{B} + \frac{(x-C)^2}{2B^2}\right)$,

   If $n = 4$, $E^* = D + A \cdot \left(1 - \exp\left(-\frac{(x-C)}{B}\right)\right) \cdot \left(1 + \frac{x-C}{B} + \frac{(x-C)^2}{2B^2} + \frac{(x-C)^3}{6B^3}\right)$,

   where $x = \ln freq + \ln aT$

4. Time-temperature relationship: $\ln aT = A \cdot \left(1 - \exp\left(-\frac{T - Tref}{B}\right)\right)$

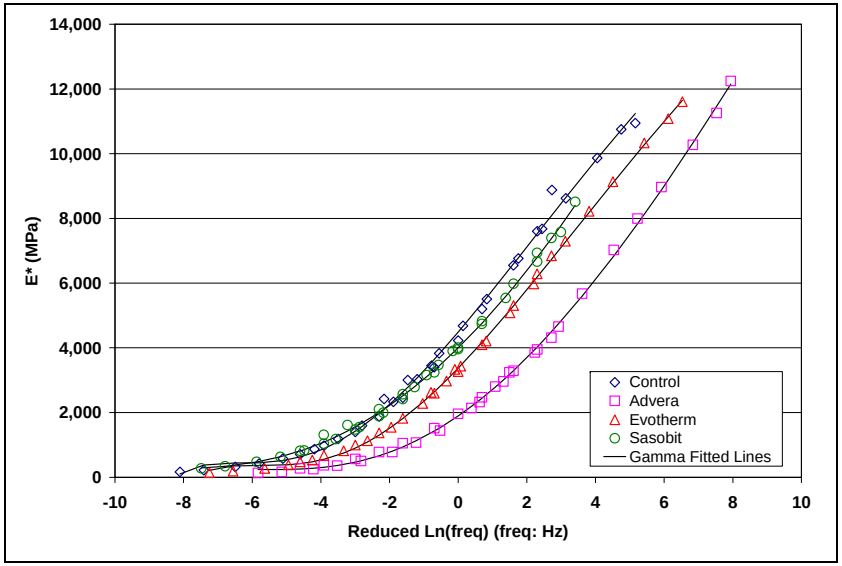

Figure 6.12: Flexural complex modulus (*E) master curves (dry).**

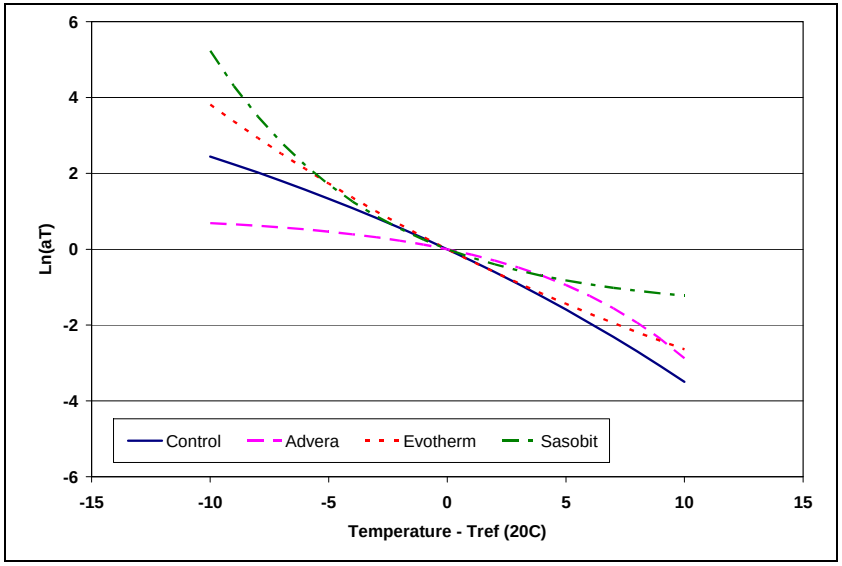

Figure 6.13: Temperature-shifting relationship (dry).

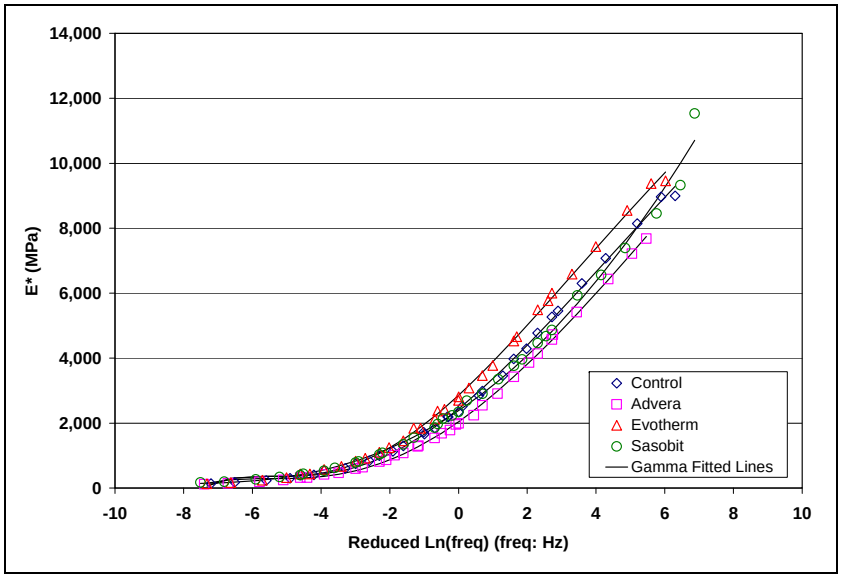

Figure 6.14: Complex modulus (*E) master curves (wet).**

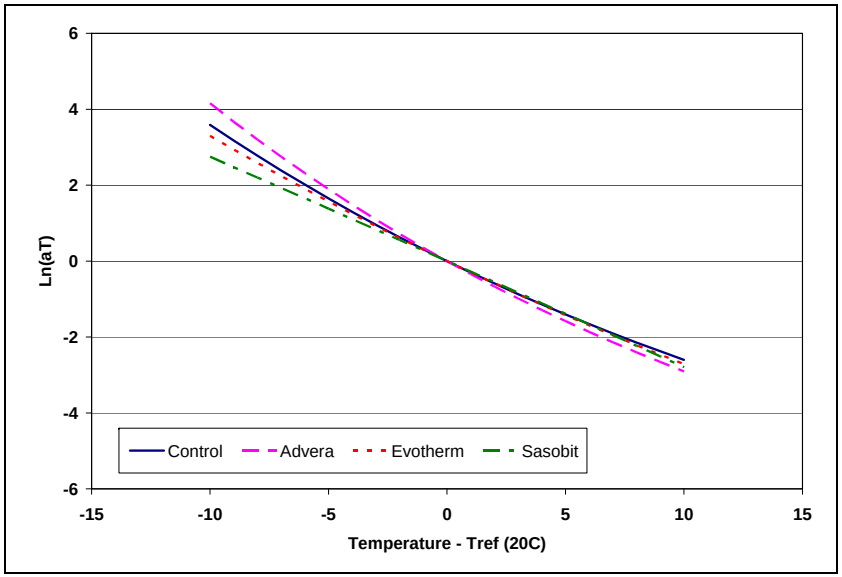

Figure 6.15: Temperature-shifting relationship (wet).

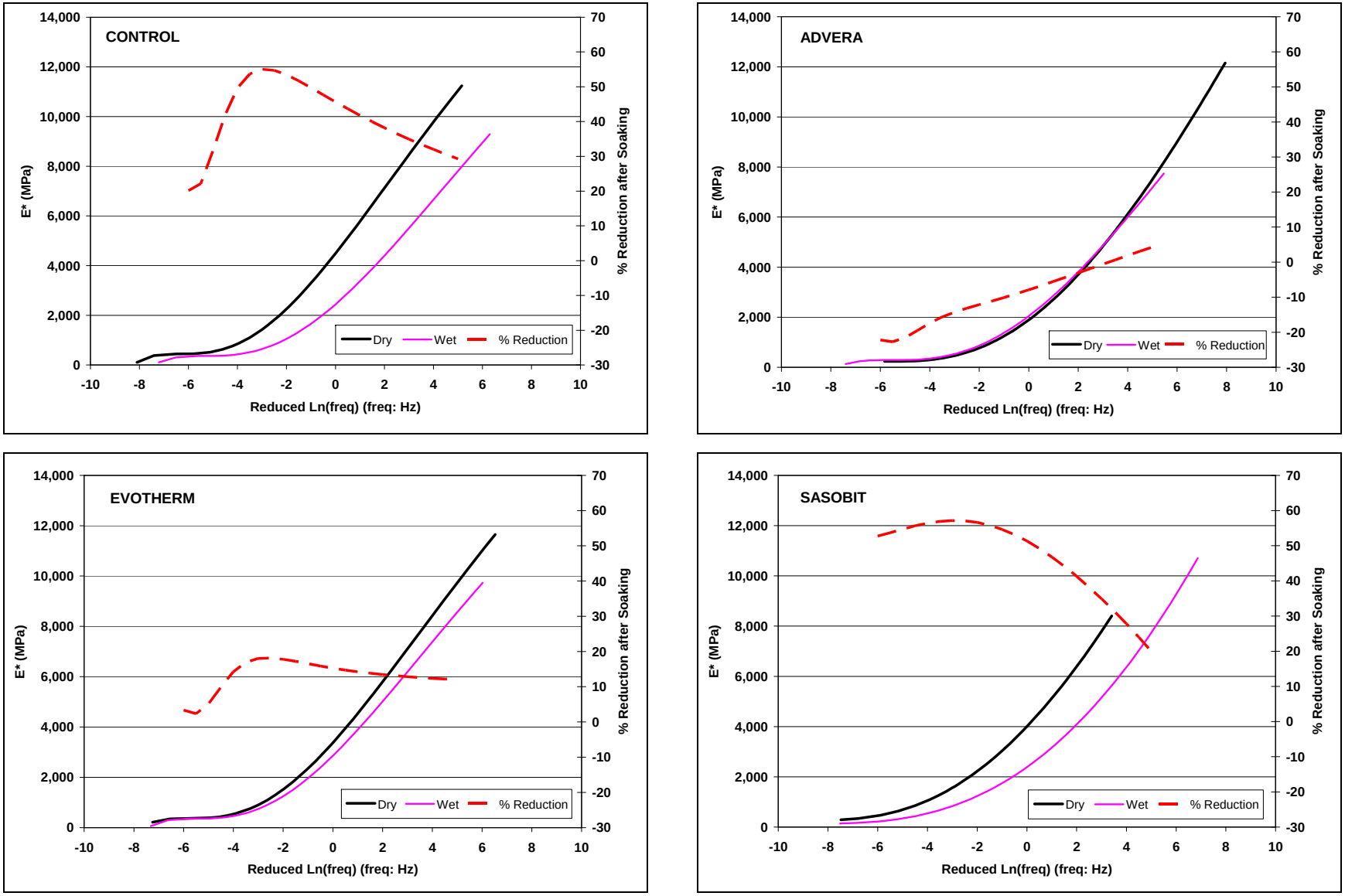

Figure 6.16: Comparison of dry and wet complex modulus master curves.
(Includes percent reduction in stiffness at each frequency from dry to wet master curve.)

6.4 Summary of Laboratory Testing Results

The laboratory test results on the field-mixed, laboratory-compacted specimens confirm the findings of the Phase 1 study in indicating that use of the three warm-mix additives assessed in this study to produce and compact mixes at lower temperatures, did not significantly influence the performance of the asphalt concrete when compared to control specimens produced and compacted at conventional hot-mix asphalt temperatures. Lower air-void contents were achieved using the laboratory compaction (rolling wheel) setup compared to those measured on the specimens removed from the test track. No difficulty was experienced in the compaction of the warm-mix specimens.

Limited moisture sensitivity testing confirmed the Phase 1 study findings in that all the mixes tested were potentially susceptible to moisture damage. There was again no difference in the level of moisture sensitivity between the Control mix and mixes with warm-mix additives.

6.5 Comparison of Phase 1 and Phase 2 Laboratory Test Results

Summary boxplots comparing the Phase 1 and Phase 2 test results are shown in Figure 6.17 through Figure 6.28.

Figure 6.17 (shear specimens) and Figure 6.18 (fatigue specimens) clearly show the difference in air-void content between the specimens tested in the two phases. Figure 6.19 through Figure 6.24 indicate that the field-mixed, laboratory-compacted specimens tested in the Phase 2 study generally performed better than the field-mixed, field-compacted specimens. This was attributed to the lower air-void contents. However, the performance trends for both phases are very similar.

A statistical analysis of the results factoring in the differences in air-void content indicated that there was no significant difference between the results from the two phases of testing if air-void content is accounted for (Figure 6.25 and Figure 6.26). Comparisons of the predicted FMFC and FMLC cycles to five-percent permanent shear strain and fatigue life for the difference mixes at the same air-void content, using a regression analysis, are shown in Figure 6.27 and Figure 6.28, respectively.

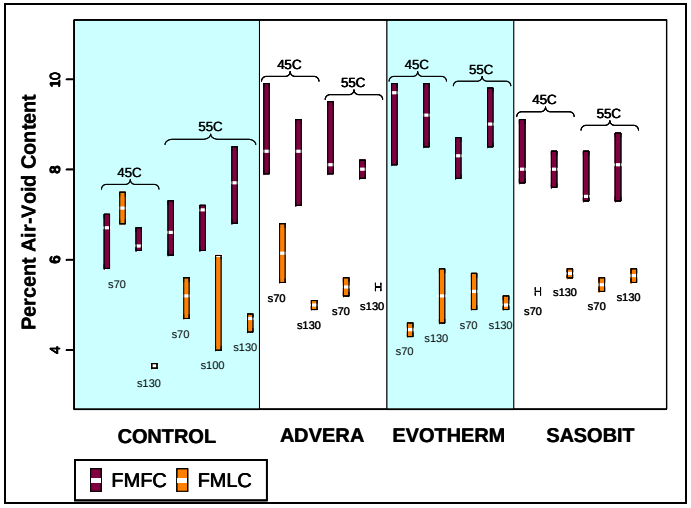

Figure 6.17: Air-void content comparison between FMFC and FMLC shear specimens.

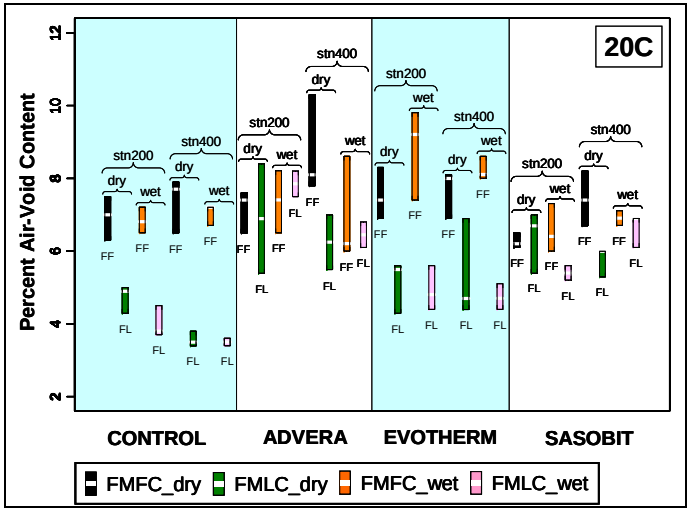

Figure 6.18: Air-void content comparison between FMFC and FMLC fatigue specimens.

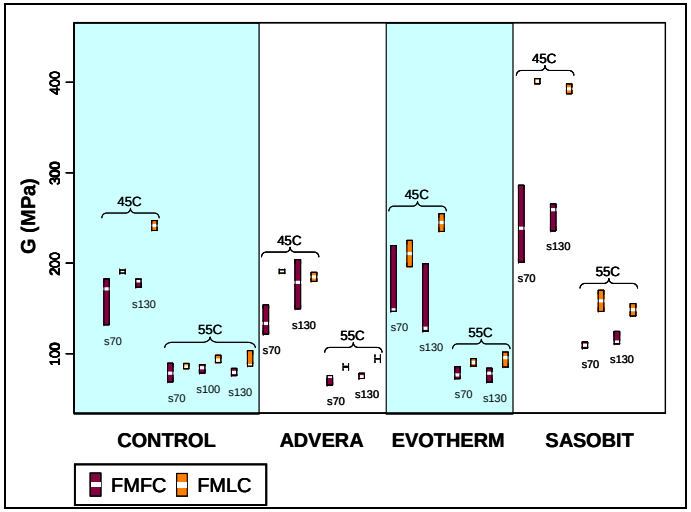

Figure 6.19: Resilient shear modulus comparison between FMFC and FMLC shear tests.

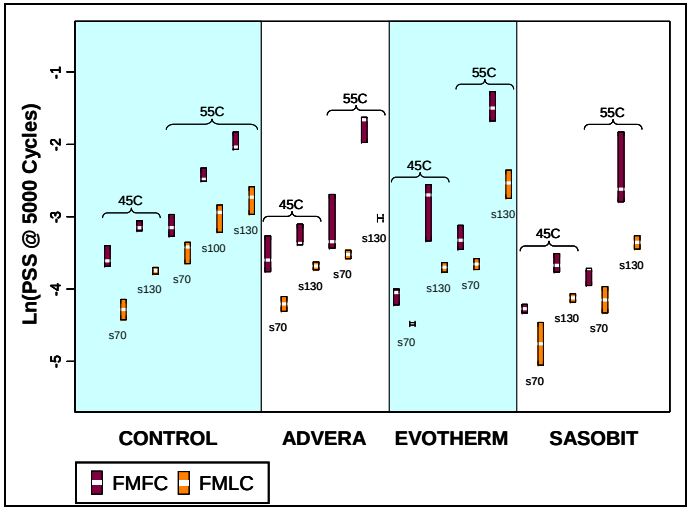

Figure 6.20: Permanent shear strain comparison between FMFC and FMLC shear tests.

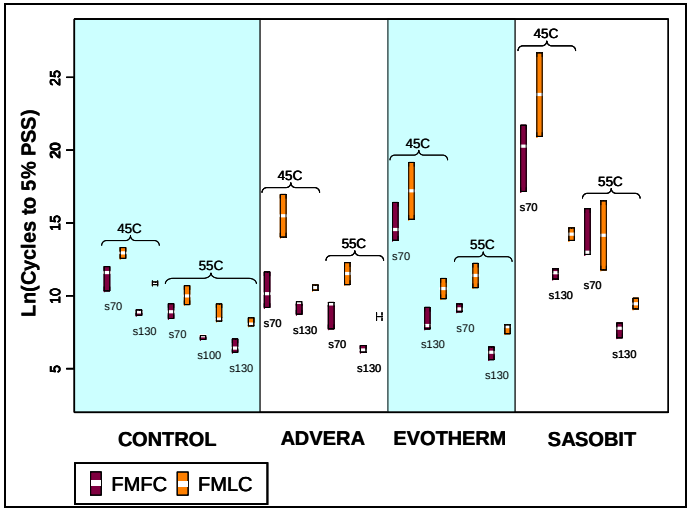

Figure 6.21: Cycles to 5% permanent shear strain comparison between FMFC and FMLC shear tests.

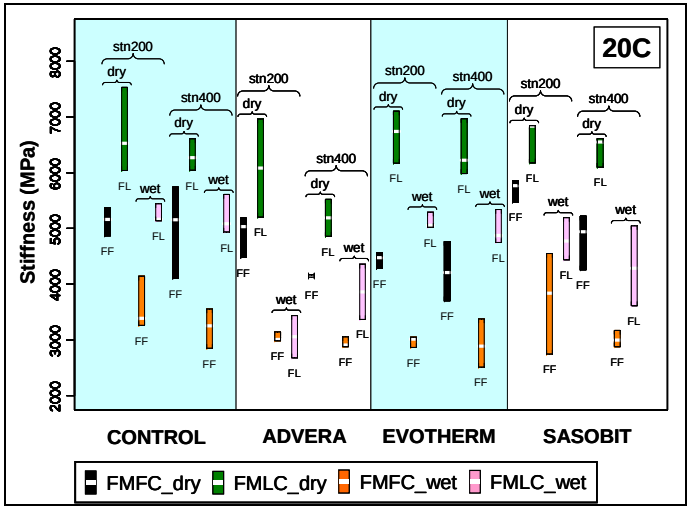

Figure 6.22: Initial stiffness comparison between FMFC and FMLC fatigue tests.

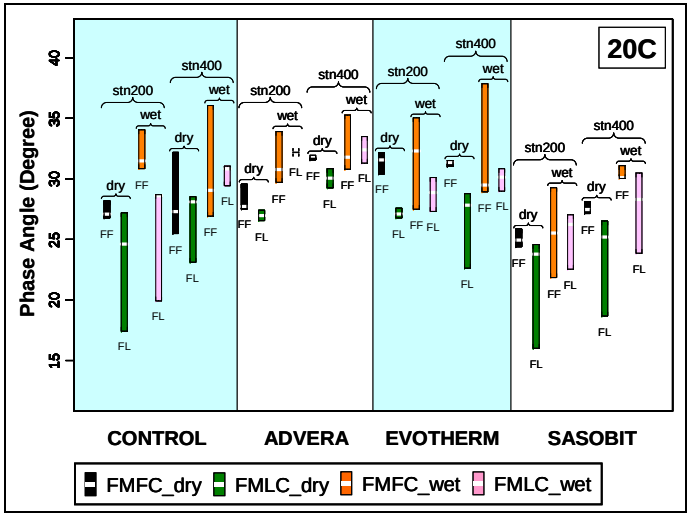

Figure 6.23: Phase angle comparison between FMFC and FMLC fatigue tests.

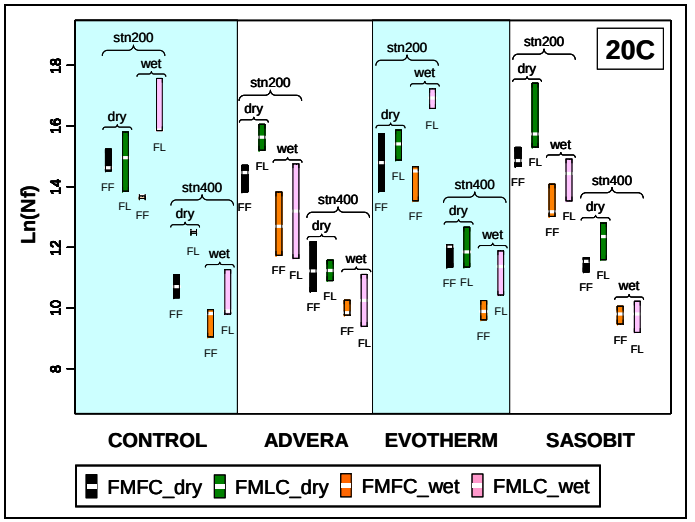

Figure 6.24: Fatigue life comparison between FMFC and FMLC fatigue tests.

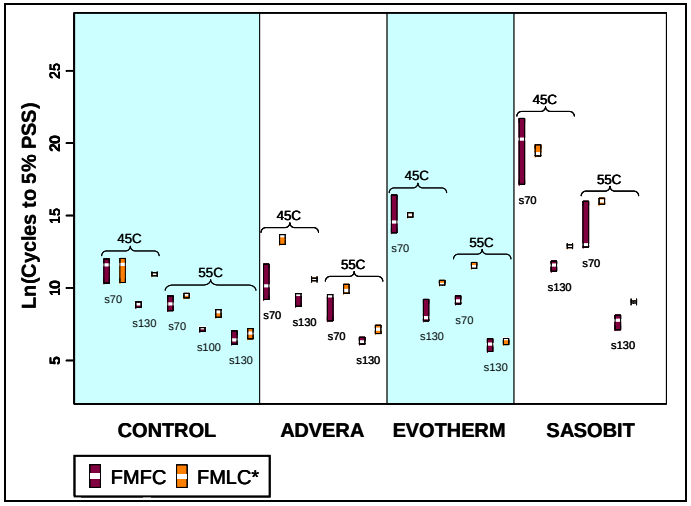

Figure 6.25: Comparison of cycles to 5% permanent shear strain after air-void content correction.

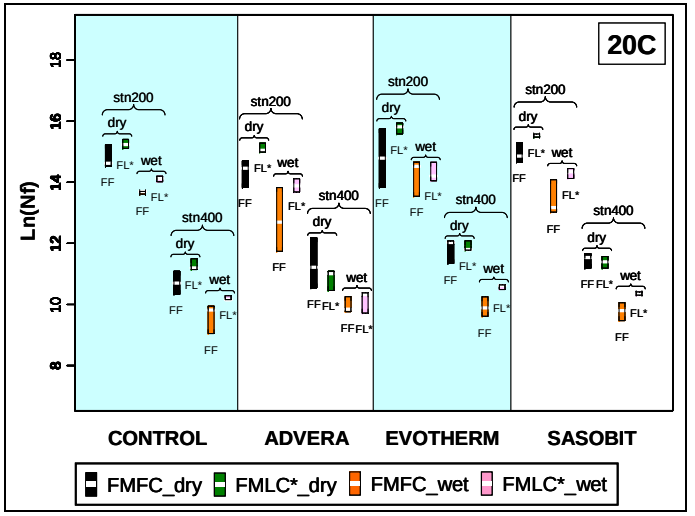

Figure 6.26: Comparison of fatigue life after air-void content correction.

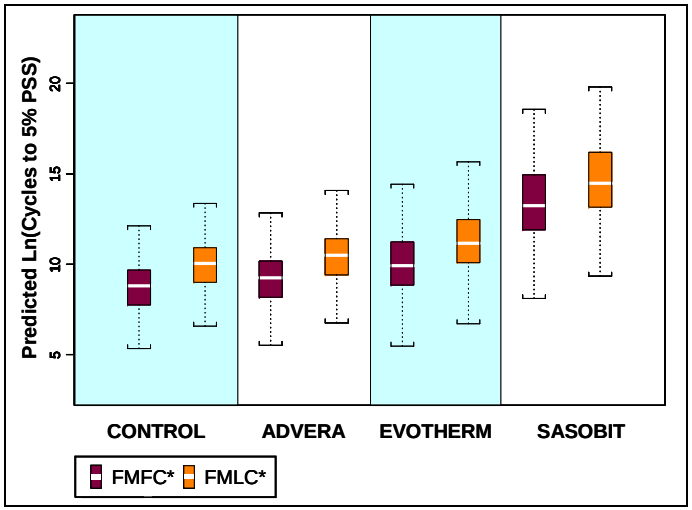

Figure 6.27: Comparison of predicted cycles to 5% permanent shear strain at same air-void content.

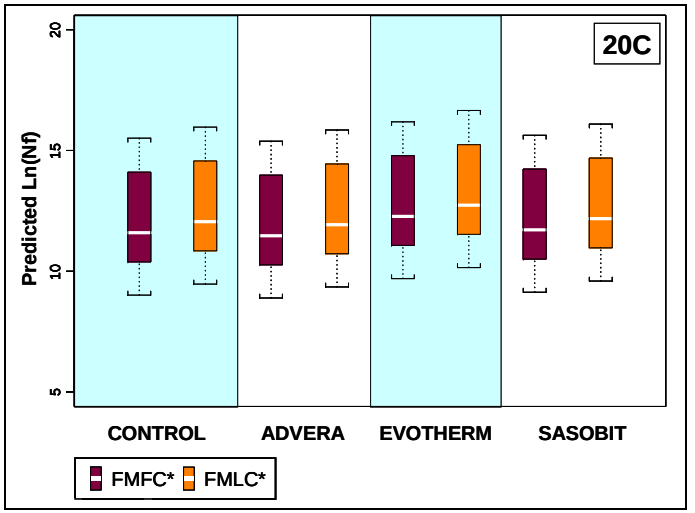

Figure 6.28: Comparison of predicted fatigue life at same air-void content.

7 CONCLUSIONS

This first-level report describes the second phase of a warm-mix asphalt study, which compares the performance of a control mix, produced and constructed at conventional hot-mix asphalt temperatures, with three mixes produced with warm-mix additives, produced and compacted at approximately 35°C (60°F) lower than the control. The additives tested included *Advera WMA®*, *Evotherm™*, and *Sasobit®*. The results of Heavy Vehicle Simulator (HVS) testing to assess moisture sensitivity of the mixes, laboratory testing of field-mixed, laboratory-compacted specimens, and a forensic investigation of the HVS test sections are discussed.

The study includes these key findings:

- HVS trafficking on each of the four sections revealed that the duration and rut depths of the embedment phase (the high early-rutting phase of the typical two-phase rutting process) of the warm-mix sections were approximately half that of the Control, an opposite trend to that observed in Phase 1, indicating that the effects of oxidation of the binder at lower production temperatures may only influence rutting performance in the first few months after construction.
- Rutting behavior of the Control and Evotherm sections was significantly different compared to that of the Advera and Sasobit sections after the embedment phase. This was attributed to the Control and Evotherm sections being predominantly in the shade of an adjacent shed for most of the day, while the Advera and Sasobit sections were predominantly in the sun for most of the day. Consequently the binder in the mixes may have oxidized more rapidly on the Advera and Sasobit sections in the year since construction, leading to potentially a higher stiffness and consequent better rutting performance. This is being investigated in a separate study.
- The Control and Evotherm tests (both predominantly in the shade) followed similar trends after the first 80,000 HVS load repetitions and reached the 12.5 mm (0.5 in.) failure point at about 300,000 load repetitions. The Advera and Sasobit tests (both predominantly in the sun) also followed similar trends with a very slow increase in rut depth after the short embedment phase. In the interests of completing this phase of the study, the Advera test was terminated after 625,000 repetitions when the rut depth was 11.5 mm (i.e., before the failure point of 12.5 mm), while the Sasobit test was terminated after 420,000 repetitions when the rut depth was 9.9 mm.
- A forensic investigation of all test sections indicated that the rutting was confined to the upper lift of the asphalt concrete. No evidence of moisture damage was noted on any of the sections, although some evidence of debonding between the two lifts of asphalt was noted on the Control section. All sections had some top-down cracking in the top lift of the asphalt concrete.
- The laboratory test results from the field-mixed, laboratory-compacted specimens confirm the findings of the Phase 1 study in indicating that use of the three warm-mix additives assessed in this study to produce and compact mixes at lower temperatures, did not significantly influence the performance of the asphalt concrete when compared to control specimens produced and compacted at conventional hot-mix asphalt temperatures. Lower air-void contents were achieved using the laboratory compaction (rolling wheel) setup compared to those measured on the specimens removed from the test track. No difficulty was experienced in the compaction of the warm-mix specimens. Limited moisture sensitivity testing confirmed the Phase 1 study findings in that all the mixes tested were potentially susceptible to moisture damage. There was again no difference in the level of moisture sensitivity between the Control mix and mixes with warm-mix additives.

These results further support the findings from the Phase 1 study in that the use of any of the three warm-mix asphalt additives tested in this experiment and subsequent compaction of the mix at lower temperatures will not significantly influence the rutting performance of the mix in the longer term. The results also indicate that if the aggregate and mix moisture contents are within specified limits and specified compaction requirements are met, the warm-mix asphalt additives tested in this experiment are unlikely to increase the moisture sensitivity of the mix. Based on the comparison of performance between Phase 1 and Phase 2 testing, it can be concluded that the effects on rutting performance of reduced binder aging attributed to lower mix production temperatures appear to be of relatively limited duration. It can therefore be concluded, based on the limited testing undertaken to date, that equal performance will be obtained in the longer term from the hot and warm mixes tested in this study. This is currently being verified in pilot studies at various locations in California.

The findings of the study are also summarized below in the form of answers to the questions identified in Section 1.3.

7.1.1 Comparative Energy Usage

Comparative energy usage during mix production has not been assessed in this study to date due to the very small mix quantities produced. Studies on energy usage will need to be carried out during larger, full-scale pilot studies on in-service pavements when large quantities of mix (i.e., more than 5,000 tons) are produced.

7.1.2 Achieving Compaction Density at Lower Temperatures

Average laboratory-determined air-void contents on field-mixed, laboratory-compacted specimens showed that adequate compaction can be achieved in the laboratory on warm-mixes at the lower temperatures, when compared to hot-mix asphalt controls.

7.1.3 Optimal Temperature Ranges for Warm-Mixes

Optimal compaction temperatures are likely to differ between the different warm-mix technologies. This study has shown that temperatures of at least 35°C (60°F) lower than conventional temperatures are appropriate for producing and compacting the modified mixes.

7.1.4 Cost Implications

The cost benefits of using the warm-mix technologies have not be assessed in this study to date due to the very small mix quantities produced.

7.1.5 Rutting Performance

Based on the results of HVS testing, it is concluded that use of any of the three warm-mix asphalt technologies tested in this experiment will not significantly influence the rutting performance of the mix.

7.1.6 Moisture Sensitivity

Laboratory moisture sensitivity testing indicated that all the mixes tested were potentially susceptible to moisture damage. There was, however, no difference in the level of moisture sensitivity between the Control mix and mixes with additives. HVS testing to assess moisture sensitivity revealed no moisture damage on any of the test sections.

7.1.7 Fatigue Performance

Laboratory testing indicated that the warm-mix technologies used in this study will not influence the fatigue performance of a mix. Given the very strong pavement structure of the test track used in this study, it is unlikely that fatigue cracking will occur under HVS testing. An assessment of fatigue performance is therefore not recommended using these test sections.

7.1.8 Rubberized and Open-Graded Mixes

Phase 3 laboratory and accelerated pavement testing on seven different rubberized warm-mix technologies was in progress at the time of this report's preparation. Performance of open-graded warm-mixes is being assessed in pilot studies at various locations in California.

8 REFERENCES

1. JONES, D. and Harvey, J. 2007. **Warm-mix Asphalt Study: Workplan for Comparison of Conventional and Warm-mix Asphalt Performance using HVS and Laboratory Testing.** Davis and Berkeley, CA: University of California Pavement Research Center. (WP-2007-01).
2. JONES, D., Wu, R., Tsai, B., Lu, Q. and Harvey, J. 2008. **Warm-Mix Asphalt Study: Test Track Construction and First-level Analysis of Phase 1 HVS and Laboratory Testing.** Davis and Berkeley, CA: University of California Pavement Research Center. (RR-2008-11).
3. JONES, D. 2005. **Quality Management System for Site Establishment, Daily Operations, Instrumentation, Data Collection and Data Storage for APT Experiments.** Pretoria, South Africa: CSIR Transportek. (Contract Report CR-2004/67-v2).

APPENDIX A: TEST PIT PROFILES

Test pit profiles for each test section are shown in Figure A.1 through Figure A.8. All test pits were excavated between Station 9 and Station 11. All profiles show the test pit face at Station 9. Test pit details are as follows:

- Figure A.1: 600FD: Phase 1 Control after 195,000 repetitions
- Figure A.2: 601FD: Phase 1 Advera after 170,000 repetitions
- Figure A.3: 602FD: Phase 1 Evotherm after 185,000 repetitions
- Figure A.4: 603FD: Phase 1 Sasobit after 285,000 repetitions
- Figure A.5: 604FD: Phase 2 Control after 371,000 repetitions
- Figure A.6: 605FD: Phase 2 Advera after 620,500 repetitions
- Figure A.7: 606FD: Phase 2 Evotherm after 352,000 repetitions
- Figure A.8: 607FD: Phase 2 Sasobit after 464,500 repetitions

It should be noted that HVS testing on Sections 603FD, 605FD and 607FD were halted before the failure criterion of 12.5 mm (0.5 in.) average maximum rut was reached.

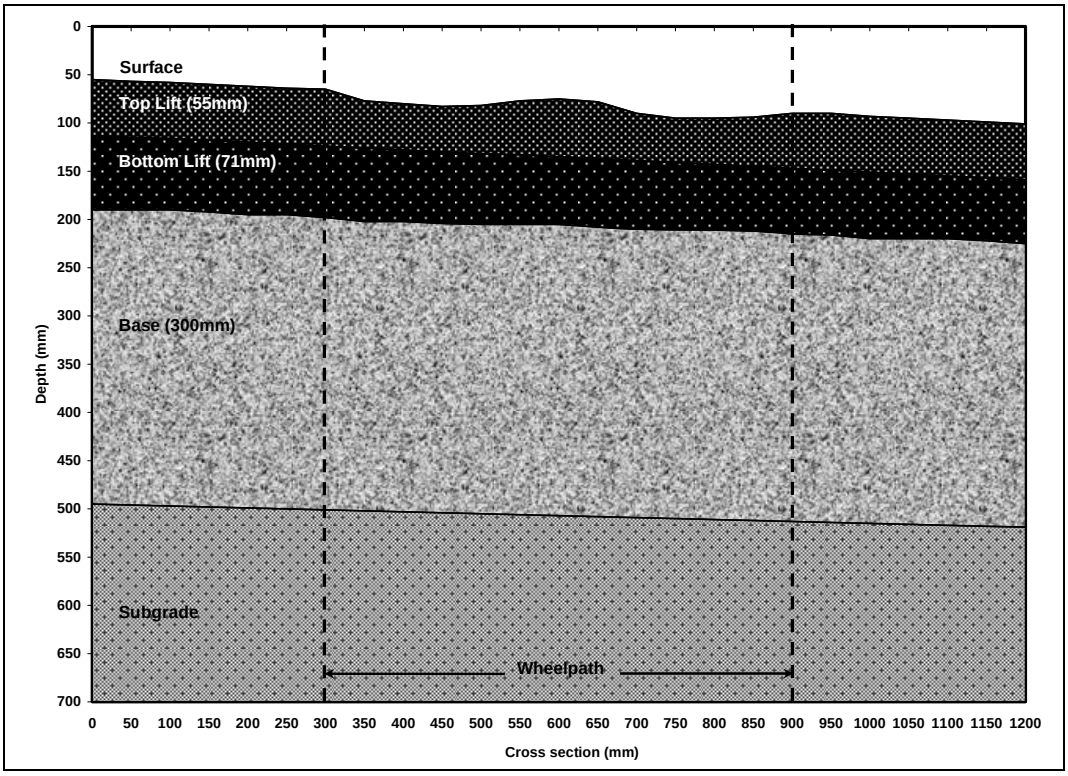

Figure A.1: 600FD: Test pit profile.

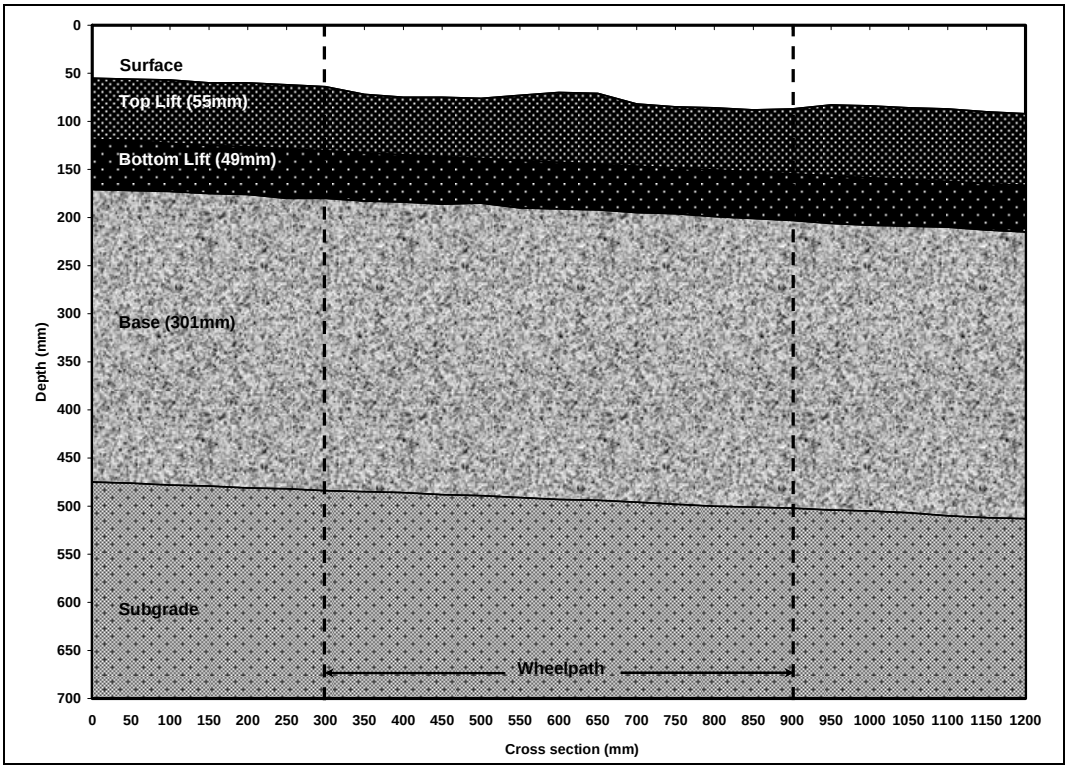

Figure A.2: 601FD: Test pit profile.

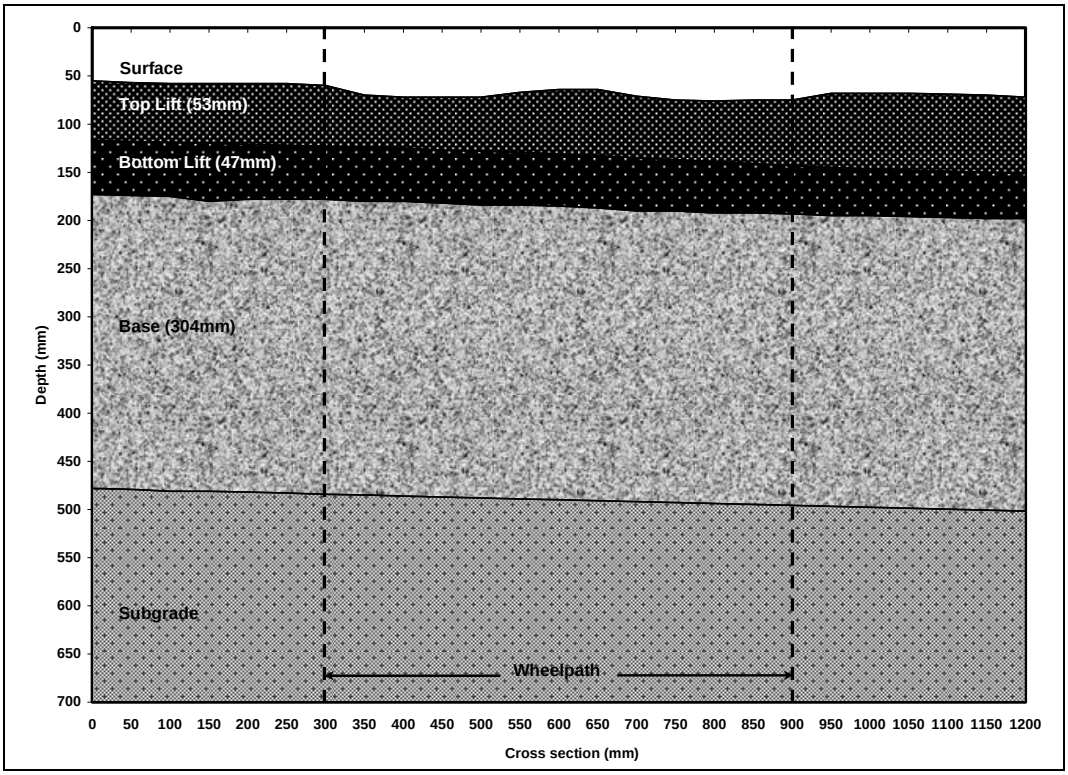

Figure A.3: 602FD: Test pit profile.

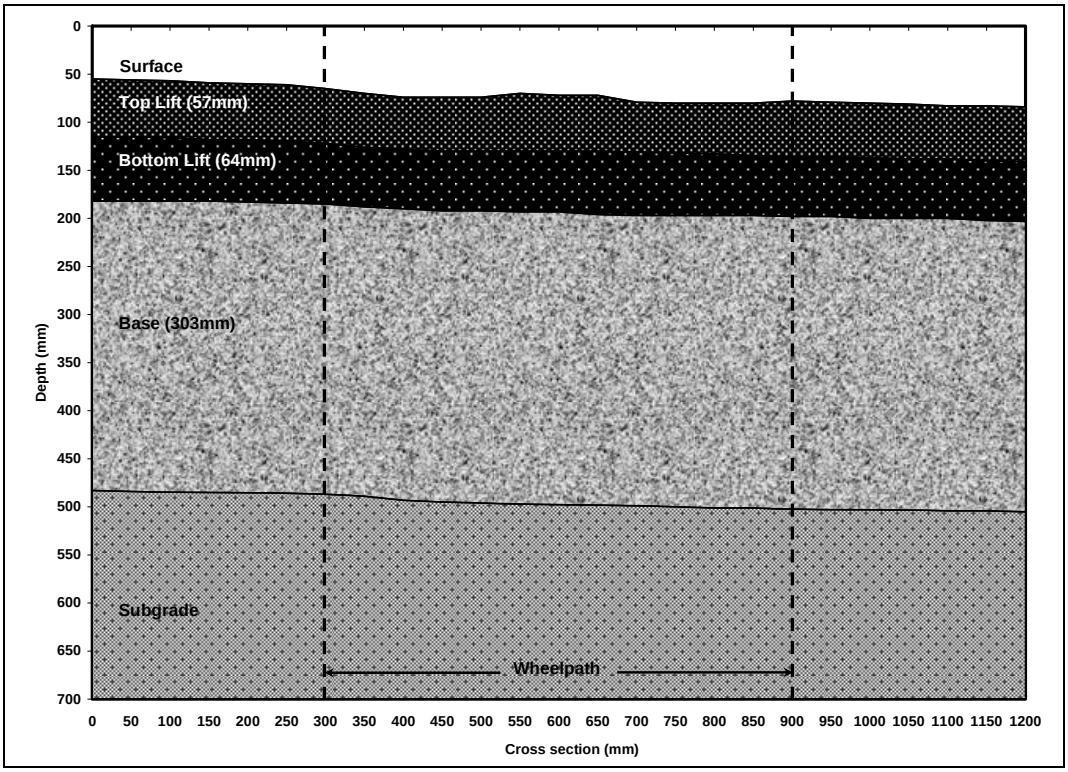

Figure A.4: 603FD: Test pit profile.

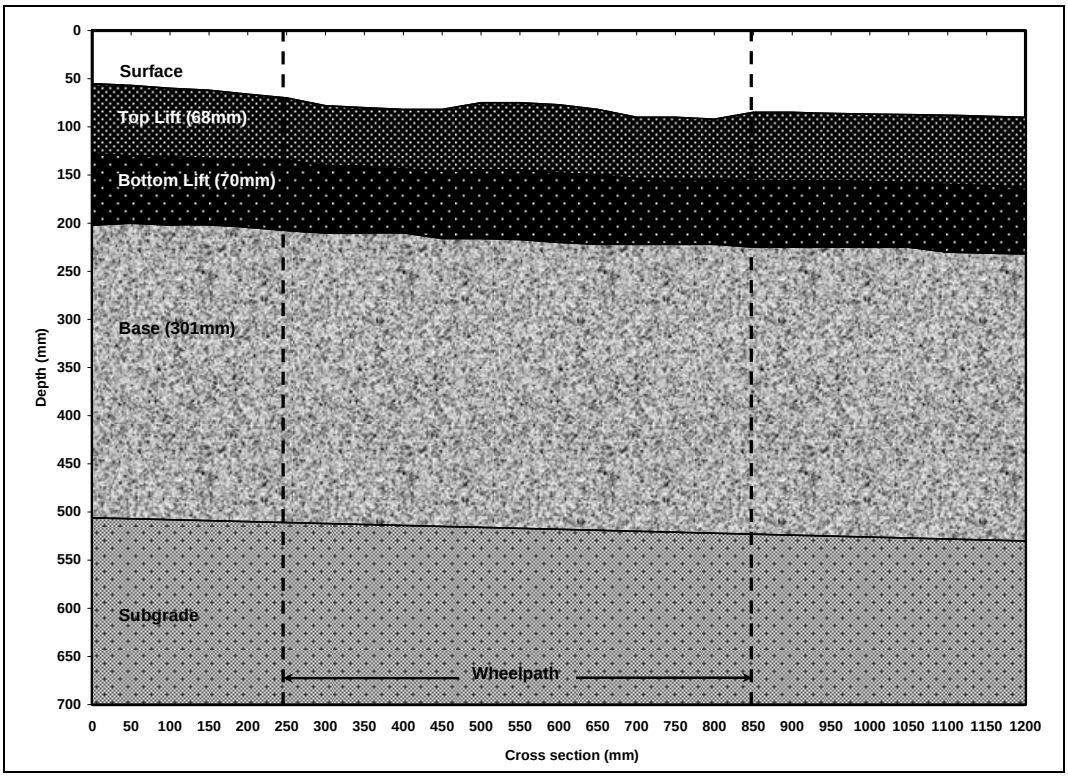

Figure A.5: 604FD: Test pit profile.

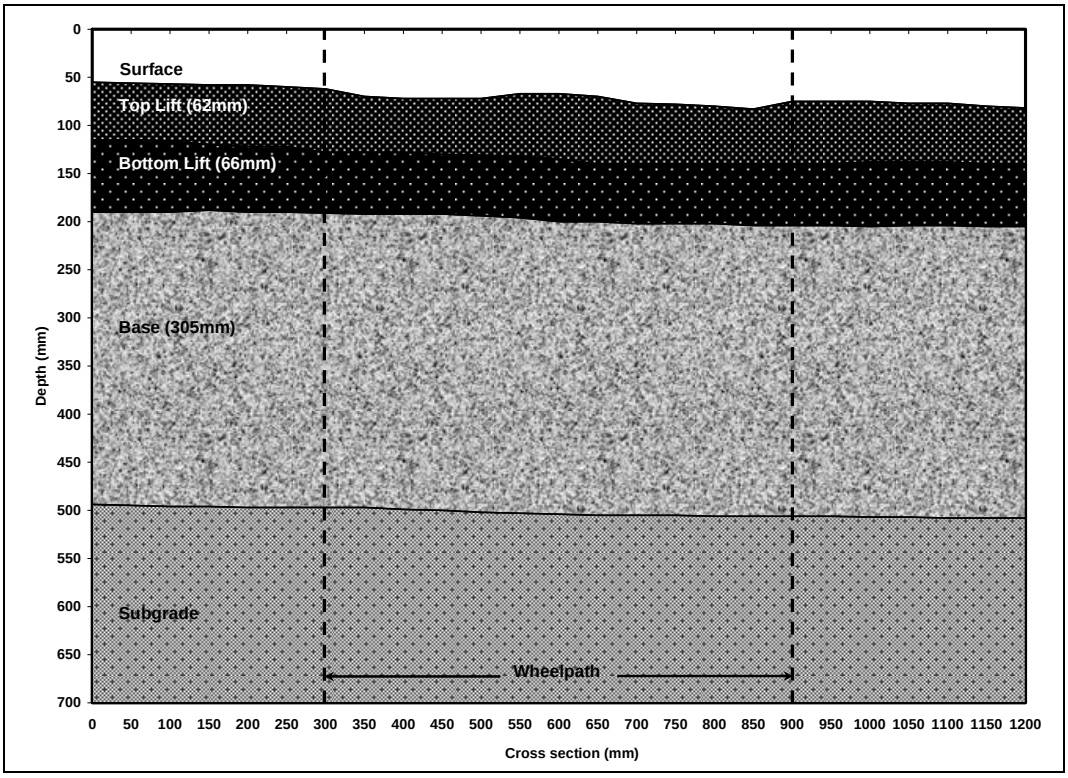

Figure A.6: 605FD: Test pit profile.

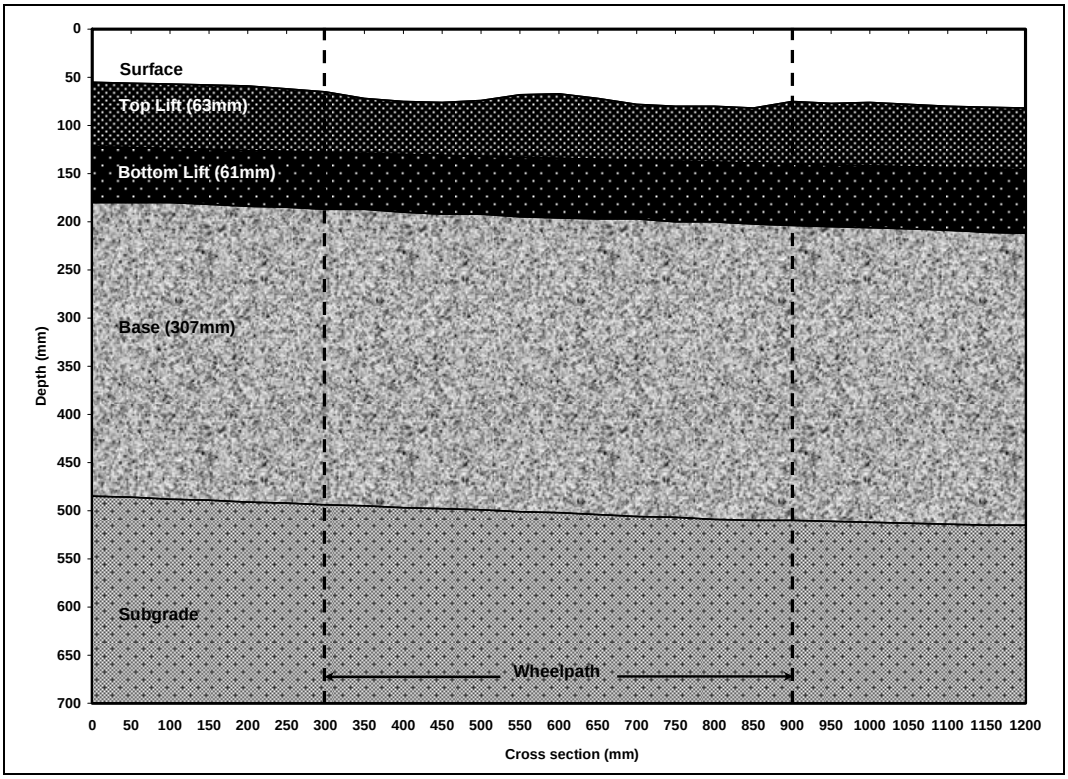

Figure A.7: 606FD: Test pit profile.

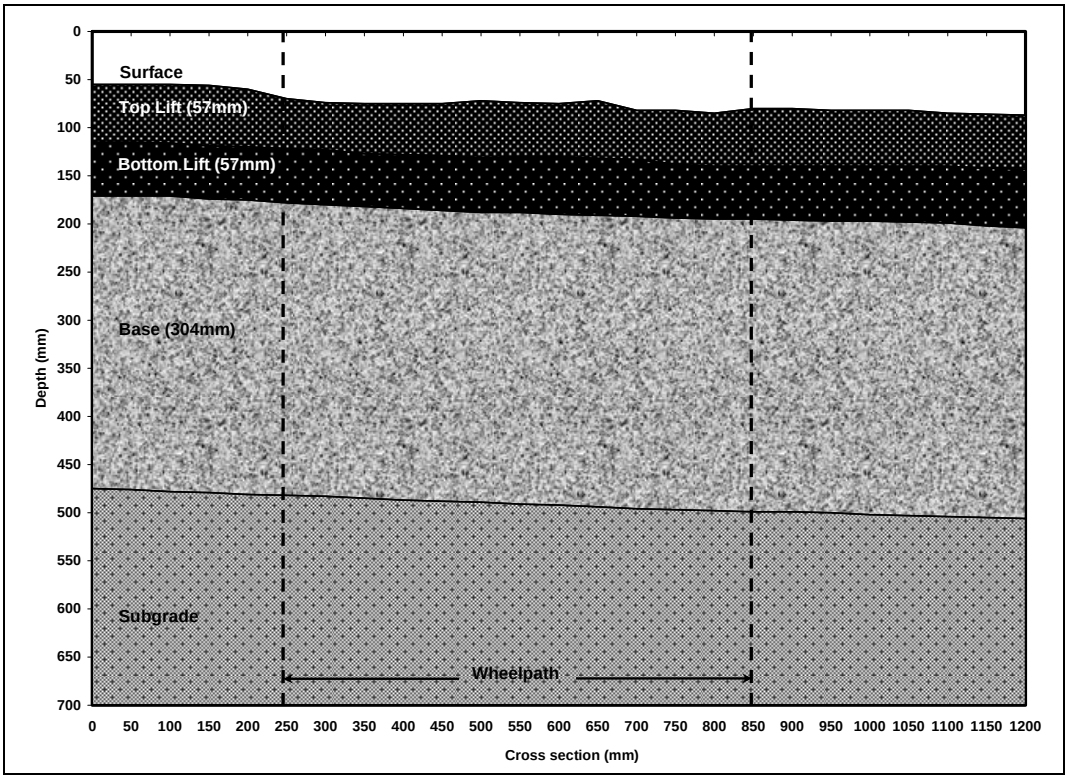

Figure A.8: 607FD: Test pit profile.

APPENDIX B: FATIGUE BEAM SOAKING PROCEDURE

B.1 Preparation of Specimens

Specimens are prepared as follows:

1. Measure and record the bulk specific gravity, width, and height of each beam.
2. Dry each beam at room temperature (around 30°C [86°F]) in a forced draft oven or in a concrete conditioning room to constant mass (defined as the mass at which further drying does not alter the mass by more than 0.05 percent at two-hour drying intervals). Record the final dry mass. Note: Place the beams on a rigid, flat surface during drying.
3. Bond the fastener for supporting the LVDT (linear variable differential transformer) to the beam using epoxy resin. Record the mass of the beam with the fastener.

B.2 Conditioning of Specimens

1. Place the beam in the vacuum container, using a spacer to provide support above the base of the container. Fill the container with water until the beam is totally submerged. Apply a vacuum of 635 mm (25 in.) of mercury for 30 minutes. Stop the vacuum and determine the saturated surface dry mass according to AASHTO T-166. Calculate the volume of absorbed water and determine the degree of saturation. If the saturation level is less than 70 percent, vacuum saturate the beam for an additional 30 minutes and determine the saturated surface dry mass again.
2. Place the vacuum-saturated beam in a water bath with the water temperature pre-set at 60°C (140°F). The beam should be supported on a rigid, flat (steel or wood) plate to prevent deformation of the beam during conditioning. The top surface of the beam should be about 25 mm (1.0 in.) below the water surface.
3. After 24 hours, drain the water bath and refill it with cold tap water. Set the water bath temperature to 20°C (68°F). Wait two hours for the temperature to equilibrate.
4. Remove the beam from the water bath, and determine its saturated surface dry mass.
5. Wrap the beam with Parafilm™ to ensure no water leakage.
6. Check the bonded fastener. If it is loose, remove it and rebond it with epoxy resin.
7. Apply a layer of scotch tape to the areas where the beam contacts the clamps of the fatigue machine. This will prevent adhesion between the Parafilm™ and the clamps.
8. Start the fatigue test of the conditioned beam within 24 hours.